The impact of diagenesis and sequestration on long-chain diols and derived marine proxies

Sophie Reiche

Members of the reading committee:

Isla Castañeda

Helge Niemann

Francien Peterse

Appy Sluijs

Jaime Toney

This research has been funded by the European Research Council (ERC) under the European Union's Seventh Framework Program (FP7/2007-2013) ERC grant agreement [339206] to S.S. S.S and J.S.S.D. receive financial support from the Netherlands Earth System Science Centre (NESSC) through a gravitation grant (NWO 024.002.001) from the Dutch Ministry for Education, Culture and Science.

Cover design by René Heistermann and Sophie Reiche

ISBN: 978-94-6332-649-0

The impact of diagenesis and sequestration on long-chain diols and derived marine proxies

De gevolgen van diagenese en sequestratie op langkettige diolen en bijbehorende mariene proxies

(met een samenvatting in het Nederlands)

Der Einfluss von Diagenese und Sequestration auf langkettige Diole und zugehörige marine Proxies

(mit einer Zusammenfassung in deutscher Sprache)

Proefschrift

ter verkrijging van de graad van doctor aan de Universiteit Utrecht op gezag van de rector magnificus, prof.dr. H.R.B.M. Kummeling, ingevolge het besluit van het college voor promoties in het openbaar te verdedigen op vrijdag 28 augustus 2020 des middags te 2.30 uur

door

Sophie Reiche

geboren op 4 maart 1988
te Greifswald, Duitsland

Promotoren:

Prof. dr. S. Schouten
Prof. dr. J.S. Sinninghe Damsté

To the Sea, to the Sea! The white gulls are crying,
the wind is blowing, and the white foam is flying.
J.R.R. Tolkien

Für meine Großeltern.

Contents

Summary

The current global warming and climate change is widely discussed in science, politics and media. To predict climate development in the future, we depend on climate models that are validated and tested on appropriate climate archives of Earth's history, e.g. marine sediments, by application of climate proxies. These climate proxies are preserved material standing in for direct measurements and provide information about past environmental and climate conditions. Their application helps in understanding past and present climate change and in turn, they give insight into potential future climate changes. A variety of inorganic and organic chemical proxies are used to reconstruct paleoenvironmental parameters that include sea surface temperature (SST), concentration of CO_2 in the atmosphere, ocean salinity or marine primary productivity. Organic proxies are based on preserved sedimentary lipids, termed biomarkers and serve as indicators for the past presence of specific groups of organism or biogeochemical processes as well as environmental parameters. For example, two frequently applied organic SST proxies are the $U^{K'}_{37}$ index, based on the degree of unsaturation of long chain alkenones produced by haptophyte algae, and the TEX_{86} index, based on the number of cyclopentane moieties in glycerol dialkyl glycerol tetraether lipids (GDGTs) biosynthesized by Thaumarchaeota.

Recently, long-chain alkyl diols (LCDs) have been developed to reconstruct SST, productivity and upwelling conditions as well as terrestrial input into marine environments. LCDs, consisting of long alkyl chains with carbon numbers commonly ranging from C_{28} to C_{32} and alcohol groups at the first carbon position and in a mid-chain position at carbon position 12 to 15, have been recognized in a wide variety of marine and lacustrine environments. While saturated and mono-unsaturated 1,14-diols have been shown to be produced by *Proboscia* diatoms in marine environments, 1,13- and 1,15-diols have been identified in cultures of freshwater/ brackish Eustigmatophyceae algae, e.g. *Nannochloropsis salina* or *Nannochloropsis oculata*, however their marine producers remain unknown. The 1,13- and 1,15-diols commonly are present as extractable-bound lipids in sediments but only occur in small abundances as freely extractable lipids in algal biomass. They have been shown to form the building blocks of the highly aliphatic and insoluble biomacromolecules termed algaenan, which are built up of mainly 1,15-diols linked by ether bonds and are part of the cell-wall. While several proxies, i.e. the Long-chain Diol Index (LDI), to reconstruct SST, and the Diol Index, to study productivity and upwelling conditions, have been defined and are increasingly used in paleo-reconstructions, many uncertainties remain. Marine organic proxies are impacted by a large number of chemical and physical changes from the time the proxy signal is generated by the producer, during the transport and settling of the signal through the water column and the subsequent burial in the sediment. An impact of these diagenetic changes, i.e. by oxic degradation or mode of occurrence, has been shown for a variety of organic proxies, but has not been studied yet in detail for LCDs and their derived proxies. Therefore, the focus of thesis was to assess potential biases that may arise when LCD proxies are impacted by diagenetic changes.

In order to constrain the impact of oxygen exposure on LCDs and the LDI, *Nannochloropsis oculata* biomass was incubated aerobically for 271 days and the concentrations of free-extractable, extractable-bound, residually ester-bound and residually-bound glycosidic ether- or amide-bound fatty acids and LCDs were determined. Both saturated and polyunsaturated fatty acids were significantly impacted, showing substantially decreasing concentrations with increasing oxic incubation time, irrespective of their mode of binding. In contrast, LCDs showed a large-scale increase in concentration from incubation day 125 until the end of incubation at day 271, in particular for residually ester-bound LCDs which showed a 30-fold

increase in concentration. This increase in concentration likely reflects a release of LCDs from the biopolymer algaenan upon oxic degradation. In contrast to this large-scale increase in LCD concentration, LDI values remained stable throughout the degradation experiment, although LDI values were dependent on their mode of occurrence. Overall these experiments indicated a likely negligible impact of oxygen exposure on the LDI.

To ascertain if prolonged oxygen exposure indeed led to a release of LCDs from the biopolymer algaenan, residues left after extraction and saponification and hydrolysis of the aerobically degraded biomass of *Nannochloropsis oculata*, were analyzed by step-wise pyrolysis. The pyrolyzate of the algaenan was characterized by a series of *n*-alkenes/ *n*-alkanes with chain lengths ranging from C_{10} to C_{33} with two maxima at C_{15} to C_{17} and C_{26} to C_{28}. Mid-chain ketones were present with chain lengths of C_{28} to C_{34} with a maximum at C_{31} and a mid-chain keto group at position 14. Additionally, a pronounced C_{19} *n*-alkan-2-one was present. These results point to a structural composition of the algaenan built-up of C_{32} 1,15-diol units, linked by ether bonds, which is in agreement with previously published studies. Analysis of residues after extraction at different time points throughout the oxic degradation experiment, however, suggests that the algaenan structure was not largely altered, indicating that oxygen exposure does not have a substantial impact on the structure of the algaenan.

Since LCDs are thought to be constituents of the algaenan and have been reported to be released after hydrolysis of algal extracts, the identification of potential macro-molecular sources of LCDs in *Nannochloropsis sp.* biomass was attempted. However, application of ultra-high pressure liquid chromatography combined with high resolution mass spectrometry (UHPLC/HRMS) and semi-preparative HPLC did not lead to the identification of potential macromolecular precursor lipids. Additionally, only freely extractable and not extractable-bound lipids could be identified, which is in contrast to previously published studies. Subsequent analysis of three different strains of *Nannochloropsis spp.* showed that LCDs mainly occur as freely extractable lipids and only minor increases in concentration were detected after application of acid hydrolysis on the biomass extracts. These results therefore call into question the common thought that LCDs occur mainly as extractable-bound lipids.

A potential bias in the application of organic biomarkers may arise, when residually-bound lipids in marine sediments are released during diagenesis and may therefore yield different distributions and abundances than freely occurring lipids. Therefore, the impact of the mode of occurrence on LCDs and structurally related mid-chain keto-ols (keto-ols) was analyzed in the S5 sapropel of the Eastern Mediterranean. Some LCDs were shown to occur partly bound to the organic sedimentary matrix; extractable-bound 1,14-diols showed a 1.5-fold increase in abundance when compared to their freely extractable counterparts. While freely extractable LCDs dominate in the sapropel, LCDs occur predominantly as residually ester-bound and residually glycosidic ether- or amide-bound lipids in sediments outside of the sapropel. However, irrespective of the mode of occurrence of the LCDs, LCD indices showed similar trends over sapropel depth. Keto-ols, which may be formed by post-depositional oxidation of LCDs, were only detected in the sapropel and not in the sediments below or above it, in agreement with the hypothesis that they reflect intermediate LCD oxidation products. Their relative abundance in the sapropel, quantified by the Diol Oxidation Index (DOXI), did not show significant changes.

Additionally, the impact of post-depositional oxidation on LCDs and keto-ols was studied in the f-turbidite of the Madeira Abyssal Plain. Comparison of lipids in the upper, oxidized part of the turbidite, which has been impacted by post-depositional oxidation, with the anoxic lower part of the turbidite, shows a higher preservation of the C_{30} 1,15-diol and C_{30} 1,15-keto-ol compared to the other LCDs and keto-ols. While the LDI showed increased values, the Diol Index and FC_{32} 1,15-diol, a proxy for the riverine input into marine environments, showed

decreased values with increasing oxygen exposure. Therefore, all three indices were impacted by post-depositional oxidation, likely resulting from a preferential preservation of the C_{30} 1,15- and C_{32} 1,15-diol over 1,13- and 1,14-diols. However, compared to GDGTs and GDGT-based organic proxies (BIT and TEX_{86} index), measured in the same turbidite, LCDs and keto-ols seem to be better preserved upon post-depositional oxidation. Changes in oxygen exposure time in sediments may therefore cause different changes in organic terrestrial and temperature proxies and care has to be taken when applying these different indices in severely oxidized sediments.

Overall, the results of this thesis represent a first step towards constraining the impact of diagenesis and sequestration on LCDs and LCD proxies. A variable impact of both oxic degradation and mode of occurrence could be shown for LCDs and LCD proxies, both in algae biomass as well as in marine sediments, which points to potential biases that have to be taken into account when applying these proxies in paleoenvironmental reconstructions.

Zusammenfassung

Der Klimawandel und die damit verbundene globale Erwärmung sind Themen, die aus aktuellem Anlass in der Forschung, Politik und den Medien diskutiert werden. Um die zukünftige Klimaentwicklung vorhersagen zu können, werden verschiedene Klimamodelle verwendet, welche anhand geeigneter Klimaarchive der Erdgeschichte durch Anwendung von Klima-Proxies getestet und validiert werden. Klima-Proxies sind dabei indirekte Anzeiger, durch welche Informationen über die Umwelt- und Klimabedingungen, unter denen z. B. marine Sedimente abgelagert wurden, ermittelt werden können. Ihre Anwendung hilft beim Verständnis vergangener und gegenwärtiger Klimaveränderungen und erlaubt einen Einblick in mögliche zukünftige Klimaveränderungen. Verschiedene anorganisch- und organisch-geochemischen Proxies werden verwendet, um Paläo-Umweltparameter zu rekonstruieren. Beispiele für Paläo-Umweltparameter sind unter anderem Meeresoberflächentemperaturen, die CO_2-Konzentrationen in der Atmosphäre, der Salzgehalt der Ozeane oder die Primärproduktivität des Meeres. In organisch-geochemischen Proxies werden dabei Biomarker angewendet, welche charakteristisch sind für bestimmte Gruppen von Organismen, biogeochemische Prozesse oder Paläo-Umweltparameter. Häufig angewendete organisch-geochemische Proxies sind unter anderem der $U^{K'}_{37}$-Index, basierend auf von Haptophyten produzierten ungesättigten langkettigen Alkenonen, und der TEX_{86}-Index, welcher die von Thaumarchaeota biosynthetisierten Membranlipide (GDGTs) berücksichtigt. In den letzten Jahren werden vermehrt langkettige Alkyldiole (Diole) genutzt um Meeres-oberflächentemperaturen, Primärproduktivität, Upwelling und die Analyse des Eintrages von terrigenem organischem Material in marine Ablagerungsmilieus zu rekonstruieren. Diese Diole, welche in einer Vielzahl von marinen und lakustrinen Ablagerungsmilieus identifiziert wurden, sind charakterisiert durch Alkylketten mit Längen von C_{28} bis C_{32} und Hydroxygruppen an der ersten Kohlenstoffposition sowie an der Kohlenstoffposition 12 bis 15. Gesättigte und einfach-ungesättigte 1,14-Diole werden von marinen *Proboscia*-Diatomeen produziert. 1,13- und 1,15-Diole wurden in Kulturen von Eustigmatophyceae-Algen, z.B. *Nannochloropsis salina* oder *Nannochloropsis oculata*, nachgewiesen, jedoch ist der marine Produzent unbekannt. Üblicherweise, liegen 1,13- und 1,15-Diole als extrahierbar-gebundene Lipide vor und kommen nur in geringen Mengen als frei-extrahierbare Lipide in der Algenbiomasse vor. Weiterhin, sind sie Bausteine des aliphatischen und unlöslichen Biomakromoleküls Algaenan, welches einen Teil der Zellwand darstellt und hauptsächlich aus durch Ether-Verbindungen vernetzte 1,15-Diole besteht. Mehrere Proxies, basierend auf Diolen, wurden bisher definiert, u.a. der Long-chain Diol Index (LDI) zur Rekonstruktion von Meeresoberflächentemperaturen, sowie der Diol Index zur Untersuchung der Primärproduktivität und Upwelling-Konditionen. Während diese zunehmend in Paläo-Rekonstruktionen verwendet werden, ist ihre Nutzung mit Unsicherheiten verbunden. Marine organisch-geochemische Proxies sind von einer Anzahl chemischer und physikalischer Veränderungen betroffen. Diese beeinflussen das Proxy-Signal sobald es vom marinen Produzenten erzeugt wird, während es durch die marine Wassersäule transportiert und schließlich in marinen Sedimenten abgelagert wird. Diese diagenetischen Veränderungen beinhalten unter anderem den Einfluss von oxidativer Degradation sowie die Sequestrierung von Lipiden in der Sedimentmatrix und der Algenbiomasse. Daher liegt der Fokus dieser Doktorarbeit auf der Untersuchung von verschiedenen diagenetischen Einflüssen auf Diole und der ihnen zugrunde liegenden Proxies, welche bisher noch nicht ausreichend von der Forschung betrachtet wurden.

Um den Einfluss der oxidativen Degradation auf Diole und den LDI zu analysieren, wurde Biomasse der Alge *Nannochloropsis oculata* über 271 Tage aerob inkubiert und die

Konzentration von frei-extrahierbaren, gebunden-extrahierbaren, residual Ester-gebundenen und residual glykosidisch Ether- oder Amid-gebundene Fettsäuren und Diolen bestimmt. Gesättigte und mehrfach ungesättigte Fettsäuren zeigen stark abnehmende Konzentrationen über die aerobe Inkubationszeit, unabhängig von der Bindungsart, in welcher sie vorlagen. Im Gegensatz dazu, steigt die Konzentration der Diole ab dem Inkubationstag 125 bis zum Ende der aeroben Inkubation stark an, welches insbesondere bei den residual Ester-gebundenen Diolen zu einem 30-fachen Konzentrationsanstieg führt. Dieser Konzentrationsanstieg spiegelt dabei wahrscheinlich eine Freisetzung von Diolen durch oxidative Degradation aus dem Biopolymer Algaenan wider. Trotz des starken Anstiegs der Diol-Konzentration, bleiben die errechneten LDI-Werte stabil, sind jedoch abhängig davon wie die zur Berechnung herangezogenen Diole in der Biomasse gebunden sind. Ein vernachlässigbarer Einfluss von oxidativer Degradation auf den LDI ist daher wahrscheinlich.

Um zu überprüfen, ob eine länger andauernde Sauerstoffexposition tatsächlich zu einer Freisetzung von Diolen aus dem Biopolymer Algaenan führt, wurden die Rückstände, welche nach der Extraktion, sowie basischen und sauren Hydrolyse der aerob degradierten Biomasse von *Nannochloropsis oculata* zurückblieben, durch schrittweise Pyrolyse analysiert. Dabei zeigt sich, dass die Pyrolysate des Algaenan durch eine Serie von *n*-Alkenen/ *n*-Alkanen mit Kettenlängen von C_{10} bis C_{33} und zwei Maxima bei C_{15} bis C_{17} und C_{26} bis C_{28} charakterisiert sind. Mittelkettige Ketone liegen mit Kettenlängen von C_{28} bis C_{34} und einem Maximum bei C_{31} mit einer mittelkettigen Ketogruppe an Position 14 vor. Besonders auffällig ist ein C_{19} *n*-Alkan-2-on. Diese Ergebnisse deuten darauf hin, dass das Algaenan durch C_{32}-1,15-Diol-Einheiten aufgebaut ist, wie in bereits veröffentlichten Studien diskutiert. Die Analyse von Rückständen zu verschiedenen Zeitpunkten der aeroben Inkubation legt nahe, dass die Algaenan-Struktur nicht durch die oxidative Degradation verändert wurde. Somit ist es wahrscheinlich, dass eine Sauerstoffexposition über die hier analysierten Zeiträume, keinen wesentlichen Einfluss auf die Struktur des Algaenans hat.

Da davon ausgegangen werden kann, dass Diole Strukturbestandteile des Algaenan sind und durch Hydrolyse von Algenextrakten freigesetzt werden, wurde versucht potentielle makromolekulare Quellen für Diole in der Biomasse von *Nannochloropsis* sp. zu identifizieren. Mittels Ultrahochdruck-Flüssigkeitschromatographie in Kombination mit hochauflösender Massenspektrometrie (UHPLC/HRMS) und semi-präparativer HPLC, können jedoch keine potenziellen makromolekulare Vorläuferlipide nachgewiesen werden. Zusätzlich können nur frei-extrahierbare und nicht-extrahierbar gebundene Lipide identifiziert werden, welches im Gegensatz zu zuvor veröffentlichten Studien steht. Eine darauf aufbauende Analyse von drei verschiedenen Spezies von *Nannochloropsis* spp. zeigt, dass Diole hauptsächlich als frei-extrahierbare Lipide vorliegen, mit einer nur geringfügigen Konzentrationserhöhung nach Anwendung von saurer Hydrolyse auf die Biomasseextrakte. Diese Ergebnisse stehen daher im Gegensatz zu früheren Veröffentlichungen und stellen die allgemeine Auffassung, dass Diole als hauptsächlich extrahierbar-gebundene Lipide vorliegen, in Frage.

Weitere systematische Fehler in der Anwendung von organischen Biomarkern können auftreten, wenn residual-gebundene Lipide in marinen Sedimenten während der Diagenese freigesetzt werden und, im Gegensatz zu frei-vorliegenden Lipiden, zu veränderten Verteilungen und Häufigkeiten von Diolen führen. Daher wurde der Einfluss des Bindungsmodus des Auftretens von Lipiden für Diole und strukturell verwandte mittelkettige Ketole (Ketole) in Sedimenten eines S5 Sapropels des östlichen Mittelmeers analysiert. Dabei konnte gezeigt werden, dass einige Diolisomere an die organische Sedimentmatrix gebunden sind, da extrahierbar-gebundene 1,14-Diole im Vergleich zu frei-extrahierbaren Diolen eine 1,5-fache Zunahme der Konzentrationen zeigen. Frei-extrahierbare Diole dominieren innerhalb des Sapropels, während Diole außerhalb des Sapropels als residual Ester-gebundene und residual glykosidische Ether- oder Amid-gebundene Lipide vorliegen. Unabhängig vom

Bindungsmodus des Auftretens von Diolen zeigen verschiedene Diol-Indizes ähnliche Trends über die Tiefe des Sapropels. Ketole können nur innerhalb des Sapropels nachgewiesen werden. Ihre relative Häufigkeit, ausgedrückt durch den Diol Oxidation Index (DOXI), welcher zur Untersuchung von Auswirkungen der post-depositionalen Oxidation herangezogen wird, zeigt jedoch keine signifikanten Änderungen.

Der Einfluss der post-depositionaler Oxidation auf Diole und Ketole wurde zusätzlich im f-Turbidit der Tiefsee-Ebene von Madeira untersucht. Eine höhere Präservation des C_{30} 1,15-Diols und des C_{30} 1,15-Ketols im Vergleich zu anderen Diolen und Ketolen liegt vor, wenn der obere oxidierte Teil des Turbidits, welcher durch post-depositionale Oxidation beeinflusst wurde, mit dem unteren anoxischen Teil verglichen wird. Während der LDI mit zunehmender Sauerstoffexposition erhöhte Werte zeigt, zeigen der Diol-Index und der FC_{32} 1,15-Diol-Index, ein Proxy für den terrigenen Eintrag in marine Ablagerungsmilieus, verringerte Werte. Daher ist wahrscheinlich, dass alle drei Indizes durch post-depositionale Oxidation beeinflusst werden, was auf eine präferentielle Konservierung der C_{30} 1,15- und C_{32} 1,15-Diole im Vergleich zu 1,13- und 1,14-Diolen zurückzuführen ist. Im Vergleich zu anderen organischen Proxies und Biomarkern, im Besonderen GDGTs, der BIT-Index und der TEX_{86}-Index, weisen Diole und Ketole eine höhere Präservation auf, wenn sie von post-depositionaler Oxidation beeinflusst werden. Bei veränderlichen Sauerstoffexpositionszeiten, kann es daher zu unterschiedlichen Beeinflussungen von organisch-terrestrischen und Meeres-oberflächentemperatur-Proxies kommen, welche bei der Anwendung von organisch-geochemischen Proxies in stark oxidierten Sedimenten berücksichtigt werden müssen.

Die Ergebnisse dieser Arbeit stellen eine erste tiefgründigere Analyse dar, wie Diole und Diol--Proxies durch Diagenese und Sequestrierung beeinflusst werden. Es konnte gezeigt werden, dass die oxidative Degradation und der Bindungsmodus des Auftretens von Lipiden zu unterschiedlichen Veränderungen von Diolen und Diol-Proxies sowohl in Algenbiomasse als auch marinen Sedimenten führt. Diese systematischen Fehler müssen daher in der Anwendung dieser Proxies in Paläo-Rekonstruktionen berücksichtigt werden.

Samenvatting

De huidige klimaatverandering en de daarmee geassocieerde opwarming van de aarde worden veel besproken in de wetenschap, politiek en media. Om de toekomstige klimaatontwikkeling adequaat te kunnen voorspellen zijn we afhankelijk van klimaatmodellen die getest zijn op het accuraat reconstrueren van het vroegere klimaatcondities. Hiertoe dienen de klimaatarchieven van de geschiedenis van de aarde, opgeslagen in bijvoorbeeld mariene sedimenten, uitgelezen te worden door toepassing van klimaatproxies. Deze klimaatproxies zijn gebaseerd op bewaard gebleven materiaal in o.a. mariene sedimenten dat de toenmalige omgevings- en klimaatomstandigheden kan reconstrueren. Toepassing van klimaatproxies helpt bij het begrijpen van vroegere en huidige klimaatveranderingen en op hun beurt geven ze inzicht in mogelijke toekomstige klimaatveranderingen. Een verscheidenheid aan anorganische en organische chemische proxies wordt gebruikt om paleomilieuparameters te reconstrueren, waaronder de oppervlaktezeewatertemperatuur (OZT), de concentratie van CO_2 in de atmosfeer, het zoutgehalte in de oceaan en de mariene primaire productiviteit. Organische proxies zijn gebaseerd op gepreserveerde sedimentaire lipiden, biomarkers genoemd, en dienen als indicatoren voor de vroegere aanwezigheid van specifieke groepen organismen, biogeochemische processen, en omgevingsparameters. Twee vaak toegepaste organische OZT-proxies zijn de $U^{K'}_{37}$-index, die gebaseerd is op de mate van onverzadiging van alkenonen met lange ketens geproduceerd door algen vallend in de groep van de haptofyten, en de TEX_{86}-index, die gebaseerd is op het aantal cyclopentaan-groepen in glycerol dialkyl glycerol tetraether lipiden (GDGTs), membraanlipiden van Thaumarchaeota, een belangrijke groep van oerbacteriën in de oceaan.

Onlangs zijn nieuwe proxies op basis van langketige diolen (LKDs) ontwikkeld om OZT, productiviteit, mate van opwelling en de aanlevering van terrestrische materiaal in mariene milieu's te reconstrueren. LKDs bestaan uit lange lineaire alkylketens met een aantal koolstofatomen dat gewoonlijk varieert van C_{28} tot C_{32} en twee alcoholgroepen die op het eerste koolstofpositie en het midden van de koolstofketen (op positie C-12 tot C-15) gepositioneerd zijn. Deze componenten worden aangetroffen in een grote verscheidenheid aan mariene en lacustriene milieu's. Verzadigde en enkelvoudig onverzadigde 1,14-diolen worden geproduceerd door *Proboscia* diatomeeën in kustzeeën en de oceaan. De 1,13- en 1,15-diolen zijn aangetroffen in culturen van Eustigmatofyten algen, b.v. *Nannochloropsis salina* of *Nannochloropsis oculata*, maar in een andere distributie dan in het mariene milieu. Hun mariene producenten zijn dan ook onbekend. De 1,13- en 1,15-diolen komen gewoonlijk voor als extraheerbare gebonden lipiden en slechts in kleine hoeveelheden als vrij extraheerbare lipiden in algenbiomassa. Er is aangetoond dat zij de bouwstenen vormen van de zeer alifatische en onoplosbare biomacromoleculen die algenaan worden genoemd en die deel uitmaken van de celwand. Verschillende op LKD gebaseerde proxies, zoals de Langketige Diol Index (LDI) om OZT te reconstrueren, en de Diol Index om productiviteit en opwelling te bestuderen, zijn ontwikkeld en worden in toenemende mate gebruikt bij paleoreconstructies. Er blijven echter nog veel onzekerheden bestaan over hun toepassing. Mariene organische proxies worden beïnvloed door een groot aantal chemische en fysische processen vanaf het moment dat de biomarkers worden geproduceerd in het oppervlaktewater van de oceaan, tijdens het transport en de bezinking van de componenten door de waterkolom en vervolgens tijdens de begraving in het sediment. De invloed van deze diagenetische veranderingen, zoals bijvoorbeeld door oxische degradatie of de manier van voorkomen, is aangetoond voor verschillende organische proxies, maar is nog niet in detail bestudeerd voor LKDs en diol-proxies. Het onderwerp van dit proefschrift is het ontstaan van mogelijke complicaties die kunnen ontstaan wanneer diol-proxies worden beïnvloed door diagenetische veranderingen.

Om de invloed van zuurstofblootstelling op de concentratie en distributie van LKDs en de LDI vast te stellen, werd gekweekte biomassa van *Nannochloropsis oculata* gedurende 271 dagen aëroob geïncubeerd. De concentraties werden bepaald van LKDs en vetzuren in verschillende verschijningsvormen: vrij extraheerbaar, extraheerbaar-gebonden, residuaal ester-gebonden en residuaal gebonden via glycosidisch ether of amide bindingen. De concentratie aan verzadigde en meervoudig onverzadigde vetzuren daalde aanzienlijk met toenemende incubatietijd, ongeacht de manier waarop zij gebonden waren. LKDs vertoonden daarentegen een toename in concentratie vanaf incubatiedag 125 tot het einde van de incubatie op dag 271, in het bijzonder voor residueel ester-gebonden LKDs, die maar liefst een 30-voudige concentratieverhoging vertoonden. Deze toename in concentratie weerspiegelt waarschijnlijk het vrijkomen van LKDs uit het biopolymeer algenaan na partiële afbraak door zuurstof. In tegenstelling tot de grootschalige toename van de LKD concentratie, bleven de LDI waarden stabiel gedurende het afbraakexperiment. De blootstelling aan zuurstof heeft dus waarschijnlijk verwaarloosbare invloed op de LDI waarden, hoewel deze wel afhankelijk zijn van de manier waarop de LKDs in de biomassa waren gebonden.

Om vast te stellen of langdurige blootstelling aan zuurstof effect heeft op het biopolymeer algenaan, werden residuen die overbleven na extractie en verzeping en hydrolyse van de aëroob afgebroken biomassa van *Nannochloropsis oculata*, geanalyseerd met behulp van stapsgewijze pyrolyse. Het pyrolysaat van het algenaan werd gekenmerkt door een reeks *n*-alkenen / *n*-alkanen met een ketenlengte van C_{10} tot C_{33} en twee maxima bij respectievelijk C_{15} tot C_{17} en C_{26} tot C_{28}. Ketonen waren aanwezig met ketenlengtes van C_{28} tot C_{34} met een maximum op C_{31} en hadden de ketogroep in het midden van de keten op positie 14. Bovendien werd er relatief veel van de C_{19} *n*-alkaan-2-on gevonden. Deze resultaten wijzen er op dat het algenaan opgebouwd is uit C_{32} 1,15-diol-eenheden, verbonden via etherbindingen. Dit is in overeenstemming met eerder gepubliceerde studies. Analyse van residuen op verschillende tijdstippen gedurende de aërobe afbraak suggereert dat de algenaan-structuur niet substantieel veranderde. Dit geeft aan dat blootstelling aan zuurstof geen grote invloed heeft op de algenaanstructuur.

Aangezien LKDs een bestanddeel vormen van het algenaan en zij pas vrijkomen bij hydrolyse van de algenextracten, is geprobeerd potentiële macromoleculaire bronnen van LKDs in *Nannochloropsis* sp. biomassa te identificeren. De toepassing van ultrahoge druk vloeistofchromatografie in combinatie met hoge resolutie massaspectrometrie (UHPLC/HRMS) en semi-preparatieve HPLC leidde echter niet tot de identificatie van potentiële macromoleculaire precursorlipiden. Bovendien konden alleen vrij extraheerbare en niet extraheerbare gebonden LKDs worden geïdentificeerd, in tegenstelling tot eerder gepubliceerd onderzoek. Analyse van drie andere *Nannochloropsis* soorten toonde aan dat LKDs ook hier voornamelijk voorkomen als vrij extraheerbare lipiden en dat kleine verhogingen van de concentratie pas gedetecteerd werden na zure hydrolyse van de biomassa-extracten. Deze resultaten trekken daarom de gangbare gedachte dat LKDs voornamelijk voorkomen als extraheerbare gebonden lipiden in twijfel.

Een mogelijke complicatie bij de toepassing van organische biomarkers kan optreden wanneer residueel gebonden lipiden in mariene sedimenten vrijkomen tijdens diagenese en daarmee de concentraties en distributies van de veel meer bestudeerde vrij-voorkomende lipiden beïnvloeden. Daarom werd de invloed van de manier van voorkomen op LKDs en structureel gerelateerde keto-olen met de keto-groep in de middenpositie geanalyseerd in mariene sedimenten van het oostelijke Middellandse Zeegebied waar de S5-sapropeel onderdeel van uit maakte. Sommige LKDs bleken in belangrijke mate gebonden te zijn aan de organische sedimentaire matrix, aangezien extraheerbaar-gebonden voorkomende 1,14-diolen een anderhalfvoudige toename in concentratie vertoonden in vergelijking met vrij extraheerbare LKDs. Terwijl vrij extraheerbare LKDs domineren in de sapropeel, komen buiten de sapropeel

LKDs alleen residuaal voor (zowel ester-gebonden als glycosidisch ether- of amide-gebonden). De verschillende LKD-indices vertoonden vergelijkbare trends met sapropeeldiepte, ongeacht de manier waarop de LKDs gebonden zijn. Keto-olen waren alleen aanwezig in de sapropeel en niet in de sedimenten onder of boven de sapropeel. Keto-olen worden wel eens gezien als intermediairen in de oxidatie van LKDs maar hun relatieve concentratie, gekwantificeerd m.b.v. de Diol Oxidation Index (DOXI), vertoonde geen significante verandering in de sapropeel.

Daarnaast werd de invloed van oxidatie na afzetting op LKDs en keto-ols bestudeerd in de f-turbidiet van de Abyssale vlakte van Madeira. Vergelijking van lipiden in het bovenste geoxideerde deel van het turbidiet, beïnvloedt door oxidatie na afzetting, met het anoxische onderste gedeelte van de turbidiet, toonde een hogere preservatie van het C_{30} 1,15-diol en C_{30} 1,15-keto-ol vergeleken met de andere LKDs en keto-olen. Terwijl de LDI verhoogd was vertoonden de Diol Index en FC_{32} 1,15-diol, een proxy voor de rivierinvoer in mariene omgevingen, verlaagde waarden bij toenemende zuurstofblootstelling. Alle drie indices werden dus beïnvloed door oxidatie na afzetting, waarschijnlijk als gevolg van een preferentiële preservatie van de C_{30} 1,15- en C_{32} 1,15-diol t.o.v. de 1,13- en 1,14-diolen. LKDs en keto-olen blijven beter bewaard na oxidatie na afzetting dan GDGTs met implicaties van op GDGTs gebaseerde organische proxies, d.w.z. de BIT en TEX_{86}-index. Veranderingen in de zuurstofblootstellingstijd in sedimenten kunnen daarom veranderingen veroorzaken in terrestrische en OZT organische proxies en daarom is voorzichtigheid is geboden bij hun toepassing in sterk geoxideerde sedimenten.

De resultaten van dit proefschrift vormen een eerste stap om de invloed van diagenese en manier van voorkomen op LKDs en LKD-proxies te bepalen. Zowel oxische degradatie als de wijze van voorkomen van LKDs, zowel in algenbiomassa als in mariene sedimenten, is aangetoond en heeft invloed op de waarden van LKD-proxies. Dit kan mogelijk tot complicatie in hun toepassing leiden en hier zal rekening mee moeten worden gehouden in hun toepassing in paleomilieu-reconstructies.

Chapter 1

Introduction

1.1. Climate reconstruction and temperature proxies

Over the last decades, the current climate change, especially the global warming induced by an anthropogenic input of greenhouse gases, is an important topic widely discussed in science (IPCC, 2014), politics and media. We depend on climate models to understand the current climate as well as to predict future climate development. These climate models are validated and tested on appropriate climate archives of Earth's history. Examples of such archives are tree rings, ice cores, speleothems as well as terrestrial and lacustrine sediments, but especially marine sediments as they provide the longest and continuous climate records of Earth's history. To extract useful information from these archives, climate records and climate proxies are applied, which are preserved environmental parameters standing in for direct measurements and which provide information about the environmental and climate conditions under which sediments were deposited. The application of these proxies therefore helps in understanding past and present climate changes, which in turn gives a potential insight into future climate development.

A variety of inorganic and organic chemical proxies are used to reconstruct paleoenvironmental parameters such as sea surface temperature (SST), the concentration of CO_2 in the atmosphere (pCO_2) as well as ocean salinity and marine primary productivity. For example, the oxygen isotopic ratio $\delta^{18}O$ and Mg/Ca ratio of foraminiferal tests are common inorganic proxies to reconstruct past SST (Urey, 1947; Epstein et al., 1953; Emiliani, 1954; Shackleton, 1974; Nürnberg et al., 1996; Rosenthal et al., 1997; Bemis et al., 1998). Organic proxies are based on preserved sedimentary lipids, termed biomarkers. These biomarkers serve as indicators for the past presence of certain (groups of) organisms and sometimes biogeochemical processes as well as certain environmental parameters (Peters et al., 2005). One of the earliest developed proxies was an SST proxy based on the degree of unsaturation of long chain alkenones produced by haptophyte algae, i.e. the $U^{K'}_{37}$ index (de Leeuw et al., 1980; Volkman et al., 1980; Brassell et al., 1986; Prahl and Wakeham, 1987). Other proxies for SST reconstruction include the TEX_{86} index (Schouten et al., 2002, 2013), based on the number of cyclopentane moieties in glycerol dialkyl glycerol tetraether lipids (GDGTs) biosynthesized by Thaumarchaeota. All these inorganic and organic proxies have, however, their own limitations and can be impacted by a variety of factors, e.g. effects of diagenesis, lateral transport, seasonality and productivity (Hoefs et al., 1998a; Gong and Hollander, 1999; Ohkouchi et al., 2002; Schouten et al., 2004; Weijers et al., 2006, 2009; Mollenhauer et al., 2008; Kim et al., 2009a, 2009b; Rontani et al., 2013). This is why a multiproxy approach is usually preferred for the reconstruction of past climate and why new proxies are continuously being developed. Among the newer proxies are the long-chain diols (LCDs) which are used for reconstructions of SST, productivity and terrestrial input.

1.2. Distribution and sources of long-chain diols and mid-chain keto-ols

LCDs consist of long alkyl chains with carbon numbers ranging from C_{26} to C_{36} with two alcohol groups at the first carbon position and in a mid-chain position at carbon position 12 to 16 (de Leeuw et al., 1981; Volkman et al., 1992; Versteegh et al., 1997). Most frequently, LCDs are detected as compounds with carbon chain lengths of C_{28} to C_{32} and alcohol moieties at 1,13, 1,14 and 1,15 (Figs. 1A, B). After their initial discovery in Black Sea sediments (de Leeuw et al., 1981), LCDs have been recognized in a large variety of marine (Smith et al., 1983; Ten Haven and Rullkötter, 1991; Ten Haven et al., 1992; Yamamoto et al., 1996; Versteegh, 1997, 2000; Pearson et al., 2001; Rampen et al., 2007; 2008, 2012; Van Soelen et al., 2010; Willmott et al., 2010; Naafs et al., 2012) and lacustrine environments (Robinson et al., 1986; Cranwell et

al., 1987; Xu et al., 2007; Shimokawara et al., 2010; Castañeda and Schouten, 2011; Romero-Viana et al., 2012; Villanueva et al., 2014).

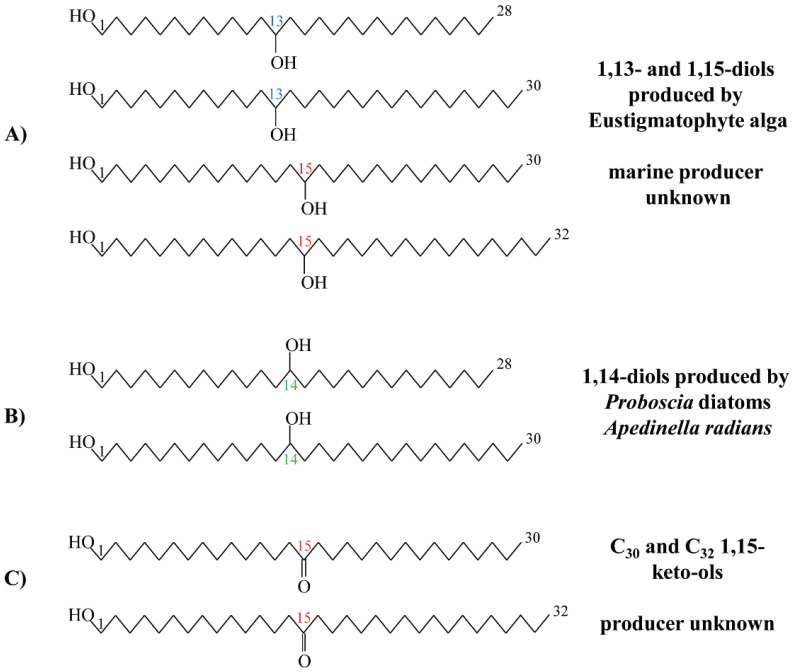

Fig. 1: Chemical structure of A) 1,13- and 1,15-diols which are produced by *Eustigmatophyte* alga although the marine producer remains unknown, B) 1,14-diols which are produced by *Proboscia* diatoms and C) C_{30} and C_{32} 1,15-keto-ols for which the producers are unknown.

LCDs were first proposed to be produced by cyanobacterial blooms of *Aphanizomenon flos-aquae* (Morris and Brassell, 1988), which could not be confirmed in laboratory studies of both *A. flos-aquae* or other cyanobacteria cultures (de Leeuw et al., 1992). LCDs were, however, identified in cultures of Eustigmatophyceae algae, e.g. *Nannochloropsis salina*, *Nannochloropsis oculata, Eustigmatos vischeri* or *Vischeria helvetica* (Volkman et al., 1992; Gelin et al., 1996; 1997a, 1997b; Rampen et al., 2014a), often showing a dominance of C_{32} 1,15-diols (Volkman et al., 1992; Méjanelle et al., 2003; Rampen et al., 2014a). This predominance of C_{32} 1,15-diols differs from the distribution of LCDs in marine surface sediments, which are generally characterized by a dominance of the C_{30} 1,13- and 1,15-diols (Versteegh et al., 1997, 2000; Rampen et al., 2012, 2014a). Therefore, the role of Eustigmatophyceae as producers of LCDs in marine environments remains uncertain. Contrastingly, LCDs produced by cultured freshwater Eustigmatophyceae are in general agreement with the LCD distribution in lacustrine environments (Volkman et al., 1999; Shimokawara et al., 2010; Rampen et al., 2014a; Villanueva et al., 2014) suggesting that they are the predominant producers of LCDs in lacustrine systems. This was confirmed by a comparison of the identity and abundance of Eustigmatophyceae 18S rRNA genes and the distribution of LCDs in the water column of Lake Challa (East Africa) (Villanueva et al., 2014).

The 1,13- and 1,15-diols (Fig. 1A) have been shown to occur as mostly extractable-bound and only in minor abundances as freely extractable lipids in algal biomass (Volkman et al., 1992) and can be released from the biomass by saponification. The LCDs have also been shown to form the building blocks of the highly aliphatic and insoluble biomacromolecules termed algaenans (Derenne et al., 1989; Tegelaar et al., 1989b; de Leeuw and Largeau, 1993; Gelin et al., 1996, 1997b; Blokker et al., 1998b, 1999, 2006; Obeid et al., 2014). These algaenans are thought to be important contributors to kerogens by selective preservation (Largeau et al., 1986; Goth et al., 1988; Tegelaar et al., 1989b). Algaenan has been analyzed by both thermal (Derenne et al., 1992a; de Leeuw and Largeau, 1993; Gelin et al., 1996, 1997b, 1999) and chemical degradation (Blokker et al., 1998b, 2000, 2006) methods and is thought to be built up of mainly 1,15-diols in Eustigmatophyte algae, linked by ether bonds. It is part of the cell wall, which has been characterized to be bi-layered, comprising both an algaenan and a cellulose-like layer. The algaenan layer has been shown to contain carboxyl, aldehyde, ketone and ester functional moieties (Scholz et al., 2014).

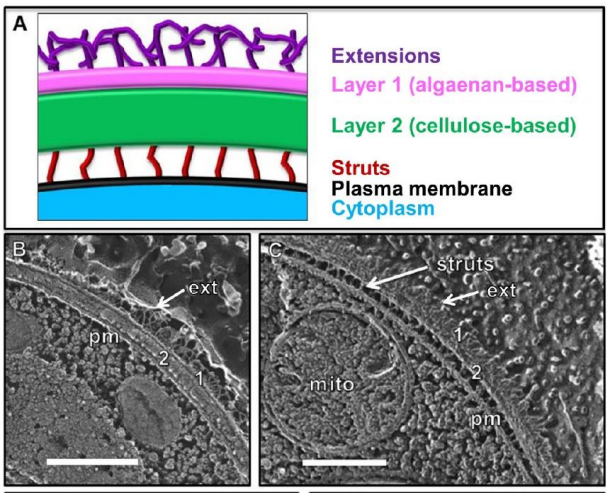

Fig. 2: A) Model of cell wall showing a bi- layer structure comprising a cellulose-based and algaenan-based layer. B, C) Quick-freeze deep-etch electron microscopy images of *Nannochloropsis gaditana* cell wall (Scholz et al., 2014).

In contrast to 1,13- and 1,15-diols, saturated and mono-unsaturated 1,14-diols have been shown to be produced by *Proboscia* diatoms (Fig. 1B), i.e. *Proboscia alata*, *Proboscia indica* and *Proboscia inermis* (Sinninghe Damsté et al., 2003; Rampen et al., 2007). They are believed to be the likely producers of 1,14-diols in marine environments based on e.g. sediment trap studies in the Arabian Sea (Rampen et al., 2007). The C_{28}, C_{30} and C_{32} 1,14-diols have also been shown to be produced by the Dictyochophycea *Apedinella radians*, however its role in the marine environments is unclear (Rampen et al., 2011).

Along with LCDs, mid-chain keto-ols (keto-ols, Fig. 1C) are often encountered in a wide range of marine and lacustrine environments and represent compounds that are structurally very similar to LCDs (Versteegh et al., 1997, 2000; Ferreira et al., 2001; Xu et al., 2007; Bogus et al., 2012). Keto-ols are usually occurring with the same carbon chain lengths and position of

functional group when compared to LCDs (Fig. 1C). In contrast to LCDs, however, producers of keto-ols have not been identified and only one study has been able to detect keto-ols in trace amounts in *Nannochloropsis gaditana* (Méjanelle et al., 2003). This has led to the idea that they are produced by oxidation in the water column and sediment (Ferreira et al., 2001; Sinninghe Damsté et al., 2003).

1.3. Paleoenvironmental proxies based on the distribution of LCDs

Two important proxies using LCD distributions have been proposed, i.e. the Long-chain Diol Index (LDI) and the Diol Index, and are discussed in detail below.

The LDI uses the fractional abundances of the C_{28} 1,13-, C_{30} 1,13- and C_{30} 1,15-diols to determine past SSTs due to a strong positive relationship of these LCDs with SST (Rampen et al., 2012). It is calculated as follows:

$$LDI = [C_{30}\ 1,15\text{-diol}]/\{[C_{28}\ 1,13\text{-diol}] + [C_{30}\ 1,13\text{-diol}] + [C_{30}\ 1,15\text{-diol}]\} \quad [1]$$

The LDI was calibrated by evaluation of the distribution of 1,13- and 1,15-diols in 162 marine surface sediments, that were globally distributed, and covered an SST range of -3 to 27 °C (Fig. 3). This yielded the following correlation:

$$\text{with SST} = (LDI-0.095)/0.033 \qquad (R^2 = 0.97;\ RSME = 2°C) \quad [2]$$

The first downcore applications in marine environments have been shown to be promising as the trends of the LDI records agree well with those of other temperature proxies (Naafs et al., 2012; Rampen et al., 2012; Lopes dos Santos et al., 2013; Smith et al., 2013; Rodrigo-Gámiz et al., 2014). So far the LDI has been applied to sediments as old as the early Pleistocene (Naafs et al., 2012). However, a potential application further back in time might be possible due to the occurrence of 1,13- and 1,15-diols, used for the calculation of the LDI, in sediments from the Miocene (Ahmed et al., 2000) and the Cretaceous-Tertiary boundary (Yamamoto et al., 1996). The LDI was also tested in lacustrine environments by analyzing the LCDs in lake surface sediments (Rampen et al., 2014a). However, only a weak correlation was observed between the LDI and annual mean air temperature, a proxy for lake surface temperature, which was probably due to different LCD producers in the different lakes. Therefore, this proxy is probably restricted to marine environments.

The 1,14-diols have been proposed to be used for the reconstruction of upwelling and productivity conditions (Rampen et al., 2008) since 1,14-diols have been shown to be produced by *Proboscia* diatoms, which are predominant in upwelling regions with high nutrient conditions. Based on this, the Diol Index was introduced (Rampen et al., 2008):

$$\text{Diol Index I} = [C_{28} + C_{30}\ 1,14\text{-diol}]/\{[C_{28} + C_{30}\ 1,14\text{-diol}] + [C_{30}\ 1,15\text{-diol}]\} \quad [3]$$

High values of the Diol Index I were shown in association with the Southwest monsoon at the onset of upwelling, when applied to the Arabian Sea, and the Diol Index I followed the same trends of other proxies reconstructing upwelling intensities, i.e. organic carbon content, barium/aluminum ratios and stable isotopic composition of foraminifera (Rampen et al., 2007, 2008). The Diol Index I was later redefined by Willmott et al. (2010) for the Western Bransfield Basin in Antarctica as the C_{30} 1,15-diol was present in very low concentration, in contrast to the C_{30} 1,13-diol which was more abundant. It is calculated as follows:

$$\text{Diol Index II} = [C_{28} + C_{30}\ 1,14\text{-diol}]/\{[C_{28} + C_{30}\ 1,14\text{-diol}] + [C_{28}\ 1,13\text{-diol}] + [C_{30}\ 1,13\text{-diol}]\} \quad [4]$$

Both indices have since been applied in a variety of study locations but uncertainties with respect to their validity remain. For example, *Proboscia* diatoms have been shown to not only bloom during periods of upwelling, but also during pre-upwelling, and even in stratified water column conditions (Contreras et al., 2010). It is therefore likely that Diol Index I and II do not represent upwelling or high nutrient conditions as such but rather are affected by various factors which influence *Proboscia* ecology.

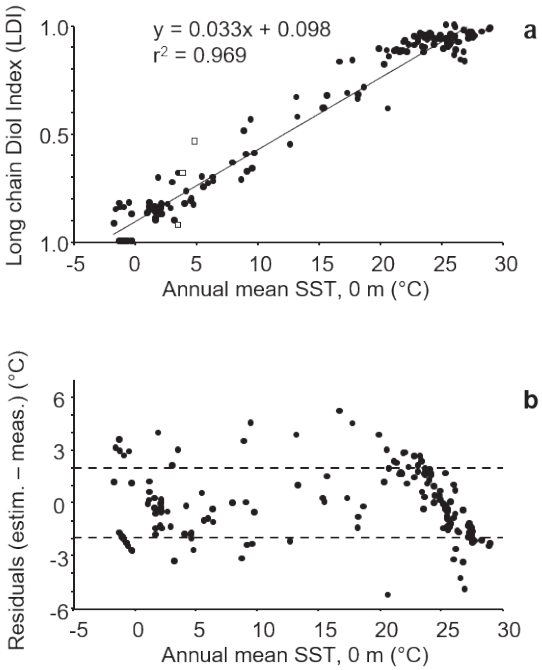

Fig. 3: a) LDI core-top calibration, correlation of LDI values of marine surface sediments with annual mean sea surface temperatures. b) Correlation of annual mean sea surface temperatures versus residual temperature errors. (Rampen et al., 2012).

1.4. Sequestration and diagenesis of long-chain diols

Although the above described LCD indices have shown some promise in paleo-reconstructions, many uncertainties remain. Marine organic proxies are impacted by a large number of physical and chemical changes from the time the proxy signal is generated by the producer. These changes may take place during their transport and settling through the water column and their subsequent burial in the sediment. These diagenetic changes can lead to changes in the composition and distribution of the organic proxies, e.g. by selective degradation of one compound over the other. Here, two important diagenetic processes, i.e. oxic degradation and matrix sequestration, are discussed.

1.4.1 Oxic and anoxic degradation

A large number of studies have analyzed the role of oxygen in the preservation of marine organic matter, in particular oxygen exposure time (Hedges et al., 1999) as well the structure and packaging of sediments (Sun and Wakeham, 1994; Canuel and Martens, 1996). A large variability in degradation rates of lipids have been shown and different lipid biomarker classes may behave significantly different with increasing levels of oxygen exposure (Hoefs et al., 2002; Sinninghe Damsté et al., 2002a). While these degradation processes have been studied in laboratory experiments by oxidation of biomass of microbes producing biomarker lipids (Harvey and Macko, 1997a, 1997b; Teece et al., 1998; Grossi et al., 2001), a number of studies have analyzed the impact of oxic degradation in natural settings. Commonly, the latter is done by comparing the abundance and distribution of lipid biomarkers in anoxic and oxic marine and lacustrine environments, i.e. in the water column and suspended particulate matter (Kim et al., 2009a; Rontani et al., 2009; Schouten et al., 2012), at the interface of water column and surface sediments (Canuel and Martens, 1996; Sun and Wakeham, 1998; Lengger et al., 2014) or in sediment cores (Cranwell, 1981; Sun and Wakeham, 1994; Hartnett et al., 1998; Hoefs et al., 1998a, 1998b, 2002; Gong and Hollander, 1999; Prahl et al., 2003; Huguet et al., 2009; Bogus et al., 2012; Lengger et al., 2012, 2013). Several locations and regions have been studied extensively due to their unique setting and formation history. For example, Mediterranean sapropels have been studied to assess post-depositional oxidation resulting from oxidation of organic matter by downward moving oxygen fronts induced by the change of redox state of the bottom water (i.e. from anoxic during sapropel deposition to oxic after sapropel deposition) (Ferreira et al., 2001; Menzel et al., 2003). Post-depositional oxidation has furthermore also been studied in organic matter-rich turbidites of the Madeira Abyssal Plain, which are influenced by downward diffusing oxygen from oxygen rich abyssal waters (Hoefs et al., 1998a, 1998b, 2002; Huguet et al., 2009; Lengger et al., 2013). Sediments were initially deposited under low oxygen conditions on the shelf and subsequently transported as turbidites and deposited in oxygen-rich bottom waters of the Madeira Abyssal Plain, allowing oxygen to diffuse into the turbidite.

Up to now, only a few studies investigated the impact of oxic and anoxic degradation on LCD abundance and distribution. Sun and Wakeham (1994) reported LCDs to be highly resistant to anoxic degradation and showed an almost 100% burial rate in Black Sea sediments. Relatively high preservation efficiencies of LCDs upon oxygen exposure compared to other biomarkers were shown in sediment cores from the Arabian Sea by Sinninghe Damsté et al. (2002), while Hoefs et al. (2002) showed a higher preservation of bound LCDs in comparison to freely extractable LCDs in turbidites of the Madeira Abyssal Plain. Furthermore, the impact of post-depositional oxidation on LCDs in S1 sapropel sediments of the Mediterranean Sea was studied and a diagenetic link between keto-ols and LCDs suggested, based on the idea that keto-ols are likely intermediate products formed by post-depositional oxidation of LCDs (Ferreira et al., 2001). To study the impact of post-depositional oxidation and paleo-oxicity, the Diol Oxidation Index (DOXI) was thus proposed by Ferreira et al. (2001) and is calculated as follows:

$$DOXI = [keto\text{-}ol]/ \{[keto\text{-}ol] + [diol]\} \quad [5]$$

Grossi et al. (2001) incubated *Nannochloropsis salina* anaerobically for 442 days, showing small increases in LCD concentration over shorter timescales, believed to be related to a release of LCDs from the algaenan, and suggesting only low degradation rates for LCDs under anaerobic conditions.

LCDs seems thus to be relatively well preserved when impacted by oxic and anoxic degradation, however the impact of these processes on LCD indices remains unclear.

1.4.2. Matrix sequestration and mode of occurrence of LCDs

Several organic biomarkers are known to not only occur as freely extractable compounds but also bound to the sedimentary matrix by e.g. ester, glycosidic, amide or ether bonds (Goossens et al., 1986, 1989b; Gelin et al., 1997b).

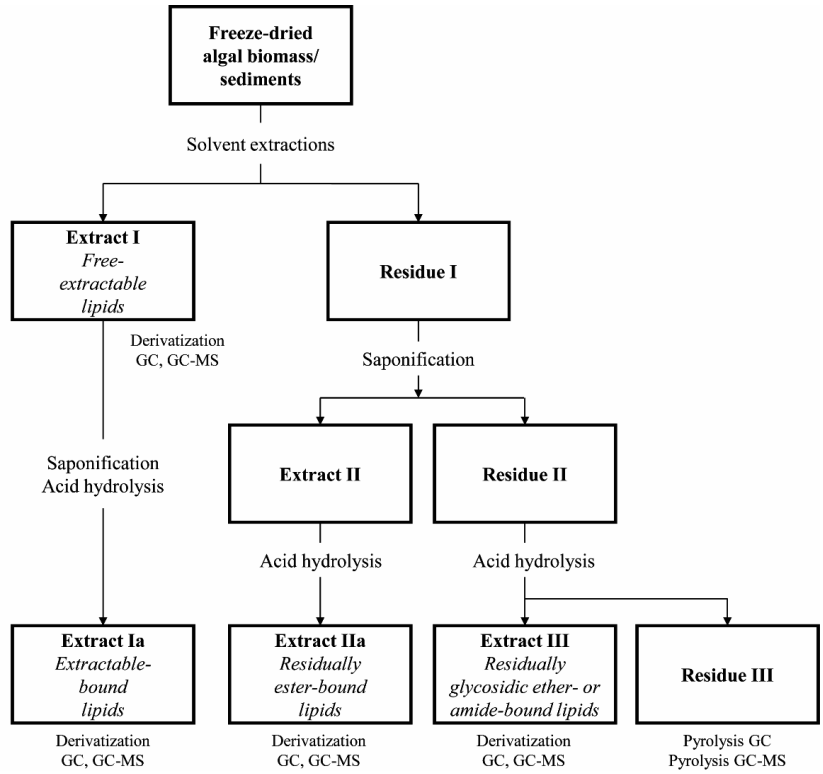

Fig. 4: Analytical scheme for analysis of mode of occurrence in algal biomass and sediments. Modified from Goossens et al. (1989b) and Gelin et al. (1997a).

These compounds are released from the sedimentary matrix by saponification and acid hydrolysis of the residue left after extraction (Fig. 4) and sometimes yield different distributions and abundances than freely occurring biomarker. If these residually-bound biomarkers are released during diagenesis, they may represent a potential bias in the application of the relevant proxies (Schouten et al., 2004; Pancost et al., 2008).

While LCDs have so far been mostly analyzed as freely extractable compounds in sediments, several studies have shown that they do occur bound to sedimentary organic matter by ester or glycosidic-ether bonds and can be released by chemical methods, i.e. saponification and acid hydrolysis. Residually ester-bound C_{30}- and C_{32} 1,15-diols and keto-ols were identified in sediments from the Monterrey Formation (Ahmed et al., 2000), while LCDs ether-linked to long-chain compounds and small amounts of ester-bound LCDs accounted for 0 – 30% of total LCDs in Lake Baikal sediments (Shimokawara et al., 2010). Additionally, Shimokawara et al. (2010) showed that the C_{32} 1,15-diol was the most abundant freely occurring LCD, while, in

contrast, the C_{30} 1,13-diol was the most abundant ester- and ether-bound LCD. However, it is unclear how much of the LCDs are occurring bound to the sedimentary matrix and whether they impact the application of LCD proxies.

1.5. Objectives and outline of the thesis

As outlined above, LCDs occur ubiquitously in a variety of environments and proxies based on these compounds show great promise when applied to reconstruct environmental conditions. However, it is apparent that uncertainties remain, which may impact our understanding of LCDs and LCD proxies. While LCDs are increasingly used in paleo-reconstructive studies, few studies as of yet have analyzed how LCDs and related proxies are impacted by diagenesis and sequestration. Therefore, this thesis aims to evaluate the impact of diagenesis, especially of oxic degradation and mode of occurrence, on LCDs and LCD proxies. To this end, LCDs were studied in aerobically degraded biomass of *Nannochloropsis oculata* in order to constrain the impact of oxic degradation on the distribution and abundance of LCDs, the LDI and the algaenan. Furthermore, the identification of possible macromolecular sources of LCDs was attempted. Finally, the impact of mode of occurrence of differently bound LCDs and the impact of post-depositional oxidation were studied in sediments from a sapropel from the Eastern Mediterranean and from a turbidite from the Madeira Abyssal Plain, respectively.

Chapter 2 presents a large-scale aerobic incubation of *Nannochloropsis oculata* biomass over 271 days in an effort to constrain the impact of oxygen exposure on LCDs and the LDI. For this, the concentrations of free-extractable, extractable-bound, residually ester-bound and residually-bound glycosidic ether- or amide-bound fatty acids and LCDs were determined. A significant impact of oxygen exposure was determined for saturated and polyunsaturated fatty acids, showing substantially decreasing concentrations over oxic incubation time, irrespective of their mode of binding. In contrast, LCDs showed a large-scale increase in concentration from incubation day 125 until the end of incubation at day 271, in particular for residually ester-bound LCDs which showed a 30-fold increase in concentration. This increase in concentration upon oxygen exposure is thought to reflect a release of LCDs from the highly aliphatic, non-hydrolysable biopolymer algaenan. LDI values remained stable throughout the degradation experiment, irrespective of the large increases in LCDs, albeit showing differences in values dependent on how the LCDs were bound to the biomass. Therefore, the impact of oxygen exposure on the LDI is likely negligible.

Chapter 3 represents a follow up on chapter 2, studying the impact of oxic degradation on the algaenan of *Nannochloropsis oculata*. Residues left after extraction and saponification and hydrolysis of aerobically degraded biomass (chapter 2) were analyzed by step-wise pyrolysis. The pyrolyzate of the algaenan was characterized by a series of *n*-alkenes/ *n*-alkanes with chain lengths of C_{10} to C_{33} and two maxima at C_{15} to C_{17} and C_{26} to C_{28}. Mid-chain ketones were present with chain lengths of C_{28} to C_{34} with a maximum at C_{31} and a mid-chain keto group at position 14. Additionally, a pronounced C_{19} *n*-alkan-2-one could be shown. These results point to an algaenan built-up of C_{32} 1,15-diol units, linked by ether bonds, which is in agreement with previously published studies. Analysis of residues at different time points throughout oxic degradation suggested that there were no large alterations of the algaenan structure, indicating that oxygen exposure has a no substantial impact on the structure of the algaenan.

In **Chapter 4** we attempted to identify macro-molecular sources of LCDs in *Nannochloropsis sp.* biomass since LCDs in algal biomass have been reported to mainly be released after hydrolysis of the extract and are thought to be a constituent of the biopolymer algaenan. However, application of ultra-high pressure liquid chromatography combined with high resolution mass spectrometry (UHPLC/HRMS) and semi-preparative HPLC did not lead to the

identification of potential macromolecular precursor lipids. Additionally, only freely extractable and not extractable-bound lipids, as commonly reported, could be identified. We subsequently analyzed 3 different strains of *Nannochloropsis spp.* and could show that LCDs mainly occur as freely extractable lipids and minor increases in concentration were only detected after application of acid hydrolysis on the biomass extracts. These results therefore call into question the idea that LCDs occur mainly as extractable-bound lipids.

In **Chapter 5** we analyzed the impact of the mode of occurrence on LCDs and keto-ols in sediments. For this, we analyzed LCDs and keto-ols in sediments of an S5 sapropel of the Eastern Mediterranean by Bligh Dyer extraction followed by base and acid hydrolysis of the extract and the residual sediment, to release additional lipids from the sedimentary matrix. Extractable-bound 1,14-diols showed a 1.5-fold increase in abundance, when compared to freely extractable LCDs, indicating some LCDs are bound to the organic sedimentary matrix. While freely extractable LCDs dominate in the sapropel, LCDs occur as residually ester-bound and residually glycosidic ether- or amide-bound lipids outside of the sapropel. LCD indices showed similar trends irrespective of the mode of occurrence of the LCDs. Keto-ols were only detected in the sapropel and not below or above it, however their relative abundance, quantified by the DOXI index, did not show significant changes in trends.

In **Chapter 6** the impact of post-depositional oxidation on LCDs and keto-ols was studied in the f-turbidite of the Madeira Abyssal Plain. Comparison of lipids in the upper oxidized part of the turbidite, impacted by post-depositional oxidation, with the anoxic lower part of the turbidite, shows a higher preservation of the C_{30} 1,15-diol and C_{30} 1,15-keto-ol compared to the other LCDs and keto-ols. While the LDI showed increased values, the Diol Index and FC_{32} 1,15-diol, a proxy for the riverine input into marine environments, showed decreased values with increasing oxygen exposure. Therefore, all three indices were impacted by post-depositional oxidation, likely resulting from a preferential preservation of the C_{30} 1,15- and C_{32} 1,15-diol over 1,13- and 1,14-diols. When compared to GDGTs and GDGT proxies, measured for the same turbidite, LCDs and keto-ols seem to be better preserved upon post-depositional oxidation. Additionally, while the BIT index showed increasing values with increasing oxygen exposure time, an impact of the TEX_{86} index by post-depositional oxidation was negligible. Therefore, changes in oxygen exposure time in sediments may cause different changes in organic terrestrial and temperature proxies and care has to be taken when applying these different indices in severely oxidized sediments.

To summarize, the work described in this thesis showed that LCDs and LCD proxies are variably impacted by diagenesis and sequestration. An impact of oxic degradation was shown for incubated algal biomass, resulting in a significant release of LCDs. The source of these LCDs however, remains unclear, since the structure of the algaenan was not impacted during incubation time. However, while a significant increase in LCD concentration occurred in algal biomass when impacted by oxic degradation, the LDI was not affected by this. Intriguingly, LCDs mainly occur as freely extractable lipids, in contrast to previous studies. In sediments, LCDs are bound in different ways to the sedimentary organic matrix and are not only available as freely extractable lipids, as commonly assumed in different paleo-environmental studies. While this mode of occurrence did not really impact the application of LCD proxies, it was shown that applying LCD indices in severely oxidized sediments may lead to a preferential preservation of certain LCDs.

The results of this thesis represent a first step towards constraining the impact of diagenesis and sequestration on LCDs and LCD proxies. Further research should aim at resolving the contrasting observation on the impact of oxic degradation on the LDI as well as the role of the biopolymer algaenan as a factor impacting the distribution and abundance of 1,13- and 1,15-LCDs in marine sediments.

Chapter 2

The impact of oxygen exposure on long-chain alkyl diols and the long chain diol index (LDI) – a long-term incubation study

Sophie Reiche[1], Sebastiaan W. Rampen[1], Denise J.C. Dorhout[1], Jaap S. Sinninghe Damsté[1,2], Stefan Schouten[1,2]

[1]NIOZ Royal Netherlands Institute for Sea Research, Department of Marine Microbiology and Biogeochemistry, and Utrecht University, PO Box 59, 1790 AB Den Burg, The Netherlands.

[2]Utrecht University, Department of Earth Sciences, Faculty of Geosciences, P.O. Box 80.021, 3508 TA Utrecht, The Netherlands.

Organic Geochemistry 124, 238-246 (2018)

https://doi.org/10.1016/j.orggeochem.2018.08.003

Abstract

In recent years, long chain alkyl diols (LCDs) have been increasingly used to study and reconstruct past sea surface temperatures using the long chain diol index (LDI), which is based on changes in the distribution of 1,15-LCDs. However, the impact of diagenesis on LCDs and the LDI is still poorly constrained. Here we studied the impact of oxygen exposure on LCDs and the LDI, by aerobically incubating biomass of the LCD-producing alga *Nannochloropsis oculata* for 271 days. The concentrations of extractable free- and bound, residually ester-bound and residually-bound glycosidic ether- or amide-bound saturated fatty acids and LCDs were determined. A significant impact of oxygen exposure was observed for C_{14}, C_{16} and C_{18} saturated fatty acids and the $C_{20:5}$ polyunsaturated fatty acid as their concentration decreased significantly over time, irrespective of their mode of binding. LCDs, in contrast, increased significantly in concentration over incubation time, e.g. up to a 30-fold increase in concentrations for residually ester-bound LCDs at day 125 compared to concentrations at the beginning of the experiment. This increase in concentration most likely represents a release of LCDs from the insoluble biopolymer algaenan due to the impact of oxygen exposure. Values of the LDI differed strongly depending on the mode of occurrence of LCDs in the biomass. However, despite the large changes in concentration of LCDs in response to oxygen exposure, the LDI remained relatively stable after prolonged degradation. This suggests that oxygen exposure may not have a substantial impact on the LDI of extractable LCDs used for its determination.

Keywords: long chain diols; long chain diol index; aerobic degradation; *Nannochloropsis oculata*; algaenan

1. Introduction

Long chain alkyl diols (LCDs) were first discovered in sediments of the Black Sea (de Leeuw et al., 1981) and since then have been studied in a large variety of marine and freshwater environments (Versteegh et al., 1997; Sinninghe Damsté et al., 2003; Rampen et al., 2007, 2008, 2014a, 2014b; Zhang et al., 2011; Romero-Viana et al., 2012; de Bar et al., 2016; Lattaud et al., 2017a). They are composed of long n-alkyl chains with chain lengths of mainly C_{28} to C_{32} and contain alcohol groups at C_1 and at a mid-chain position, most notably between positions C_{12} to C_{15} (Versteegh et al., 1997). Saturated and unsaturated C_{28} and C_{30} 1,14-LCDs have been shown to be produced by *Proboscia* diatoms (Sinninghe Damsté et al., 2003; Rampen et al., 2007) and C_{28}-C_{32} 1,14-LCDs have also been identified in *Apedinella radians* (Rampen et al., 2011). C_{28} to C_{32} 1,13- and 1,15-LCDs have been identified in cultures of freshwater and marine Eustigmatophyte algae (Volkman et al., 1992; Gelin et al., 1997b, 1999; Méjanelle et al., 2003; Shimokawara et al., 2010; Rampen et al., 2014a; Balzano et al., 2017; Zhang and Volkman, 2017), but the diol distributions in marine environments are dissimilar to those of cultured algae (Volkman et al., 1992; Versteegh et al., 1997; Rampen et al., 2012, 2014a), suggesting unknown marine sources. LCDs in algal cell material of Eustigmatophytes and in the sediment have been shown to occur in different forms, i.e. as free-extractable, extractable-bound (released by hydrolysis of the extract) and residually-bound lipids (released by hydrolysis of the residual biomass left after extraction) (Gelin et al., 1997b; Ahmed et al., 2000; Grossi et al., 2001; Hoefs et al., 2002; Shimokawara et al., 2010). Additionally, they are also thought to be the building blocks of the insoluble biopolymer algaenan which occurs in the cell wall of Eustigmatophytes (de Leeuw et al., 1981; Tegelaar et al., 1989a; Gelin et al., 1997b; Volkman et al., 1998; Scholz et al., 2014; Zhang and Volkman, 2017).

Several indices based on LCD distributions have been proposed to reconstruct past conditions such as upwelling, oxic degradation, riverine input as well as sea surface temperatures (SST).

The long chain diol index (LDI) is based on the fractional abundances of C_{28} 1,13-, C_{30} 1,13- and C_{30} 1,15-LCDs and correlates strongly with SST (Rampen et al., 2012). Upwelling indices use the relative abundances of C_{28} and C_{30} 1,14- to C_{28}/C_{30} 1,13- or C_{30} 1,15-LCDs (Rampen et al., 2008; Willmott et al., 2010). The diol oxidation index (DOXI), calculated as the ratio of 1,15-keto-ols versus LCDs, is used to study oxic degradation in sediments thereby assuming that keto-ols are oxidative products of LCDs (Ferreira et al., 2001). Finally, the %C32 1,15 of all LCDs (de Bar et al., 2016; Lattaud et al., 2017a, 2017b) is used to study riverine inputs into the marine environment.

These indices have since shown promise in paleo-environmental reconstruction studies and have been applied in different marine environments (Pancost et al., 2009; Willmott et al., 2010; Rampen et al., 2012, 2014b; Seki et al., 2012; Lopes dos Santos et al., 2013; Rodrigo-Gámiz et al., 2014, 2015, 2016; Nieto-Moreno et al., 2015; Plancq et al., 2015).

Certain uncertainties in the application of LCD indices still remain to be addressed. Only a few studies have considered the impact of diagenesis on the abundance and distribution of LCDs (Ferreira et al., 2001; Versteegh et al., 2010; Bogus et al., 2012). As shown by various studies, biomarker distributions can be altered substantially by oxygen exposure (Sun and Wakeham, 1994; Hoefs et al., 1998b; Prahl et al., 2003; Rontani et al., 2009, 2013), but only Sinninghe Damsté et al. (2002), Hoefs et al. (2002) and Rodrigo-Gámiz et al. (2016) analyzed the impact of oxic degradation on LCD distributions. Sinninghe Damsté et al. (2002) analyzed sediment cores from the northern Arabian Sea studying the impact of oxygen exposure time on the preservation potential of various biomarkers, finding relatively high preservation efficiencies of LCDs. Hoefs et al. (2002) studied free and bound lipid biomarkers in oxidized and un-oxidized parts of Madeira Abyssal Plain turbidites, finding higher preservation of bound LCDs compared to free LCDs. Analysis of Arabian Sea surface sediments deposited under contrasting redox conditions by Rodrigo-Gámiz et al. (2016) showed a strong decrease in concentration of LCDs with increasing oxygen exposure as well as a slightly higher degradation rate of 1,15-LCDs compared to 1,14- and 1,13-LCDs. This resulted in a drop of the LDI from 0.94 to 0.85 with increasing water depth. Additionally, the DOXI ratios showed no distinctive trends over water depth and only slight increases in value with increasing oxygen concentration were observed. The impact of anoxic degradation on LCDs has been constraint by a few studies, most notably by Sun and Wakeham (1994) and Grossi et al. (2001). Sun and Wakeham (1994) reported a high level of resistance to anoxic degradation during early diagenesis and an almost 100% burial efficiency of LCDs in Black Sea sediments. Grossi et al. (2001) incubated *Nannochloropsis salina* anaerobically over 442 days, revealing short-term increases (degradation days 50 to 100) in LCD concentrations, which were proposed to be caused by a release of LCDs from the algaenan. Following this, concentrations of LCDs decreased over time, albeit to a lesser extent than other associated compounds, such as alkenes, phytol, sterols and fatty acids. Both studies thus show relatively low degradation rates for LCDs under anoxic conditions.

Here we present a laboratory study analyzing the impact of oxygen exposure on LCD concentrations and distributions in *Nannochloropsis oculata* biomass, which was aerobically incubated for 271 days. The concentrations of free and bound LCDs and major other lipids were monitored over degradation time. Furthermore, the impact of oxic degradation on the LDI was constrained.

2. Material and methods

2.1. Set up of aerobic biomass incubations

A large batch of the LCD-producing alga *Nannochloropsis oculata*, strain CCMP525, was ordered from Reed Mariculture Inc and kept frozen at 20 °C until the set-up of incubation. 20 g of defrosted biomass were transferred to Erlenmeyer flasks each containing 10 g of sediment and 210 ml of sea water, both collected from the Dutch Wadden Sea in March 2015 and acclimatized after collecting for 24h at 25°C. 42 Erlenmeyer flasks were prepared and placed into a shaker table in the dark, at 25 °C and stirred at 100 rpm for 271 days under aerobic conditions. Sea water levels were monitored weekly and bi-distilled water was added when required to keep the water volume constant and to counteract evaporation effects.

2.2. Lipid analysis

At predetermined sampling days, three Erlenmeyer flasks were randomly selected. For each flask, the water layer was separated from the particulate matter by centrifugation at 3000 rpm for 120 min. The particulate matter was subsequently freeze dried and processed using the analytical scheme outlined in Fig. 1.

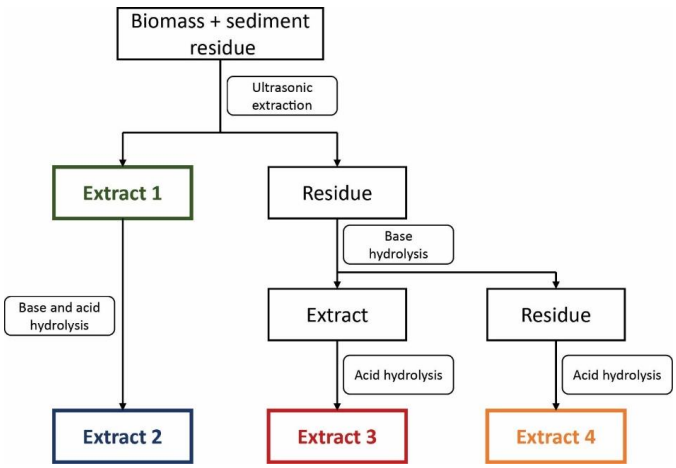

Fig.1: Analytical scheme representing the work up steps of *Nannochloropsis oculata* biomass + sediment, as described in 2.2.

The particulate matter was ultrasonically extracted with methanol/dichloromethane (MeOH/DCM) (2:1, v/v, 4x). DCM phases were combined and dried using rotary evaporation and drying under N_2. The extract resulting from this work-up step was labelled Extract 1 (E1).

An aliquot of E1 was subsequently saponified by refluxing with 1 M KOH in MeOH for 1 h. The DCM phase was separated from the H_2O/MeOH phase and dried under N_2. This fraction was subsequently acid hydrolyzed in a last step by refluxing with 1.5 M HCl in MeOH for 3 h. After cooling, the mixture was neutralized using 2 N KOH in MeOH and extracted with DCM/H_2O (1:1, v/v, 3x). The DCM phases were separated from the H_2O/MeOH phase and

combined to be dried under N_2. The base and acid hydrolyzed E1 extract is termed Extract 2 (E2).

The residue obtained after ultrasonic extraction of the particulate phase of the incubation experiment was dried under N_2 and saponified by refluxing with 1 M KOH in MeOH for 1 h. The mixture was centrifuged and the liquid phase was collected into a separatory funnel and acidified to a pH of 3 using 2 N HCl in MeOH. The residue was subsequently extracted using H_2O/MeOH (1:1, v/v), MeOH (2x) and DCM (3x) and all solvents were combined into the separatory funnel. The DCM layer was separated from the MeOH/H_2O layer and collected, the MeOH/H_2O layer was extracted with DCM (3x) and the combined DCM phases were dried under N_2. This extract was subsequently acid hydrolyzed using the conditions described above and yielded Extract 3 (E3). In a last step, the saponified residues were acid hydrolyzed by refluxing with 1.5 M HCl in MeOH for 3 h. Solvents were collected into a separatory funnel after cooling and neutralized using 2 N KOH in MeOH. Residues were subsequently extracted using H_2O/MeOH (1:1, v/v), MeOH (2x) and DCM (3x) and solvents were collected into the separatory funnel. The DCM layer was separated from the MeOH/H_2O layer and collected, the MeOH/H_2O layer was extracted with DCM (3x) and the combined DCM phases were dried under N_2. The extracted residue after base hydrolysis was subsequently also acid hydrolyzed following the procedures described above yielding Extract 4 (E4).

E1-E4 were eluted with DCM over a small pasteur pipette containing Na_2SO_4 to remove remaining salts. An internal standard C_{22} 7,16 - diol (MolPort SIA, Latvia) was added to aliquots of E1-E4 which were subsequently methylated with diazomethane in diethylether. Very polar components were removed by eluting the methylated E1-E4 with ethyl acetate over a small pasteur pipette containing silica gel.

Prior to analysis by gas chromatography (GC) and gas chromatography/ mass spectrometry (GC/MS), E1-E4 were silylated by adding BSTFA [N,O-bis(trimethyl-silyl)trifluoroacetamine] and pyridine and heated up to 60 °C for 20 min. Subsequently, samples were dissolved in ethyl acetate.

2.3. GC-MS analysis of LCDs

Samples were analyzed for LCDs on an Agilent 7890B gas chromatograph coupled to an Agilent 5977A mass spectrometer, equipped with a fused silica capillary column (25 m x 0.32 mm) coated with CP Sil-5 (film thickness 0.12 µm). Samples were injected at 70 °C oven temperature, increasing to 130 °C at 20 °C/min and then 320 °C at 4°/min which was held for 25 min with a helium flow of 2 mL/min. The mass spectrometer operated with an ionization energy of 70 eV. LCDs were quantified in selective ion monitoring (SIM) of m/z 187, 313, 339 and 341 characteristic for the different LCDs (Versteegh et al., 1997; Rodrigo-Gámiz et al., 2015). Additional compounds, e.g. fatty acids, polyunsaturated fatty acids, phytol and sterols, were identified on the same GCMS in full scan (m/z 50-800) and analyzed on an Agilent 7890B gas chromatograph with helium as the carrier gas at a flow of 2 ml per minute using the same temperature program as that of the GCMS. Fatty acids were identified by comparison with published mass spectra and quantified by integration of respective peak areas of fatty acids and the internal standard. The calculated concentrations given in this paper were normalized on dry weight of the biomass, in mg/g or µg/g.

The LDI was calculated as follows (Rampen et al., 2012):

$$\text{Long chain Diol Index (LDI)} = \frac{F_{C_{30}1,15-\text{diol}}}{F_{C_{28}1,13-\text{diol}} + F_{C_{30}1,13-\text{diol}} + F_{C_{30}1,15-\text{diol}}} \quad [1]$$

3. Results

Biomass of the LCD-producing alga *Nannochloropsis oculata* was incubated in the presence of sediment and water from the North Sea under aerobic conditions for a period of 271 days. Four extracts (E1-E4), each representing lipids occuring in the biomass in a different way, were obtained (Fig. 1) following the work-up procedures of e.g. Gelin et al. (1997) or Goossens et al. (1986). E1 contains freely occurring and –extractable lipids, while E2 contains free-extractable lipids from E1 as well as extractable lipids which are ester-bound or bound by glycosidic ether- or amide bonds. E3 represents residually ester-bound lipids while E4 contains residually-bound glycosidic ether- or amide-bound lipids (Goossens et al., 1986, 1989a). LCDs were detected in all fractions. Both E1 and E2 contained saturated and polyunsaturated fatty acids, phytol and sterols, predominantly cholesterol and minor amounts of $C_{29}\Delta^{5,24}$ sterols. E3 contained saturated and polyunsaturated fatty acids, α-hydroxy and β-hydroxy fatty acids with chain lengths of C_{24} to C_{26} and C_{12} to C_{18}, respectively, and to a lesser extent sterols, predominantly cholesterol. E4, was mostly comprised of α- and β-hydroxy fatty acids with chain lengths of C_{24} to C_{26} and C_{12} to C_{18}, respectively, and to a lesser extent, of saturated fatty acids. Long chain keto-ols were not detected and mid-chain hydroxy methyl alkanoates were only present in trace amounts. This lipid composition is in good agreement with previous studies of the lipids of *Nannochloropsis* species (Volkman et al., 1992, 1993; Olofsson et al., 2012; Mitra et al., 2015; Balzano et al., 2017; Zhang and Volkman, 2017). Analysis of the sediment and sea water from the Dutch Wadden Sea used, did not show the presence of LCDs. Saturated fatty acids and the $C_{20:5}$ PUFA were present in low abundances in the Wadden Sea sediment and water and are ignored here. Additionally, the pure biomass of strain CCMP525 was analyzed to confirm that the reported LCDs in this study were solely derived from this alga.

In this study, we will mainly focus on LCDs, as well as the dominant saturated fatty acids and the $C_{20:5}$ polyunsaturated fatty acid (PUFA), to contrast their different responses to oxygen exposure.

3.1 Fatty acids

C_{14}, C_{16} and C_{18} saturated fatty acids were identified in E1-E4. The concentrations of summed saturated fatty acids ($C_{14} + C_{16} + C_{18}$) were highest in E1 and E3 with 7.9 ± 1.4 and 10.1 ± 1.6 mg/g respectively (Fig. 2A). The concentration of free-extractable saturated fatty acids (E1) decreased by 98% during the first 35 days of incubation and stayed low at 0.2 ± 0.1 mg/g throughout the remainder of the experiment. Free- and extractable-bound (E2) saturated fatty acids initially increased during the first 3 days of incubation up to 30.7 ± 8.3 mg/g and subsequently showed a continuous slow decrease until reaching a plateau of 6.1 ± 0.7 mg/g at 169 incubation days for the remainder of the experiment. The concentration of residually ester-bound (E3) saturated fatty acids decreased slowly, reaching concentrations of 2.9 ± 0.1 mg/g by the end of the experiment. Residually-bound glycosidic ether- or amide-bound (E4) fatty acids stayed low in concentration at 0.3 ± 0.1 mg/g throughout the experiment.

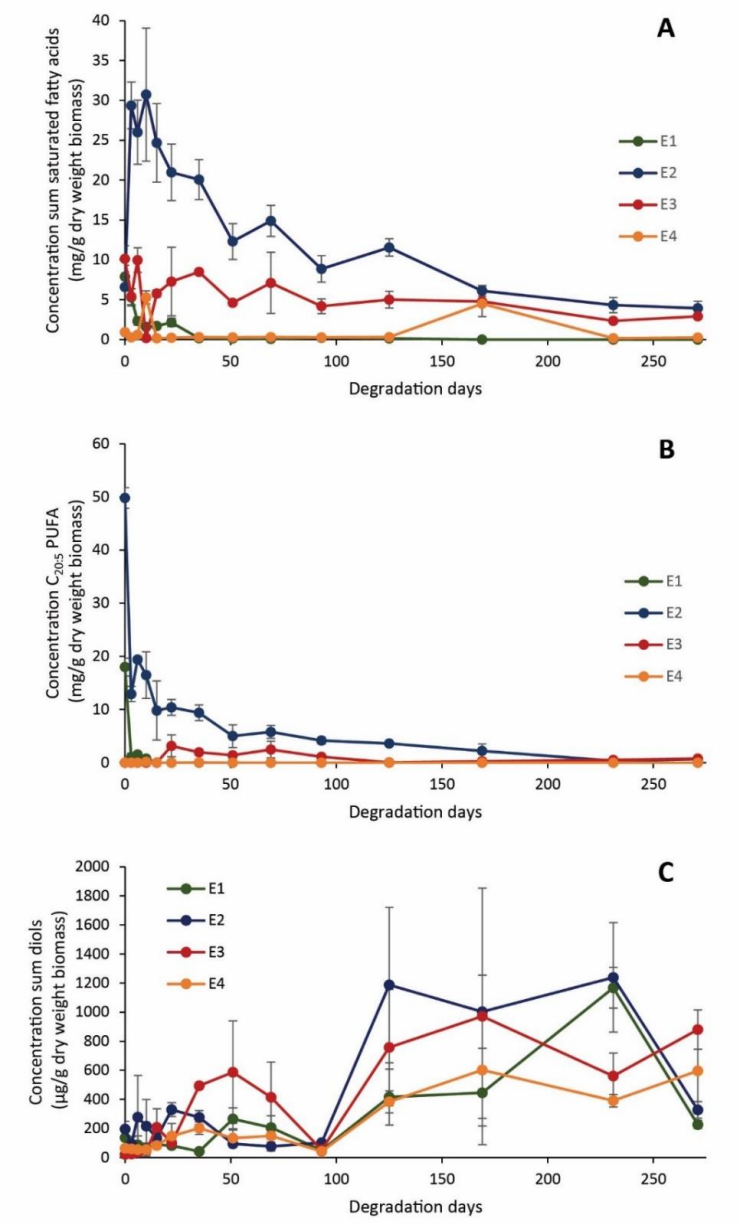

Fig. 2: Concentrations of lipids over time in an incubation experiment where biomass of the Eustigmatophyte alga *Nannochloropsis oculata* is exposed to oxygen in the presence of sediment and sea water: A) concentration of the sum of saturated fatty acids, B) concentration of $C_{20:5}$ PUFA, C) concentration of the sum of LCDs. Concentrations are given over degradation time for free-extractable (E1), free- and extractable-bound (E2), residually ester-bound (E3) and residually-bound glycosidic ether- or amide-bound compounds (E4). Error bars represent standard deviations calculated from triplicate incubations.

The $C_{20:5}$ PUFA is also a prominent lipid in addition to saturated fatty acids in *N. oculata* biomass. In this incubation study it occurred in the free-extractable (E1) and free- and extractable-bound (E2) extracts, but was not identified in E3 and E4 (Fig. 2B). Its concentration in the free-extractable (E1) form decreased rapidly during the first 15 days of incubation from initial values of 18.0 ± 1.7 mg/g to below detection limits. The concentration of free- and extractable-bound (E2) $C_{20:5}$ PUFA decreased rapidly from 49.8 ± 2.0 mg/g to 12.9 ± 1.4 mg/g during the first 3 days and stayed approximately constant until 35 days. Subsequently, values slowly decreased until the end of incubation time to concentrations of 0.7 ± 0.1 mg/g. The residually ester-bound $C_{20:5}$ PUFA was first detected at day 22 of incubation at 3.2 ± 2.1 mg/g, but subsequently decreased and was not detected from 125 days onwards.

3.2 Long chain alkyl diols

Four major LCDs were identified in this incubation study at the beginning of incubation, i.e. the C_{28} 1,13-, C_{30} 1,13-, C_{30} 1,15- and C_{32} 1,15-LCD. The C_{28} 1,13-LCD (Fig. 3A) showed concentrations of 0.7 ± 0.1 µg/g (E1), 1.1 ± 0.2 µg/g (E2), 0.4 ± 0.2 µg/g (E3) and 0.3 ± 0.0 µg/g (E4) and was the least abundant of the four major LCDs. The concentration of the C_{30} 1,13-LCD (Fig. 3B) was 7.5 ± 4.7 µg/g (E1), 19.7 ± 4.7 µg/g (E2), 2.9 ± 1.6 µg/g (E3) and 4.4 ± 1.7 µg/g (E4), while the C_{30} 1,15-LCD (Fig. 3C) showed concentrations of 5.2 ± 2.3 µg/g (E1), 11.0 ± 2.9 µg/g (E2), 1.4 ± 0.7 µg/g (E3) and 4.2 ± 1.3 µg/g (E4). The C_{32} 1,15-LCD (Fig. 3D) was the most dominant LCD with 124 ± 61 µg/g (E1), 163 ± 47 µg/g (E2), 17.4 ± 8.7 µg/g (E3) and 55.0 ± 26.7 µg/g (E4). Additionally, a low abundance of the $C_{32:1}$ 1,15-LCD was detected.

The concentration trends of LCDs over time developed in two phases and individual LCDs show similar concentration patterns. In the first phase, spanning the first 93 incubation days, summed LCD concentrations increased and then decreased to a minimum at 93 degradation days (Fig. 2C). Free-extractable (E1) and free- and extractable-bound (E2) LCDs decreased in concentration during the first 3 days of incubation by 42% and 52% and subsequently increased to reach maximum concentration at days 51 with 270 ± 80 µg/g for free-extractable (E1) LCDs and maximum concentration at day 22 with 330 ± 50 µg/g for free- and extractable-bound (E2) LCDs. Residually ester-bound (E3) LCDs showed the highest maximum concentrations in this first phase at day 51 with 590 ± 350 µg/g, while residually-bound glycosidic ether- or amide-bound (E4) LCDs stayed overall lower and showed highest concentration at day 35 with 200 ± 40 µg/g.

In the second phase, summed LCD concentrations reached even higher concentrations. At day 125, concentrations were substantially higher compared to initial values at day 0 of incubation time: double in concentration to 420 ± 190 µg/g in the E1 fraction, a five-fold increase to 1190 ± 540 µg/g in fraction E2, a thirty-fold increase to 760 ± 400 µg/g in fraction E3 and a five-fold increase to 380 ± 80 µg/g in fraction E4. After this maximum, concentrations stayed approximately constant until the end of the experiment for residually ester-bound (E3) and glycosidic ether- or amide-bound (E4) LCDs, while both free-extractable (E1) and free- and extractable-bound (E2) LCDs decreased sharply at the end of the experiment to concentrations of 230 ± 30 and 330 ± 60 µg/g respectively.

In two instances, at incubation days 51 and 69, the concentrations of LCDs in E2 were below concentrations of E1, which is unexpected as hydrolysis should potentially result in additional release of LCDs. However, in most cases the majority of LCDs are present as free-extractable LCDs and the amount released by base and acid hydrolysis is relatively low. Possibly the lower amount of LCDs after the hydrolysis steps are due to work up losses during consecutive hydrolyses or artifact formation (unpublished data).

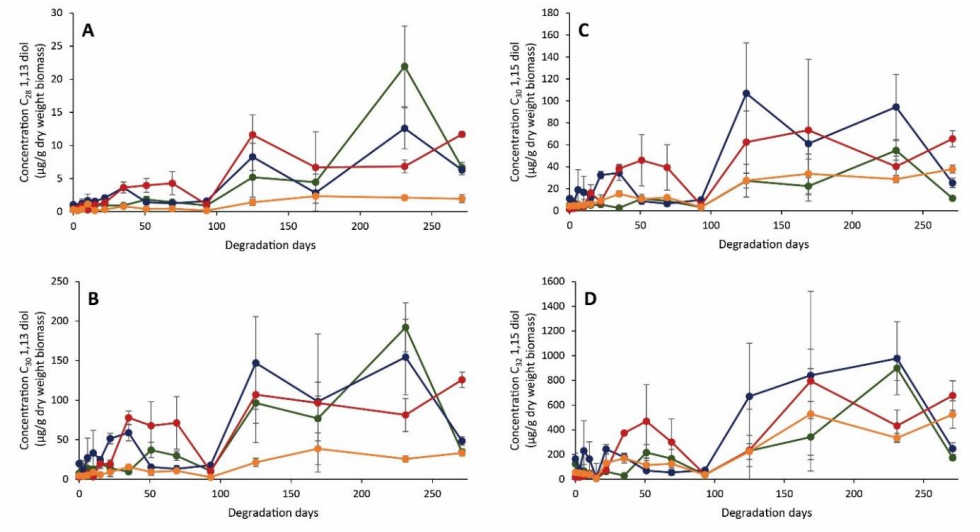

Fig. 3: Concentrations of LCDs over time in an incubation experiment where biomass of the Eustigmatophyte alga *Nannochloropsis oculata* is exposed to oxygen in the presence of sediment and sea water: C_{28} 1,13- (A), C_{30} 1,13- (B), C_{30} 1,15- (C) and C_{32} 1,15-LCDs (D) as free-extractable compounds (E1 in green), free- and extractable-bound compounds (E2 in blue), residually ester-bound compounds (E3 in red) and residually-bound glycosidic ether- or amide-bound compounds (E4 in yellow). Error bars represent standard deviations calculated from triplicate incubations.

The LDI showed some variation over the course of the experiment, each fraction having distinct values (Fig. 4). The LDI calculated from residually-bound glycosidic ether- or amide-bound (E4) LCDs ranged from 0.34 ± 0.03 (day 10) to 0.55 ± 0.03 (day 125), free- and extractable-bound (E2) and residually ester-bound (E3) ranged from 0.31 ± 0.02 (day 15) to 0.40 ± 0.01 (day 125) and 0.28 ± 0.01 (day 22) to 0.52 ± 0.04 (day 10), respectively. The LDI calculated from free-extractable (E1) LCDs had the lowest values and ranged from 0.19 ± 0.03 (day 15) to 0.43 ± 0.25 (day 0). The largest variability was observed during the first 35 incubation days. The LDI for the free-extractable (E1) LCDs dropped from 0.43 ± 0.25 at the beginning of the experiment to 0.25 ± 0.02 at day 3, thereafter remaining approximately constant. The LDI for the residually ester-bound (E3) LCDs showed a maximum at day 10 of 0.52 ± 0.04 and slowly dropped to constant values by day 35 of 0.32 ± 0.00, approximately remaining at that level for the remainder of the experiment, while the LDI for the residually-bound glycosidic ether- or amide-bound LCDs decreased from an initial value of 0.48 ± 0.01 to 0.34 ± 0.03 by day 10, recovering to initial values by degradation day 15 and staying constant throughout the rest of the experiment.

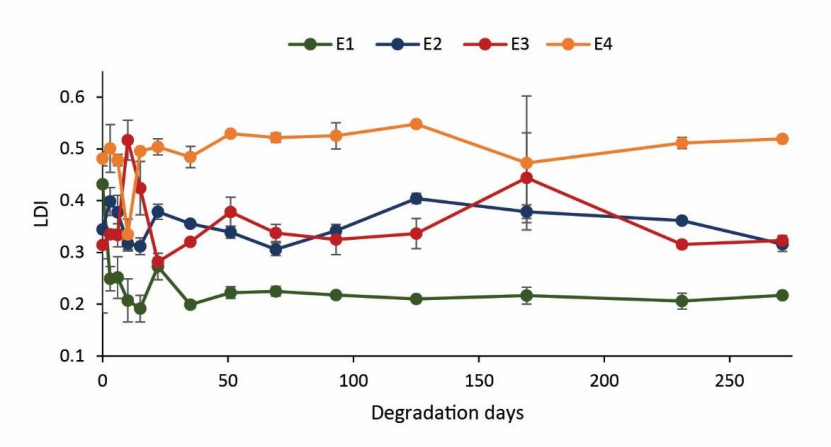

Fig. 4: LDI in an incubation experiment where biomass of the Eustigmatophyte alga *Nannochloropsis oculata* is exposed to oxygen in the presence of sediment and sea water: calculated from free-extractable (E1), free- and extractable-bound (E2), residually ester-bound (E3) and glycosidic ether- or amide-bound LCDs (E4). Error bars represent standard deviations calculated from triplicate incubations.

4. Discussion

4.1 Impact of oxygen exposure on the abundance of fatty acids and LCDs

The occurrence of C_{14}, C_{16} and C_{18} saturated fatty acids and the $C_{20:5}$ PUFA in *Nannochloropsis oculata* is consistent with earlier studies of the lipid composition of *Nannochloropsis* species (Volkman et al., 1993; Olofsson et al., 2012; Xiao et al., 2013; Mitra et al., 2015; Balzano et al., 2017). These lipids showed significant decreases in concentration when exposed to aerobic conditions during 271 days of incubation, to the point of non-detection in the case of the $C_{20:5}$ PUFA. This was independent of the mode of occurrence of these lipids (i.e. as free-extractable, free- and bound-extractable and residually ester-bound or residually-bound glycosidic ether- or amide-bound). Thus, a significant impact of oxygen exposure was observed, especially for the $C_{20:5}$ PUFA. This mirrors previous studies, which showed the relatively rapid degradation of fatty acids and PUFAs in both incubation studies and in sediment cores under oxic as well as anoxic conditions (Farrington and Quinn, 1973, 1977; Sun and Wakeham, 1994, 1997; Canuel and Martens, 1996; Harvey and Macko, 1997a; Grossi et al., 2001; Hoefs et al., 2002).

In contrast to the fatty acids, the impact of oxygen exposure on LCDs resulted in substantially different concentration trends. Following a first minor phase of increase in concentration of LCDs, which was most pronounced in the residually ester-bound fraction (Fig. 2C), a second more significant phase of increasing concentrations was observed. During this second phase from 93 days onwards, LCD concentrations increased discernibly in all four fractions and subsequently plateaued from 125 days onwards, indicating a large-scale release of LCDs from a source outside of our analytical window. The most likely source for these LCDs is the insoluble biopolymer algaenan, which is produced in substantial amounts by Eustigmatophyte algae. Based on chemical degradation methods such as RuO_4 and/or HI or thermal degradation

methods such as pyrolysis GC-MS (Gelin et al., 1997b, 1999; Blokker et al., 1998a, 2000, 2006) this algaenan is thought to be composed of LCDs linked by ether bonds (Zelibor et al., 1988; Tegelaar et al., 1989b; de Leeuw and Largeau, 1993; Gelin et al., 1997b; Blokker et al., 1998b, 2000). If so, it is difficult to envisage how oxidation of ether-linked diols would result in the release of LCDs themselves, i.e. it would be expected that oxidized products of LCDs such as dicarboxylic acids (Blokker et al., 2000) would be detected. However, Scholz et al. (2014) extended the commonly accepted algaenan structure by identifying a bi-layer cell wall composed of a cellulose layer and an algaenan layer while in addition to ether bonds, the algaenan was found to comprise carboxyl, aldehyde, ketone and ester functional groups. Possibly, the impact of oxygen exposure on the algaenan of *N. oculata* may have led to the release of LCDs bound intra-polymeric by ester bonds as opposed to ether bonds, possibly during the initial stage of break-down of the cell and cell wall containing the algaenan. This would mean that the algaenan has remained relatively intact during oxygen exposure but that weakly bonded LCDs attached to the algaenan may have been released and entered our analytical window. It is unclear why this would happen in two phases but possibly is the result of different steps in the breakdown of algal cell and cell wall. Further research examining the integrity of structure of the algaenan during oxygen exposure may shed more light on this.

At 271 degradation days, the time span our incubation was set up for, a substantial decrease of LCD concentrations can be observed in the free-extractable (E1) and free- and extractable-bound fractions (E2), while the residually ester-bound (E3) and glycosidic ether- or amide-bound (E4) fractions showed an increase in concentration. If a constant supply by release of LCDs from the algaenan and a simultaneous degradation of released LCDs by oxic degradation is assumed, free-extractable and free- and extractable-bound LCDs consequently show a higher degradation rate compared to the rate of release from the algaenan, at the end of incubation time.

In a similar incubation study, set up under anaerobic conditions, complete degradation of LCDs in *Nannochloropsis salina* was also not observed (Grossi et al., 2001) but in contrast to our results, only a transient minor increase in LCD concentrations was observed. This is possibly due to the anaerobic nature of the incubation experiment of Grossi et al. (2001), which may have led to a limited release of LCDs from the algaenan over the studied time span. A further comparison is complicated by the fact that Grossi et al. (2001) only considered LCDs that are ester-bound to the biomass and did not take into account the individual patterns of degradation of free-extractable or residually-bound glycosidic ether- or amide-bound LCDs.

The results of this incubation study potentially have implications for our understanding of the fate of LCDs in the context of organic matter settling through the water column and the subsequent burial into the sediment. On short time scales i.e. the settling of organic matter through an oxic water column which is in the order of days to weeks, oxygen exposure is not expected to exert a substantial effect on the LCD concentrations. Only on longer time scales, i.e. in the context of organic matter burial into the sediment which may take multiple years to decades, does oxic as well as anoxic degradation lead to decreasing concentrations of LCDs in the sediment, as previously shown by Hoefs et al. (2002) and Rodrigo et al. (2016).

Keto-ols were not detected in this study, indicating that they were not formed by oxidation of LCDs in the timespan that this incubation study covered. Possibly, the time frame of our study was too short to form these products or the hypothesis that keto-ols are formed by oxic degradation of LCDs is not correct.

4.2. Impact of oxic degradation on the LDI

To examine the impact of oxic degradation of LCD distributions we focused on the LDI although we realize that the alga species used in our study is not the main producer of LCDs in the marine environment and thus LDI values cannot be converted to temperature values following Rampen et al. (2012). Despite the large changes in concentrations of LCDs, the calculated LDI showed only some variability at the initial stages of oxygen exposure, while after 35 days, no substantially changes in the LDI were observed anymore. Values of the LDI, however, differed strongly depending on how the respective LCDs were present in the algal biomass, i.e. the LDI calculated from free-extractable LCDs (E1) showed much lower values compared to e.g. the LDI calculated from residually-bound glycosidic ether- or amide- bound LCDs (E4) (Fig. 4). Since the values for the LDI remained distinctly different between these differently bound LCDs throughout the degradation experiment, it suggests that LCDs were not transferred between the differently bound compound pools. Furthermore, a strong preferential degradation of one diol over another diol was not observed. This consistent difference in LCD distributions between the differently bound compound pools is difficult to reconcile with the hypothesis that LCDs are released from the algaenan upon oxygen exposure as it might be expected that these released LCDs would have a rather uniform distribution. Possibly, these results suggest that LCDs are bound to the algaenan in certain ratios and are also released in these ratios upon oxygen exposure.

The fact that the LDI is not substantially affected by oxic degradation is in contrast to the study of Rodrigo et al. (2016), which showed a preferential preservation of 1,13- over 1,15-LCDs, which consequently impacted the LDI. However, the studies differ in time scales of oxic degradation on LCDs, i.e. while our study represents a time window of less than a year, Rodrigo et al. (2016) analyzed the long term (years to decades) impact of oxic exposure on LCDs during burial in sediments. Thus, short term exposure to oxygen, for instance during the settling of LCDs through an oxic water column, is unlikely to alter the LDI.

5. Conclusion

Nannochloropsis oculata biomass was aerobically degraded for 271 days. While saturated fatty acids and the polyunsaturated fatty acid $C_{20:5}$ were degraded to a large extent, the concentrations of LCDs increased over time and were probably released from the biopolymer algaenan. A substantial impact of oxic exposure on the LDI was not observed.

Acknowledgements

We thank Anchelique Mets for analytical support and Dr. Rodrigo-Gámiz for help with the initial set-up of the experiments. This research has been funded by the European Research Council (ERC) under the European Union's Seventh Framework Program (FP7/2007-2013) ERC grant agreement [339206] to S.S. S.S and J.S.S.D. receive financial support from the Netherlands Earth System Science Centre (NESSC) through a gravitation grant (NWO 024.002.001) from the Dutch Ministry for Education, Culture and Science.

Chapter 3

The impact of oxic degradation on the algaenan of *Nannochloropsis oculata* (Eustigmatophyceae)

Sophie Reiche[1], Zhirong Zhang[2], John K. Volkman[2,3], Klaas G.J. Nierop[4], Jaap S. Sinninghe Damsté[1,4], Stefan Schouten[1,4]

[1]*NIOZ Royal Netherlands Institute for Sea Research, Department of Marine Microbiology and Biogeochemistry, and Utrecht University, PO Box 59, 1790 AB Den Burg, The Netherlands.*

[2]*Wuxi Institute of Petroleum Geology, PEPRIS, SINOPEC, 2060 Lihu Road, Wuxi, Jiangsu 214126, China.*

[3]*CSIRO Oceans and Atmosphere, GPO Box 1538, Hobart 7001, Tasmania, Australia.*

[4]*Utrecht University, Department of Earth Sciences, Faculty of Geosciences, P.O. Box 80.021, 3508 TA Utrecht, The Netherlands.*

To be submitted to Organic Geochemistry

Abstract

Certain freshwater and marine alga, such as Chlorophyceae and Eustigmatophyceae, have been shown to form highly aliphatic and insoluble biopolymers termed algaenan located in the cell wall, which might be preserved in sediments. However, the exact fate of these biopolymers during diagenesis is not well established. Here, in an effort to study the impact of oxic degradation on algaenans, insoluble residues left after hydrolysis of biomass of the Eustigmatophyte *Nannochloropsis oculata* (*N. oculata*) degraded under oxic conditions for up to 271 days, were analyzed by stepwise pyrolysis gas chromatography mass spectrometry. These pyrolyzates were characterized by *n*-alkene/ *n*-alkane doublets with chain lengths from C_{10} to C_{33} and two maxima at C_{15} to C_{17} and C_{26} to C_{28}. Additionally, ketones, with a mid-chain keto group at position 14, were identified with chain lengths of C_{28} to C_{34} with a maximum at C_{31}. A further pronounced abundance of C_{19} *n*-alkan-2-one was observed. These results are in line with an algaenan structure composed of C_{32} 1,15-diol units linked by ether bonds, as proposed previously. Importantly, analysis of residues at four different time points in the oxic degradation experiment did not show a difference in the algaenan chemical composition. The structure of the algaenan of *N. oculata* is therefore relatively resistant to oxic degradation over time scales of at least 270 days.

1. Introduction

There is a long-standing debate on the composition and sources of marine sedimentary organic matter, in particular the insoluble part termed kerogen. While kerogen forms the majority of organic matter in marine sediments and has been analyzed by using a large variety of physical and chemical methods, its formation remains largely disputed (Vandenbroucke and Largeau, 2007). Research in the Seventies and Eighties favored formation of kerogen by biodegradation of proteins and carbohydrates of organic matter into amino acids and sugars and subsequent abiotic recondensation into complex insoluble geopolymers (Durand, 1980; Tissot and Welte, 1984). Later research focused on the preservation and enrichment of highly aliphatic and insoluble biomacromolecules produced by a variety of higher plants and freshwater algae (Largeau et al., 1986; Goth et al., 1988; Tegelaar et al., 1989b). Among the latter, several microalgae from the classes Eustigmatophyceae, Chlorophyceae and Dinophyceae are known to contain these selectively preserved highly aliphatic biopolymers, which are located in the cell wall and are termed algaenan (Derenne et al., 1989; de Leeuw and Largeau, 1993; Gelin et al., 1996, 1997b, 1999; Blokker et al., 1998b, 2006; Kodner et al., 2009; Obeid et al., 2014). Algaenans mostly occur in freshwater microalgae (Largeau et al., 1986; Goth et al., 1988; Zelibor et al., 1988; Tegelaar et al., 1989b; Kodner et al., 2009), e.g. *Botryococcus braunii* or *Tetraedron minimum*, and have only been detected in some marine alga, i.e. *Nannochloropsis oculata (N. oculata)* and other *Nannochloropsis* species (Volkman et al., 1992; Gelin et al., 1997b, 1999). While the algaenan only represents a small percentage of living cell material, its resistance against diagenesis is thought to lead to selective preservation, eventually forming the main part of kerogen (Hutton, 1987; Goth et al., 1988; Tegelaar et al., 1989b; de Leeuw and Largeau, 1993; Largeau and de Leeuw, 1995; Blokker et al., 2000; van Bergen et al., 2004). However, to the best of our knowledge, this resistance has not been tested extensively, e.g. by degradation experiments of algaenans.

Due to their insoluble nature, algaenans are often analyzed by thermally degradative methods, e.g. pyrolysis gas chromatography mass spectrometry (pyrolysis GC-MS). Analysis of algaenan by pyrolysis GC-MS gives rise to a suite of characteristic *n*-alkene/ *n*-alkane doublets (Derenne et al., 1992b; de Leeuw and Largeau, 1993; Gelin et al., 1996, 1999; Zhang and Volkman, 2017). The distribution of *n*-alkene/ *n*-alkane doublets of algaenan pyrolyzates of various

Eustigmatophytes showed maxima at C_{15} to C_{17} and C_{26} to C_{28} for *Nannochloropsis salina* (*N. salina*) and *Nannochloropsis sp.* (Gelin et al., 1997b) and maxima at C_{10} and C_{27} for *N. oculata* and *Nannochloropsis granulata* (*N. granulata*) (Gelin et al., 1999). Additionally, mid-chain ketones, indicating that ether cross bridges occur in the algaenan structure, are present with chain lengths varying from C_{25} to C_{36} in e.g. *N. salina* and *Nannochloropsis sp.* (Gelin et al., 1996, 1997b, 1999). Small amounts of prist-1-ene, toluene and traces of aromatic, isoprenoid and branched hydrocarbons were detected as well (Gelin et al., 1997b). Further information has been gained from the application of chemical degradation, i.e. RuO_4 and/ or $HI/LiAlH_4$ (Blokker et al., 1998b, 2000, 2006), which showed that the algaenan of Eustigmatophytes is likely composed mainly of long-chain 1,15-diols (LCDs) linked by ether bonds (Zelibor et al., 1988; Tegelaar et al., 1989b; de Leeuw and Largeau, 1993; Gelin et al., 1997b; Blokker et al., 1998b, 2000). Additionally, Scholz et al. (2014), identified a bi-layer cell wall composed of an outer algaenan and an inner cellulose layer in *Nannochloropsis gaditana* (*N. gaditana*) and used Fourier transform infra-red spectroscopy to show that the algaenan layer comprised carboxyl, aldehyde, ketone and ester functional moieties.

More recently, Zhang and Volkman (2017) analyzed the algaenan of *Nannochloropsis oceanica* (*N. oceanica*), formerly *N. oculata* (Fawley et al., 2015; Zhang and Volkman, 2017, 2018), by stepwise pyrolysis GC-MS, enabling a more in-depth analysis of the algaenan by generation of products at different temperatures. Importantly, they found a series of mid-chain ketones from C_{29} to C_{33}, the most abundant being the C_{31} ketone, as well as an abundant C_{17} *n*-alkan-2-one. These results confirmed LCDs as important building blocks of the algaenan, described earlier by Gelin et al. (1997), albeit with 1,17-diols, as the building blocks of the algaenan, rather than 1,15-diols. This is in contrast with lipid analyses which showed a dominance of 1,15-diols and only trace amounts of 1,17-diols in this alga (Volkman et al., 1992).

In a recent study, we analyzed the impact of oxygen exposure on lipids of *N. oculata* by aerobic incubation of its biomass for over 271 days (Reiche et al., 2018). During degradation, the concentrations of freely-extractable, but also bound-extractable and residually bound LCDs increased over oxygen exposure time, which was hypothesized to result from a potential break-up of the algaenan and therefore a release of these differently bound LCDs. This would suggest that, in contrast to previous hypotheses, the algaenan is not stable upon oxic degradation and therefore not selectively preserved.

Here, in an effort to study the fate of algaenan during oxic degradation, we analyzed extracted and hydrolyzed biomass of *N. oculata* from the oxic degradation incubations of Reiche et al. (2018) using stepwise pyrolysis GC-MS following the approach outlined by Zhang et al. (2016) and Zhang and Volkman (2017). The results give insights into potential chemical alterations of algaenan during oxic degradation.

2. Material and methods

2.1. Oxic degradation incubations

The oxic degradation incubation of *N. oculata* was previously described in Reiche et al. (2018). Briefly, biomass of *N. oculata* strain CCMP525 (20g) was incubated aerobically with sediment (10 g) and water from the Dutch Wadden Sea (210 ml) for 271 days at 25 °C in the dark and stirred at 100 rpm on a shaker table. Forty-two slurries were prepared and at fourteen predetermined sampling days, the water layer of the biomass slurries was separated from the particulate matter by centrifugation and the obtained particulate matter was freeze dried.

2.2. Work-up procedure

Four time points, i.e. at the start of the oxic degradation experiment (t_0), at the conclusion of a first minor phase of increase in LCD concentrations (t_{93}), at the beginning of a large scale second increase in LCD concentration (t_{125}) and the end of the incubation experiment (t_{271}), were selected for the work-up (see Reiche et al. 2018 for details). The work-up procedure followed a modified approach by Gelin et al (1997) and Goossens et al. (1986).

In a first step, the particulate matter was ultrasonically extracted with methanol/ dichloromethane (MeOH/ DCM) (2:1, v/v, 4x). The resulting residue was dried under N_2 and in a second step saponified by refluxing with 1 M KOH in MeOH for 1 h. The residue was subsequently extracted using H_2O/ MeOH (1:1, v/v), MeOH (2x) and DCM (3x) and dried under N_2. In a last step, the saponified residues were acid hydrolyzed by refluxing with 1.5 M HCl in MeOH for 3 h and subsequently extracted using H_2O/ MeOH (1:1, v/v), MeOH (2x) and DCM (3x) and dried under N_2. The dried, extracted, saponified and acid hydrolyzed residues were homogenized using a mortar and pestle. A blank, consisting of only sediment and sea water was worked up in the same way and prepared for analysis as outlined above.

2.3. Stepwise pyrolysis GC-MS

The residues and blanks were analyzed by sequential stepwise pyrolysis GC-MS as outlined in Zhang et al. (2016) and Zhang and Volkman (2017) . Briefly, ca. 1 mg of the respective residue was placed into a deactivated stainless-steel sample cup, which was subsequently pushed into a pyrolysis quartz tube of a Frontier PY-3030D pyrolyzer and maintained for 20 s to accomplish flash pyrolysis at the pre-set temperature. After flash pyrolysis, the residue was pulled from the pyrolysis zone and a blank run was carried out at 700 °C in preparation for the subsequent higher temperature step. The sample was pyrolyzed in 4 steps at temperatures from 360 - 660 °C in 100 °C intervals. In each step, the formed pyrolyzate was directly swept into the GC injector with He as the carrier gas and analyzed using an Agilent 7890B-5977 A GC-MS system with a J&W DB-5MS column (60 m x 0.25 mm i.d., 0.25 µm film thickness) and an ionization voltage of 70 eV in full scan mode (*m/z* 50-800). Peak assignment was accomplished by comparison with literature data (Volkman et al., 1992) and the library spectra.

3. Results

As described in Reiche et al. (2018), biomass of *N. oculata* with sediment and sea water was incubated in the dark at 25 °C for 271 days. Particulate matter (i.e. biomass and sediment) from four time points in the degradation experiment (t_0, t_{93}, t_{125} and t_{271}) was collected. The time points at t_{93} and t_{125} were chosen because they represent time points where large increases in LCD concentrations were observed (Fi. 1). The particulate matter was extracted, saponified and acid hydrolyzed and analyzed by stepwise pyrolysis GC-MS at different temperatures, e.g. 360 °C to 660 °C in 100 °C steps.

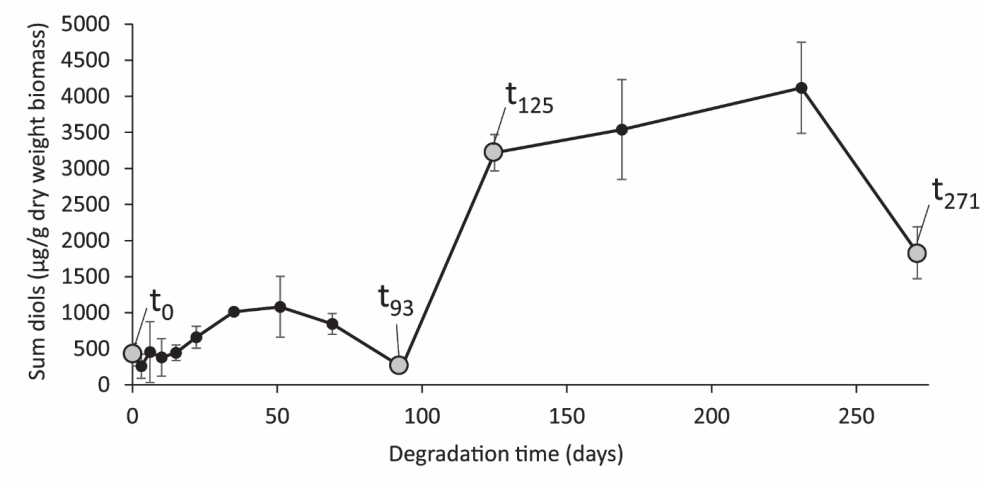

Fig. 1: Summed concentrations of LCDs over time in an incubation experiment where biomass of the Eustigmatophyte alga *N. oculata* was exposed to oxygen in the presence of sediment and water (modified from Reiche et al., 2018). T_0, t_{93}, t_{125} and t_{271} represent sampling points for analysis of the residue by pyrolysis GC-MS methods. Error bars represent standard deviations calculated from triplicate incubations.

For the residue at t_0, at 360 °C, C_{16} fatty acids and a series of C_{24} to C_{30} fatty acids were detected. Furthermore, tocopherol and small amounts of aromatic compounds including indole and benzenepropanenitrile, could be identified. At 460 °C, a series of C_{28} to C_{34} mid-chain ketones with a maximum at C_{31} and a series of *n*-alkenes/ *n*-alkanes with chain lengths from C_{24} to C_{30} predominated. The *n*-alkenes/ *n*-alkanes were most pronounced at 560 °C with chain lengths of C_{10} to C_{33} and two maxima at C_{15} to C_{17} and C_{26} to C_{28} (Fig. 2). Mid-chain ketones were again identified with chain lengths of C_{28} to C_{34} with a maximum at C_{31}. GC-MS analysis showed that for the C_{31} mid-chain ketones, the keto group is predominantly at position 14, based on the major fragment ions of *m/z* 211 and *m/z* 267 resulting from cleavage either side of the carbonyl group (Fig. 3). Furthermore, an abundant C_{19} *n*-alkan-2-one was detected (Fig. 4). At 660 °C, only minor amounts of products were detected in the pyrolyzate. A blank, which consisted of only sediment and sea water and worked up in the same way as the other samples, did not generate any significant products when analyzed by stepwise pyrolysis GC-MS, indicating that all detected pyrolysis products were derived from *N. oculata* biomass.

Comparison of the chemical composition of the pyrolyzates of t_0, t_{93}, t_{125} and t_{271}, shows similar distributions and products for the different pyrolysis temperatures, although a few subtle differences are distinguishable (Fig. 2-4). While a slight maximum at C_{15} *n*-alkane is visible for *n*-alkene/ *n*-alkanes at t_{93}, in contrast, t_0, t_{125} and t_{271} show a maximum at C_{16} *n*-alkane in the pyrolyzate at 560 °C. Additionally, a more pronounced C_{27} *n*-alkane maximum can be observed for t_0, whereas t_{93}, t_{125} and t_{271} show more equal maxima between C_{26} to C_{28} *n*-alkanes (Fig. 2). While for t_0 and t_{93} mid-chain ketones showed a maximum at C_{31} in the 560 °C pyrolyzate, a slight shift to a maximum of C_{32} is visible at t_{125} and t_{271} (Fig. 3). In contrast, the C_{19} n-alkan-2-one was pronounced in all incubation time points (Fig. 4).

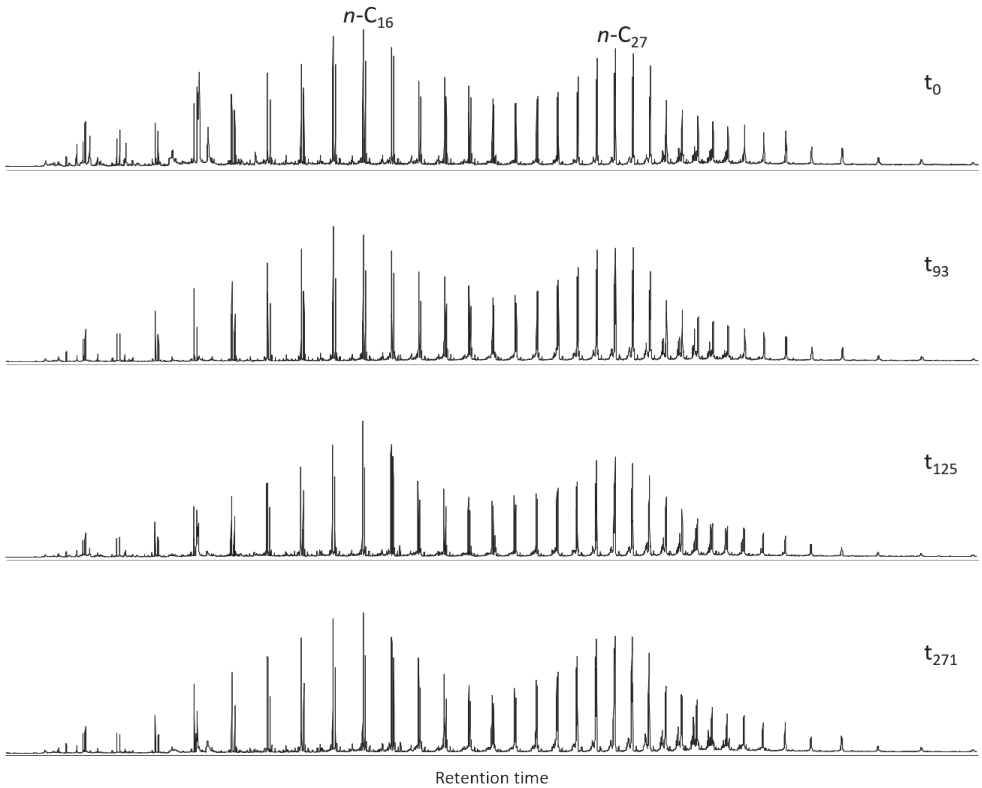

Fig. 2: Summed mass chromatograms of *m/z* 83 + 85 showing the distributions of *n*-alkene/*n*-alkane pairs with chain lengths of C_{10} to C_{33} and two maxima at C_{15} to C_{17} and C_{26} to C_{28} in the pyrolyzates obtained at 560 °C at different timepoints in oxic incubation experiment.

4. Discussion

4.1. Stepwise pyrolysis results of *Nannochloropsis* biomass

We first compared the results of stepwise pyrolysis at t_0, i.e. the start of degradation, with those obtained by Zhang and Volkman (2017) who studied the stepwise pyrolysis of biomass of *N. oceanica*. At lower temperatures (360 °C) both pyrolyzates were relatively clean, showing only low amounts of aromatic compounds, such as indole and benzenepropanenitrile, which have been interpreted to reflect pyrolysis products of proteins (Valdés et al., 2013; Biller and Ross, 2014). In contrast to Zhang et al. (2017), only small amounts of fatty acids, which represent freely extractable compounds in *Nannochloropsis* species (Reiche et al., 2018), could be detected. This is likely due to differences in the initial material that was analyzed. Zhang and Volkman (2017) analyzed freeze dried biomass of *N. oceanica* while the material used here was extracted, saponified and acid hydrolyzed resulting in a removal of most of the carbohydrates, proteins and ester- and amide-bound fatty acids. *N*-alkene/ *n*-alkane doublets were first identified at 460 °C and more clearly visible at 560 °C in our study, which is somewhat different to Zhang and Volkman (2017). That study showed the clear presence of *n*-alkene/ *n*-alkane doublets at 460 °C and 510 °C, but could not detect higher molecular weight compounds at

temperatures > 510 °C. However, in our study we analyzed the residues in temperature steps of 100 °C, i.e. 460 °C and 560 °C, while Zhang and Volkman (2017) used temperature steps of 50 °C and thus also generated pyrolyzates at 510 °C. The distribution of the series of *n*-alkenes/ *n*-alkanes in our experiments (Fig. 2) is characterized by a carbon chain length range of C_{10} to C_{33} and two maxima at C_{15} to C_{17} and C_{26} to C_{28}. This is similar to the results of *N. oceanica* (Zhang and Volkman, 2017) and is representative for algaenan pyrolyzates of different species of Eustigmatophytes, i.e. *Nannochloropsis sp*. or *N. granulata* (Gelin et al., 1997b).

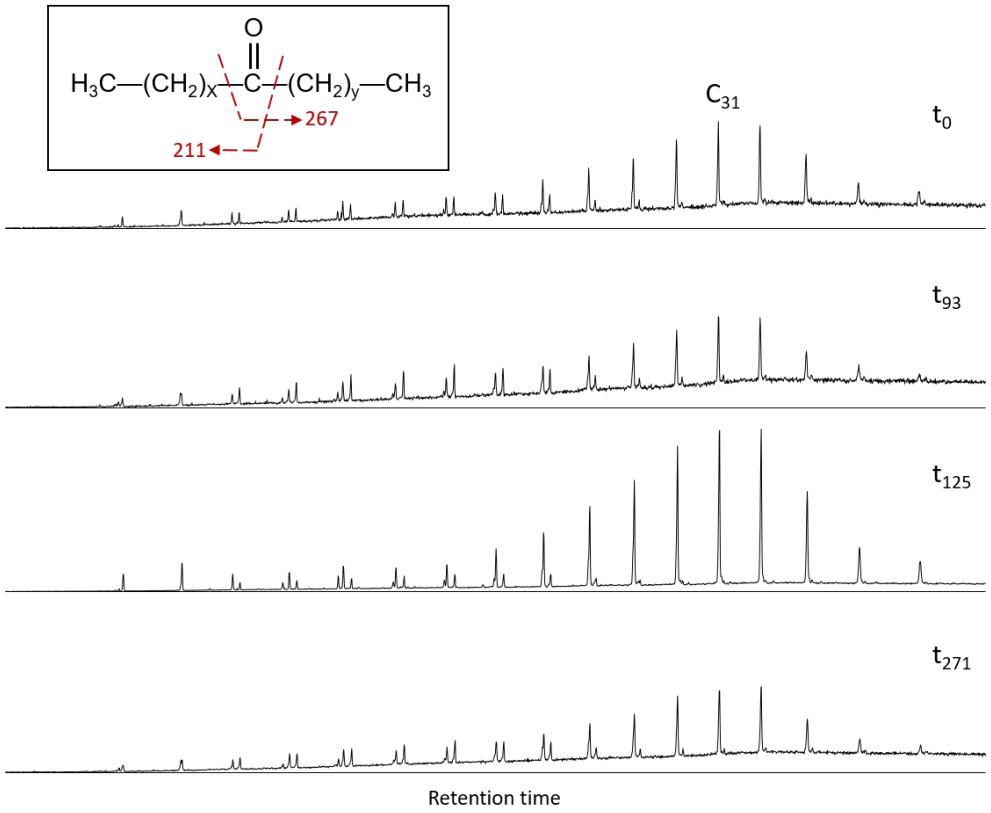

Fig. 3: Mass chromatograms of *m/z* 267 showing the predominance of C_{24} – C_{35} mid-chain ket-14-ones (peaking at C_{31}) in the pyrolysates obtained at 560 °C at different timepoints in the oxic incubation experiment. The structural formula (x =16, y = 12) shows the C_{31} 14 mid-chain ketone and depicts the formation of the observed major fragment ions at *m/z* 211 and 267 by cleavage at both sides of the carbonyl group.

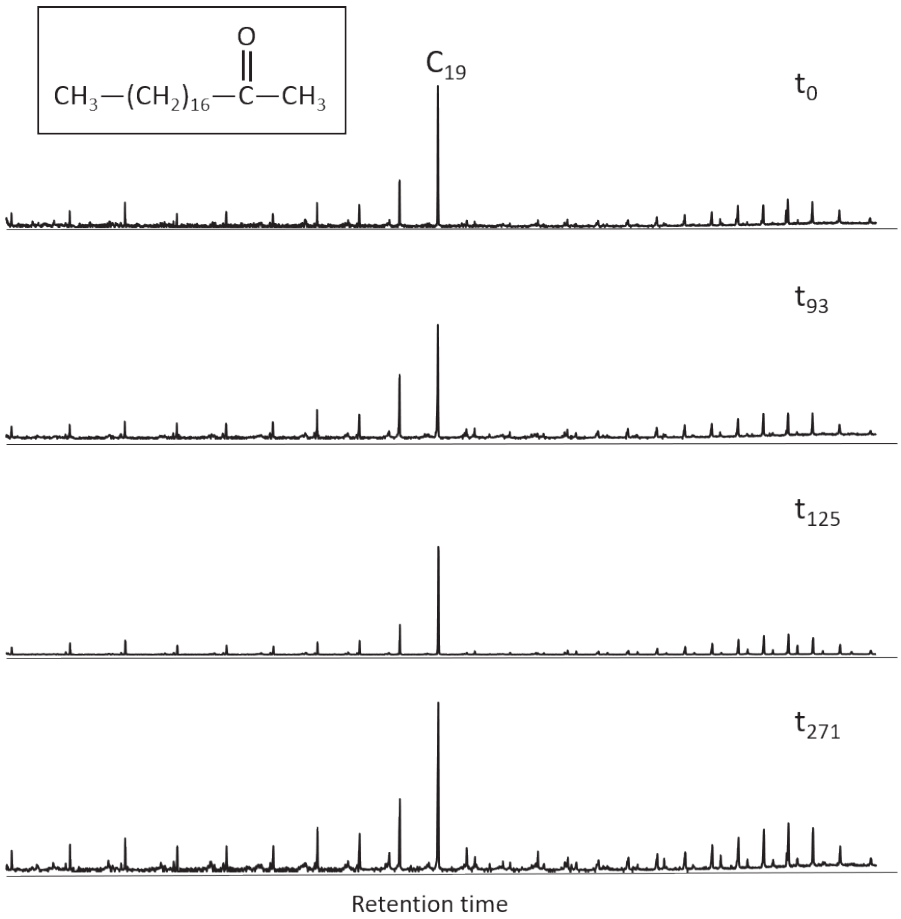

Fig. 4: Mass chromatograms of *m/z* 59 showing the predominance of the C_{19} n-alkan-2-one in the pyrolyzates obtained at 560 °C at different timepoints in the oxic incubation experiment. The chemical structure shown depicts the C_{19} n-alkan-2-one in the pyrolyzates obtained at 560 °C at different timepoints in the oxic incubation experiment.

Mid-chain ketones were detected first at 460 °C and were abundant at 560 °C in our study. This is different from the study of *N. oceanica* by Zhang and Volkman (2017), which showed the highest abundances of mid-chain ketones at 460 °C, but did not detect them at temperatures >460 °C. Possibly, this may be due to the different residues that were analyzed, i.e. freeze dried biomass versus extracted, saponified and acid hydrolyzed biomass. Mid-chain ketones were present with chain lengths of C_{28} to C_{34} with a maximum at C_{31} and a keto-group at position 14 in our analyzed residues. In combination with a pronounced C_{19} *n*-alkan-2-one detected at 560 °C, this strongly suggests that the C_{32} 1,15-diol comprised the main building block of the algaenan, bound by ether bonds. This is consistent with the results of lipid analyses of the biomass of *N. oculata* (Reiche et al., 2018), in which the C_{32} 1,15-diol was the predominant LCD, as a freely extractable, bound extractable and residually bound compound. It contrasts the results of Zhang and Volkman (2017), who found a predominance of the C_{17} *n*-alkan-2-one

and mid-chain ketones with the keto group at position 16 which would indicate an algaenan built up of 1,17-diols. These differences might be a result of the different species that were analyzed, e.g. *N. oculata* here and *N. oceanica* for the study of Zhang and Volkman (2017). Interestingly, *N. oceanica* was also previously analyzed by Volkman et al. (1992), who reported only small amounts of 1,17-diol isomers and the predominance of 1,15-diols in the extractable biomass. This is similar to our work on the *N. oculata* strain (Reiche et al., unpublished data 2018). Possibly, this difference may again be explained by the fact that residues were analyzed here, in contrast to Zhang and Volkman (2017) who analyzed the whole, freeze-dried biomass. Indeed, the C_{19} *n*-alkan-2-one detected here occurred in the pyrolyzates at the temperature step of 560 °C, while the C_{17} *n*-alkan-2-one of Zhang and Volkman (2017) was predominant at 460 °C and was not detected at temperatures higher than 510 °C, suggesting it was less well bound. Therefore, the *n*-alkan-2-one in their case may have not been generated from the algaenan, but from another hydrolysable macromolecule, which is removable by saponification and acid hydrolysis. However, most LCDs do not seem to be bound to soluble macromolecules (Reiche et al. unpublished results, chapter 4). Alternatively, these contrasting results represent real differences between different strains of *Nannochloropsis* species. Indeed, for flash pyrolyzates of *Nannochloropsis sp.* mid-chain ketones with chain lengths of C_{22} to C_{32}, a maximum at C_{26} and keto groups at position 17 and 18 were observed (Gelin et al., 1996). Additionally, Gelin et al. (1996) indicated the presence of *n*-alkan-2-ones with chain lengths of C_7 to C_{25} and a maximum at C_{19} for flash pyrolyzates of *Nannochloropsis sp*. Therefore, there may be potential differences between the basic building blocks of algaenan of different *Nannochloropsis* species and further research is needed, e.g. by application of chemical degradation.

4.2. Impact of oxic degradation on the algaenan of *N. oculata*

In our incubation experiments, we previously showed a large-scale increase in LCD concentration when biomass of the Eustigmatophyte *N. oculata* was aerobically degraded (Fig. 1). We interpreted this large-scale increase in LCD concentration as a release of LCDs from a source outside of our analytical window, most likely the algaenan, as an impact of oxygen exposure. However, it remains chemically unclear how oxidation of ether-bound LCDs in the algaenan would lead to a release of LCDs and why the release of LCDs would happen in two phases (Fig. 1). We, therefore, chose, besides the residues at the beginning (t_0) and the end of incubation (t_{271}), residues from a first minor phase of increase in LCD concentrations (t_{93}) and the large scale second increase in LCD concentration (t_{125}) (Fig. 1) as subjects for study. When comparing the different pyrolyzates for the four different timepoints in degradation, it is however apparent that there are no major changes in the distributions of the *n*-alkenes/ *n*-alkanes (Fig. 2), mid-chain ketones (Fig. 3) and *n*-alkan-2-ones (Fig. 4). Their distribution remained approximately constant throughout the various stages of *N. oculata* biomass degradation indicating only minimal alterations in the structure of the algaenan over the course of the experiment. Since we did not determine the absolute abundance of the pyrolysis products per g of biomass, we cannot say if the algaenan decreased in abundance. However, the relative intensity of the signal of pyrolysis products remained relatively similar (Fig. 2-4). Interestingly, no additional compounds that may have been formed by oxidation of ether-bonds or other parts of the algaenan, e.g. peroxides or dicarboxylic acids (Blokker et al., 1998b, 2000), were detected when analyzed by GC-MS. Overall, our results thus suggest that oxic degradation did not alter the composition of the algaenan itself substantially, making it unlikely that the observed releases of LCDs in the degradation experiment are derived from the core of the algaenan. Alternatively, the release of LCDs may reflect the release of weakly-bonded LCDs of the outer parts of the algaenan, which perhaps were becoming more sensitive to release during degradation of the outer structure of the algaenan. Scholz et al. (2014) have shown that the algaenan is comprised of a two-member algaenan outer layer together with a cellulose-like

layer. If during degradation, the more labile cellulose layer was degraded, parts of the algaenan may have become exposed and accessible for extraction and hydrolysis. The reason that the increase in LCD concentration was happening in two phases may reflect releases of LCDs from different parts of the algaenan. In any case our results suggest that algaenans are relatively resistant against oxic degradation as their structure is not substantially altered after >270 days of exposure to oxygen. They are therefore expected to preserve well during settling in the water column and sediment burial.

5. Conclusion

In order to constrain the impact of oxygen exposure on the chemical composition of the algaenan of *N. oculata*, residues of ultrasonically extracted, saponified and acid hydrolyzed biomass, subjected to oxic degradation, were analyzed by stepwise pyrolysis. Homologous series of *n*-alkenes/ *n*-alkanes, characteristic pyrolysis products of the algaenan, were detected with chain lengths ranging from C_{10} to C_{33} with two maxima at C_{15} to C_{17} and C_{26} to C_{28}. Mid-chain ketones were identified with chain lengths of C_{28} to C_{34} with a maximum at C_{31} and a mid-chain keto group at position 14. Additionally, an abundant C_{19} *n*-alkan-2-one was present. This suggests that the building block of the algaenan of *N. oculata* comprised the C_{32} 1,15-diol, bound by ether bonds into a macromolecular network. This is different from a previous study of *N. oceanica*, in which the building block of the algaenan was predominantly the C_{32} 1,17-diol, suggesting different building blocks of the algaenan within Eustigmatophytes. Analysis of the different time points in oxic degradation did not reveal a pronounced impact of oxygen exposure on the chemical structure of the algaenan. This suggests that the algaenan is relatively resistant to oxic degradation on timescales of at least 270 days and well preserved during settling in the water column und subsequent burial in the sediment.

Acknowledgements

We thank Denise Dorhout and Sebastiaan Rampen for help with the incubation study. This research has been funded by the European Research Council (ERC) under the European Union's Seventh Framework Program (FP7/2007-2013) ERC grant agreement [339206] to S.S. S.S and J.S.S.D. receive financial support from the Netherlands Earth System Science Centre (NESSC).

Chapter 4

A search for macromolecular sources of long-chain alkyl diols

Sophie Reiche[1], Ellen C. Hopmans[1], Jaap S. Sinninghe Damsté[1,2], Stefan Schouten[1,2]

[1]*NIOZ Royal Netherlands Institute for Sea Research, Department of Marine Microbiology and Biogeochemistry, and Utrecht University, PO Box 59, 1790 AB Den Burg, The Netherlands.*

[2]*Utrecht University, Department of Earth Sciences, Faculty of Geosciences, P.O. Box 80.021, 3508 TA Utrecht, The Netherlands.*

Abstract

C_{28} to C_{32} 1,13- and 1,15- long chain diols (LCDs) have been shown to occur in cultured freshwater and marine Eustigmatophytes and are thought to be the building blocks of the insoluble biopolymer algaenan, which forms a constituent of their cell wall. Commonly, LCDs are reported to occur as bound, yet extractable lipids in biomass, which can be released by base hydrolysis of the extract or biomass, while only minor amounts of LCDs occur freely. Here, we attempted to identify potential (macro-)molecular sources of LCDs in extracts of cell material of *Nannochloropsis* sp. by application of ultra-high pressure liquid chromatography combined with high resolution mass spectrometry (UHPLC/HRMS) and semi-preparative HPLC. However, no LCD precursor lipids could be identified by UHPLC-HRMS, while semi-preparative HPLC led to the identification of freely occurring, but not of bound-extractable LCDs, in contrast to previous studies. Subsequent analysis of biomass of three different strains of *Nannochloropsis* spp. showed that LCDs largely occur as free-extractable lipids with only minor increases in LCD concentration after application of acid hydrolysis on the extract. These results therefore call the common hypothesis that LCDs occur as bound-extractable lipids in alga biomass into question.

1. Introduction

Long chain alkyl diols (LCDs) occur in a variety of environments, i.e. freshwater, soil or marine environments. In the latter, they are used to reconstruct sea surface temperatures (Rampen et al., 2012), upwelling and productivity conditions (Rampen et al., 2008; Willmott et al., 2010) and riverine input into the marine environment (de Bar et al., 2016; Lattaud et al., 2017a, 2017b; He et al., 2020). LCDs are composed of long, even carbon-numbered n-alkyl carbon chains with chain lengths of C_{28} to C_{36} with alcohol groups at the first carbon and at a varying mid-chain position at C_{12} to C_{15} (Versteegh et al., 1997). Saturated and unsaturated 1,14-diols with chain lengths of C_{28} to C_{32} have been shown to be produced by *Proboscia* diatoms and have also been identified in *Apedinella radians* (Sinninghe Damsté et al., 2003; Rampen et al., 2007, 2011). C_{28} to C_{32} 1,13- and 1,15-diols have been shown to be produced by cultured freshwater and marine Eustigmatophytes, i.e. *Nannochloropsis oculata* and *Nannochloropsis oceanica* (Volkman et al., 1992; Gelin et al., 1997b, 1999; Méjanelle et al., 2003; Shimokawara et al., 2010; Rampen et al., 2014a; Balzano et al., 2017; Zhang and Volkman, 2017), however the distributions of LCDs in marine environments and cultures differ, suggesting unknown marine sources (Volkman et al., 1992; Versteegh et al., 1997; Rampen et al., 2012, 2014a).

The 1,13- and 1,15-diols have been postulated as the building blocks of the insoluble biopolymer algaenan occurring in the cell wall of Eustigmatophytes (de Leeuw et al., 1981; Tegelaar et al., 1989b; Gelin et al., 1997b; Volkman et al., 1998; Scholz et al., 2014). Several studies have characterized the algaenan using chemical degradation methods, e.g. RuO_4 or HI (Blokker et al., 1998b, 2000, 2006), or thermal degradation methods such as pyrolysis GC-MS (Gelin et al., 1997b, 1999) These studies led to the conclusion that the algaenan is mainly composed of ether-bound LCDs (Zelibor et al., 1988; Tegelaar et al., 1989b; de Leeuw and Largeau, 1993; Gelin et al., 1997b; Blokker et al., 1998b, 2000). A more recent characterization by Scholz et al. (2014) has extended the commonly accepted algaenan structure, by identifying carboxyl, aldehyde, ketone and ester moieties in a bi-layer cell wall composed of a cellulose and an algaenan layer. Besides being part of the insoluble algaenan, LCDs also occur in extracts obtained by ultrasonic or Bligh Dyer extraction of algal biomass (Volkman et al., 1992; Gelin et al., 1997b) and as bound lipids which can be released by base and acid hydrolysis of the extract or residue left after extraction (Gelin et al., 1997b; Grossi et al., 2001; Shimokawara et al., 2010; Reiche et al., 2018). Since LCDs are commonly detected in e.g. *Nannochloropsis*

oculata and *Nannochloropsis salina* as bound-extractable lipids and are not detected as free-extractable lipids or only in minor quantities (Volkman et al., 1992; Gelin et al., 1997b), LCDs seem to be bound to an as of yet unknown polar (macro)molecule. Holguin et al. (2013) analyzed the intact polar lipids of different *Nannochloropsis* spp. and also could detect LCDs only after hydrolysis and not in their free-extractable form. Analysis of a *Nannochloropsis salina* enrichment culture using FT-ICR mass spectrometry, suggested that long-chain sulfate lipids as the source of LCDs released by base and acid hydrolysis. Additionally, Shimokawara et al. (2010) identified LCDs in Eustigmatophyte alga as free-extractable lipids and as lipid bound by ester bonds to more polar compounds, e.g. hydroxy fatty acids bound to amino acids and saccharides, or by ether bonds to macromolecules.

However, none of these studies were successful in unambiguously identifying the polar (macro-)molecules that represent the precursors from which LCDs are released by base and acid hydrolysis.

Here, we attempted to identify the polar (macro-)molecular sources of LCDs in extracts of *Nannochloropsis* biomass by application of ultra-high pressure liquid chromatography high resolution mass spectrometry (UHPLC-HRMS) in combination with semi-preparative HPLC. Furthermore, we quantified the amount of free and bound-extractable LCDs in extracts of different *Nannochloropsis* sp. strains.

2. Methods

2.1. Cultivation of alga strains

In this study, three strains of *Nannochloropsis* sp. were analyzed, e.g. *Nannochloropsis oculata* CCMP525 (hereafter *N. oculata* CCMP525), *Nannochloropsis oculata* CCMP2195 (hereafter *N. oculata* CCMP2195) and *Nannochloropsis oceanica* CCMP1779 (hereafter *N. oceanica* CCMP1779). *N. oculata* CCMP525 was originally ordered and grown by Mariculture Inc and kept frozen at -20°C until analysis.

N. oculata CCMP2195 and *N. oceanica* CCMP1779 were cultured according to Balzano et al. (2017). In short, both strains were cultured in f/2 medium (Guillard, 1975) and maintained under a 16: 8 light: dark cycle at 15°C for *N. oculata* CCMP2195 and 20°C for *N. oceanica* CCMP1779. Both strains were grown in 0.25 L volumes within 0.5 L Erlenmeyer flasks until reaching late exponential phase at 10 days as described by Balzano et al. (2017). The number of cells per culture were counted by flow cytometry (Marie et al., 1999) and subsequently the batch culture was harvested by filtration through 0.7 µm GF/F filters (Whatman, Maidstone, UK).

2.2. Lipid analysis

Frozen filters were freeze dried using a LyoQuest (Telstart, Life Sciences) prior to analysis and were subsequently ultrasonically extracted with methanol/ dichloromethane (MeOH/ DCM) (2:1, v/v, 4x). DCM phases were combined and dried using rotary evaporation and subsequent drying under N_2.

An aliquot of the extract was subsequently saponified by refluxing with 1 M KOH in MeOH for 1 h. The DCM phase was separated from the H_2O/ MeOH phase and dried under N_2. Finally, aliquots of both the extract and the saponified extract were acid hydrolyzed by refluxing with 1.5 M HCl in MeOH for 3 h. After cooling, the mixture was neutralized using 2 N KOH in

MeOH and extracted with DCM/ H_2O (1:1, v/v, 3x). The DCM phases were separated from the H_2O/MeOH phase and combined to be dried under N_2.

The different extracts were eluted with DCM over a small pasteur pipette containing Na_2SO_4 to remove remaining salts. A known amount of the internal standard C_{22} 7,16- diol (MolPort SIA, Latvia) was added to the extracts. Prior to analysis by gas chromatography (GC), extracts were silylated by adding BSTFA [N,O-bis(trimethyl-silyl)trifluoroacetamine] and pyridine and heated up to 60 °C for 20 min. Subsequently, samples were dissolved in ethyl acetate.

Samples were analyzed for LCDs on an Agilent 7890B gas chromatograph equipped with a fused silica capillary column (25 m x 0.32 mm) coated with CP Sil-5 (film thickness 0.12 µm). Samples were injected at 70 °C oven temperature, increasing to 130 °C at 20 °C/min and then 320 °C at 4°/min which was held for 25 min with a helium flow of 2 mL/min. LCDs were quantified by integration of respective peak areas of LCDs and the internal standard.

2.3. Ultra-High Pressure Liquid Chromatography-Electro Spray Ionization/High Resolution Mass Spectrometry (UHPLC-ESI/HRMS) analysis

An aliquot of extract obtained from *N. oculata* CCMP525 biomass was analyzed by normal phase high performance liquid chromatography on an Ultimate 3000 RS UHPLC, equipped with thermostatted auto-injector and column oven, coupled to a Q Exactive Orbitrap MS with Ion Max source with heated electrospray ionization (HESI) probe (Thermo Fisher Scientific, Waltham, MA). Separation was achieved on a YMC-Triart Diol-HILIC column (250 x 2.0 mm, 1.9 µm particles, pore size 12 nm; YMC Co., Ltd, Kyoto, Japan) maintained at 30 °C. The following elution program was used with a flow rate of 0.2 mL min-1: 100% A for 5 min, followed by a linear gradient to 66% A: 34% B in 20 min, maintained for 15 min, followed by a linear gradient to 40% A: 60% B in 15 min, followed by a linear gradient to 30%A:70%B in 10 min, where A = hexane/2-propanol (80:20 [volume in volume, v/v]) and B = 2-propanol/water (90:10 [v/v]). Total run time was extended to 100 min to allow detection of potentially late eluting lipids. HESI settings were as follows: T 50 ˚C, sheath gas (N2) pressure 35 (arbitrary units), auxiliary gas (N2) pressure 10 (arbitrary units), sweep gas (N2) pressure 5 (arbitrary units), spray voltage 4.0 kV for positive ion ESI and -5,5 kV for negative ion ESI, capillary temperature 275 °C, S-Lens 70 V. Lipids were analyzed in both positive and negative ion mode with a mass range of *m/z* 375 to 2000 and *m/z* 1000-4000 (resolution 70,000), followed by data dependent MS^2 (resolution 17,500), in which the ten most abundant masses in the mass spectrum (with the exclusion of isotope peaks) were fragmented successively (stepped normalized collision energy 15, 22.5, 30; isolation window 1.0 *m/z*). A dynamic exclusion window, with a mass tolerance of 3 ppm, of 6 sec was applied.

2.4. Normal and reverse phase semi-preparative high-performance liquid chromatography (HPLC)

In an attempt to isolate macromolecular sources of LCDs, normal phase semi-preparative HPLC following the method described by Bauersachs et al. (2009), and reverse phase semi-preparative HPLC following the method described by Zhu et al. (2013) and Wörmer et al. (2013) , was applied to an extract of *N. oculata* biomass CCMP525.

In short, for normal phase semi-preparative HPLC using a 1260 Infinity Binary HPLC (Agilent, San Jose, CA), a filtered ultrasonically extracted *N. oculata* CCMP525 biomass extract was injected onto a LiChrospher DIOL column (250mm x 10 mm, 5µm, Alltech Deerfield, IL, USA) following the gradients and mobile phase described in 2.3, at a flow rate of 3 mL min^{-1}.

For reverse phase semi-preparative HPLC, the same *N. oculata* CCMP525 extract was injected onto a C18 column (SymmetryPrep C18, 150 mm x 7.8 mm, 5 µm, Waters Corporation, USA). Lipids were eluted at 3 mL min^{-1} using a linear gradient: 100% eluent A for 2 min, increase to 15% eluent B at 2.10 min, 43,5 % eluent B at 15 min and holding to 16 min, washing with 100% eluent B from 16 min to 24 min before returning to 100% eluent A for 5 min. Eluent A was methanol/ water (85:15, v/v) and eluent B was methanol/ 2-propanol (50:50, v/v).

For both normal and reverse phase semi-preparative HPLC, eluents were collected in 1 min fractions. For initial screening purposes, aliquots of the 1 min fractions were combined into 10 min fractions. Aliquots of the 10 min fractions were subsequently saponified according to the procedure described above. The C_{22} 7,16- diol internal standard was added to both the HPLC fractions as well as the saponified fractions, which were subsequently silylated and analyzed using gas chromatography as described above.

3. Results and discussion

3.1. UHPLC-ESI/HRMS analysis of an extract of *N. oculata* CCMP525

In a first attempt to identify sources of bound LCDs in extracts of Eustigmatophyte alga, we analyzed an extract of *N. oculata* CCMP525 biomass by UHPLC-ESI/HRMS. With ESI in positive mode, phosphatidylcholines, diacylglyceryl-trimethylhomoserine (DGTS), diacylglyceryl-hydroxymethyltrimethylalanine (DGTA), dihexoses, sulfoquinovosyl-diacylglycerol (SQDG), inositolphosphoceramide (IPC) as well as lyso forms of these intact polar lipids (IPLs) were detected (Fig. 1A). With ESI in negative mode, SQDGs and lyso SQDGs as well as C_{32} sulfate lipids, i.e. with elemental formula $C_{32}H_{63}O_4S$ (based on accurate mass) and a C_{32} hydroxyl sulfate lipids, i.e. $C_{32}H_{65}O_5S$, were identified (Fig. 1B). Common esterified fatty acid moieties of the identified IPLs included saturated and unsaturated C_{16} and C_{18} fatty acids and $C_{20:5}$ polyunsaturated fatty acids. This composition agrees with previous studies of IPLs of *Nannochloropsis* species (He et al., 2011; Holguin and Schaub, 2013). In order to find polar lipids potentially containing LCDs, we analyzed the MS^2 data in search for diagnostic mass fragments or mass losses related to LCDs, e.g. *m/z* 18 or *m/z* 57, 71, 85 indicating the loss of a hydroxyl group or alkyl chains, respectively. However, this did not lead to any tentative identification of lipids containing LCD moieties. While C_{32} (hydroxy) sulfate lipids were identified, in agreement with earlier findings of Holguin and Schaub (2013), we could not replicate the hypothesis that sulfate lipids serve as a source of LCDs upon release by hydrolysis.

3.2. Semi-preparative HPLC of extract of *N. oculata* CCMP525

The large abundances of IPLs in the biomass extract dominated the base peak chromatograms and, in combination with the unknown nature (and hence unknown mass spectra) of the precursors of the bound LCDs, severely complicated their identification. Therefore, we took an alternative approach. An extract of *N. oculata* CCMP525 obtained by ultrasonication was subjected to semi-preparative HPLC and the eluent was collected in 10 min fractions which were analyzed directly by GC as well as saponified and analyzed for LCDs in order to identify the HPLC retention time of free and bound LCDs, respectively.

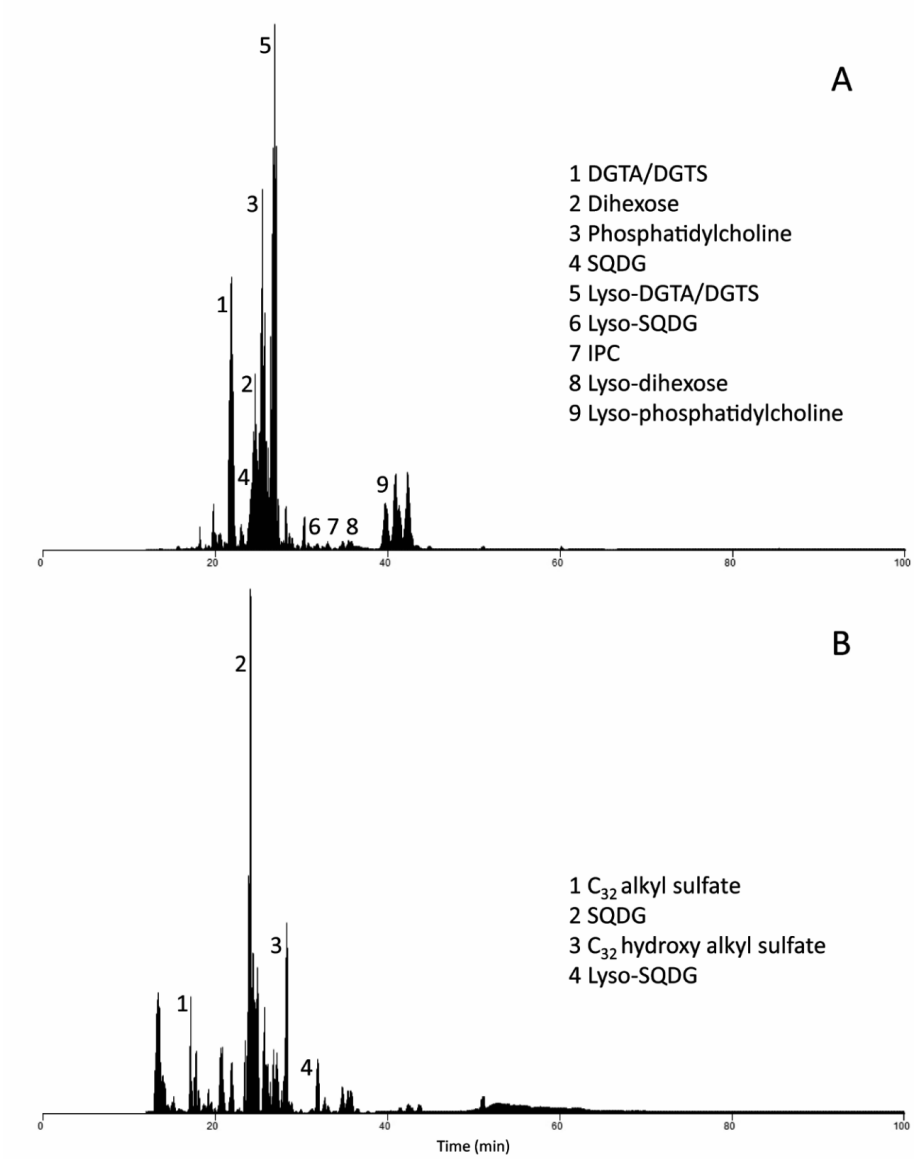

Fig. 1: UHPLC base peak chromatograms of *N. oculata* CCMP525 biomass with identified IPLs in A: positive ion mode and B: negative ion mode. Identified IPLs include among others diacylglyceryl-trimethylhomoserine (DGTS), diacylglyceryl-hydroxymethyltrimethylalanine (DGTA), sulfoquinovosyldiacylglycerol (SQDG) and inositolphosphoceramide (IPC).

We first attempted normal phase semi preparative HPLC (Bauersachs et al., 2009) which resulted in the detection of freely occurring LCDs in the first 10 min fraction, with summed up LCD concentrations of 0.98 µg/g dry weight biomass (Fig. 2A). Very small abundances of freely occurring LCDs were also detected in the second to fourth 10 min fractions. Surprisingly,

saponification of all collected fractions (in the time window 0-70 min) did not lead to the detection of any additional LCDs suggesting that extractable, polar macromolecular sources of bound LCDs did not elute from the column under normal phase HPLC conditions. Therefore, we repeated the experiment using the reversed phase semi-preparative HPLC methods described by Wörmer et al. (2013) and Zhu et al. (2013) as any compound that elutes very late or not at all using normal phase liquid chromatography should elute early when using a reverse phase column. Applying reverse phase semi-preparative HPLC resulted again in the detection of freely occurring LCDs, but now in the second fraction (20-30 min), with summed up LCD concentrations of 0.67 µg/g dry weight biomass (Fig. 2B). Small amounts of LCDs were also detected in the third fraction (30-40 min). Again, however, application of saponification on the collected 7 fractions did not lead to the detection of bound LCDs.

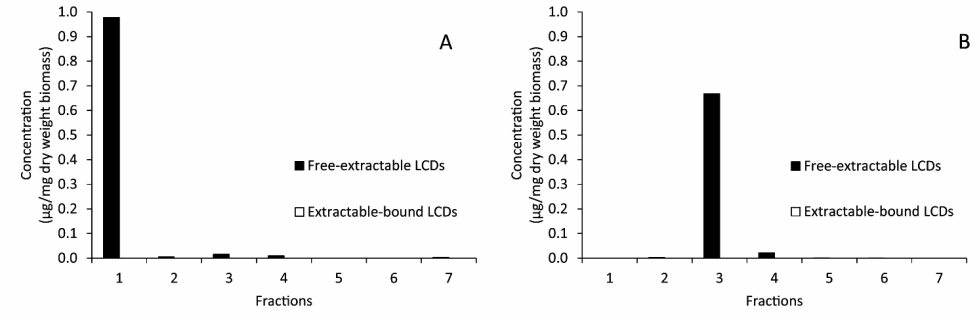

Fig. 2: Yields of free- and bound extractable LCDs after semi-preparative HPLC. A: yields of summed up LCD concentrations following normal phase semi-preparative HPLC. B: yields of summed up LCD concentrations following reverse phase semi-preparative HPLC. Fractions 1-7 represent 10 min intervals of eluent collection.

3.3. Occurrence of LCDs in *Nannochloropsis* species

The relatively high abundances of freely occurring LCDs and the lack of bound LCDs released by base hydrolysis in the fractions obtained by both normal and reverse phase semi-preparative HPLC are in contrast to the common hypothesis that LCDs occur as bound-extractable LCDs and that relatively minor amounts of freely occurring LCDs can be detected (Volkman et al., 1992). However, only few studies have studied free-extractable LCDs, instead analyzing LCDs in biomass cultures by either immediate base hydrolysis of the extract (Gelin et al., 1997b; Rampen et al., 2007) or of the biomass directly (Balzano et al., 2017). Therefore, we re-examined the mode of occurrence of LCDs in extracts by analyzing three different strains of *Nannochloropsis* species, e.g. *N. oculata* CCMP2195, *N. oceanica* CCMP1779 and *N. oculata* CCMP525. The different strains were ultrasonically extracted und subsequently subjected to base hydrolysis, acid hydrolysis and consecutive base and acid hydrolysis following the methodological approaches presented by Volkman et al. (1992), Gelin et al. (1997) and Reiche et al. (2018).

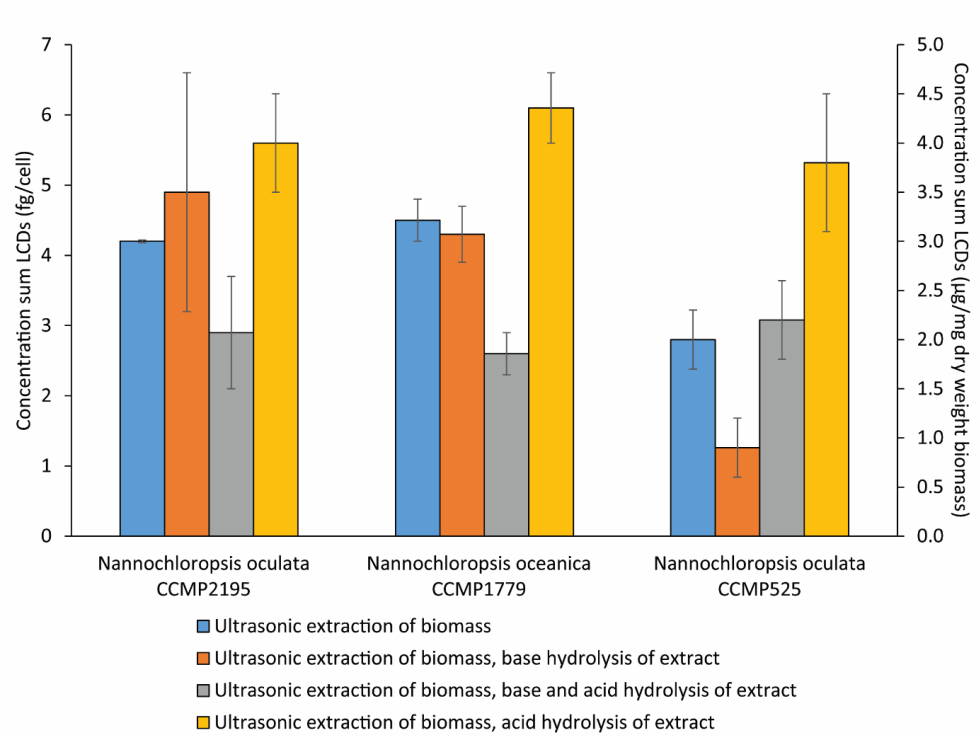

Fig. 3: Yields of summed LCDs in three different *Nannochloropsis* strains following the application of ultrasonic extraction and subsequent base hydrolysis of the extract, base and acid hydrolysis of the extract and acid hydrolysis of the extracts. Yields for *N. oculata* CCMP2195 and *N. oceanica* CCMP1779 given in fg/ cell. Yields for *N. oculata* CCMP525 given in µg/ mg dry weight biomass. Standard deviations calculated from duplicate work-ups.

Both *N. oculata* CCMP2195 and *N. oceanica* CCMP1779 showed similar concentrations of freely occurring summed LCDs with 4.2 ± 0.02 and 4.5 ± 0.3 fg/ cell respectively (Fig. 3), with *N. oculata* CCMP525 showing concentrations of 2.0 ± 0.3 µg/ mg dry weight biomass. The LCDs in base hydrolyzed extracts, which represent both freely extractable and LCDs released by base hydrolysis, showed a slight increase in concentration to 4.9 ± 1.7 fg/ cell for *N. oculata* CCMP2195 and a decrease to 4.3 ± 0.4 fg/ cell for *N. oceanica* CCMP1779. *N. oculata* CCMP525 showed a larger decrease in concentration to 0.9 ± 0.3 µg/mg dry weight biomass. Subsequent acid hydrolysis of the base hydrolyzed extract, thus representing freely extractable LCDs and LCDs released by base and acid hydrolysis, showed decreasing concentrations for summed LCDs for *N. oculata* CCMP2195 and *N. oceanica* CCMP1779 to 2.9 ± 0.8 fg/ cell and 2.6 ± 0.3 fg/ cell respectively. In contrast, the concentration of summed LCDs for *N. oculata* CCMP525 increased to 2.2 ± 0.4 µg/mg dry weight biomass. Finally, when direct acid hydrolysis to the extract was applied, thus representing freely extractable LCDs and LCDs released by acid hydrolysis, all three strains showed an increase in LCD concentration compared to the freely occurring LCDs, increasing to 5.6 ± 0.7 fg/ cell for *N. oculata* CCMP2195, 6.1 ± 0.5 fg/ cell for *N. oceanica* CCMP1779 and 3.8 ± 0.7 µg/mg dry weight biomass for *N. oculata* CCMP525.

Our results clearly show that applying base hydrolysis does not lead to a substantial increase in concentration due to a release of bound LCDs, but instead often led to a decrease in concentration. In principle, an extract treated by base hydrolysis should at least contain the same amount of LCDs as detected directly in the extract. This decrease might be explained by losses through artifact formation as also described in the context of algaenan isolation (Allard et al., 1997, 1998). Harsh consecutive hydrolyses in alkaline or acidic conditions may form melanoidin-like polymers due to the recondensation of polar molecules present in the cell material and our work-up, albeit of less harsh nature, may have led to the formation of similar artifacts binding LCDs to other compounds. Alternatively, work up losses during the hydrolysis procedures, e.g. from shaking against water and subsequent dissolution or micelle formation, may have led to a decrease. Furthermore, weak hydrolysis might be induced when the solvents used for ultrasonic extraction are stored over longer timescales, e.g. leading to the generation of phytadienes from chlorophylls. However, if that would be the case, common work-up products by base and acid hydrolyses of biomass (Grossi et al., 1996) would be found as freely extractable lipids in our *Nannochloropsis* spp biomass, which was not the case. Applying a straight acid hydrolysis on the extract did result in a significant increase in LCD concentration in all three strains and therefore to a release of bound LCDs from unknown sources. Since base, in contrast to acid, hydrolysis did not release any LCDs, these LCDs might have been ether-bound to a glycosidic moiety or amide bound (Goossens et al., 1986, 1989a). Nevertheless, the amount of LCDs released after acid hydrolysis is still only around 30-40% of freely occurring LCDs and so the large majority of LCDs occur as free- extractable lipids in Eustigmatophyte algae, contrasting previous studies. Thus, studies analyzing LCD-containing biomass and not taking free-extractable LCDs into account, might have overlooked a large pool of lipids leading to potential misinterpretations, i.e. creating a bias in distribution and an underestimation of LCD occurrences.

4. Conclusions

In an attempt to identify and characterize macromolecular sources of LCDs, LCD-containing biomass was analyzed by various HPLC methods. Identification of potential polar macromolecules containing LCDs by UHPLC-ESI/HRMS proved to be unsuccessful. Subsequently, an isolation of macromolecular sources by semi-preparative HPLC was attempted. However, both in normal and reverse phase semi-preparative HPLC no ester-bound LCDs and only free-extractable LCDs were detected. Analysis of three strains of *Nannochloropsis* species showed high abundances of free-extractable LCDs and lower amounts of ester-bound LCDs, partially explaining the unsuccessful attempt to isolate macromolecular sources by HPLC methods. Our results thus call into question the current hypothesis that extractable LCDs occur mainly as bound lipids in extracts of biomass of Eustigmatophyte alga.

Acknowledgements

We thank Denise J.C. Dorhout and Monique Verweij for analytical support. This research has been funded by the European Research Council (ERC) under the European Union's Seventh Framework Program (FP7/2007-2013) ERC grant agreement [339206] to S.S. S.S and J.S.S.D. receive financial support from the Netherlands Earth System Science Centre (NESSC) through a gravitation grant (NWO 024.002.001) from the Dutch Ministry for Education, Culture and Science.

Chapter 5

The impact of mode of occurrence of long chain diols and keto-ols and related indices in an S5 sapropel from the Eastern Mediterranean

Sophie Reiche[1], Caglar Yildiz[1], Rick Hennekam[2], Gert-Jan Reichart[2,3], Jaap S. Sinninghe Damsté[1,2], Stefan Schouten[1,2]

[1]NIOZ Royal Netherlands Institute for Sea Research, Department of Marine Microbiology and Biogeochemistry, and Utrecht University, PO Box 59, 1790 AB Den Burg, The Netherlands.

[2]NIOZ Royal Netherlands Institute for Sea Research, Department of Ocean Systems, and Utrecht University, PO Box 59, 1790 AB Den Burg, The Netherlands.

[3]Utrecht University, Department of Earth Sciences, Faculty of Geosciences, P.O. Box 80.021, 3508 TA Utrecht, The Netherlands.

To be submitted to Biogeosciences

Abstract

Long chain diols (LCDs), mid-chain keto-ols (keto-ols) and associated indices are increasingly used as proxies in paleoenvironmental reconstructions, i.e. to determine sea surface temperatures, upwelling conditions, riverine inputs into marine environments and post-depositional oxidation. However, few studies consider that LCDs have different modes of occurrence, i.e. they occur not only as free-extractable compounds but also bound to organic matter by ester- or glycosidic ether- or amide-bonds which may result in an underestimation of LCD abundances and possible differences in LCD indices in the sedimentary record. Here, we studied the effect of matrix sequestration on LCDs, keto-ols and associated indices in a well-defined S5 sapropel from the Eastern Mediterranean by analyzing freely occurring extractable lipids but also LCDs and keto-ols released by base and acid hydrolysis of the extract as well as the residue after sediment extraction. Our results show that the concentrations of 1,14-diols are higher after base and acid hydrolysis, indicating that some LCDs are bound to organic matter and the sedimentary matrix. While freely occurring LCDs dominate the sapropel, LCDs are only detected as residually ester-bound and residually glycosidic ether- or amide-bound lipids above or below the sapropel. However, LCD indices in the S5 sapropel are quite similar to each other irrespective of the mode of occurrence, suggesting that matrix sequestration does not have a large impact on the application of LCD indices in paleoenvironmental reconstructions. Finally, keto-ols were only identified in the sapropel and their relative amount, quantified using the DOXI index, did not show significant trends throughout the sapropel.

1. Introduction

In order to reconstruct past environmental conditions, several organic proxies have been established. Among them, long chain diols (LCDs) have been described in a large number of marine and freshwater environments (Versteegh et al., 1997; Sinninghe Damsté et al., 2003; Rampen et al., 2007, 2008, 2014a; 2014b; Zhang et al., 2011; Romero-Viana et al., 2012; de Bar et al., 2016; Lattaud et al., 2017a) and are increasingly used in paleo-environmental reconstructions. LCDs are commonly composed of a long n-alkyl chain of C_{28} to C_{32} carbon atoms with alcohol groups at the first carbon atom and at a mid-chain position, commonly at position C_{12} to C_{15} (Versteegh et al., 1997) and were first described in Black Sea sediments (de Leeuw et al., 1981). C_{28} and C_{30} 1,14- saturated and unsaturated diols have been shown to be produced by *Proboscia* diatoms (Sinninghe Damsté et al., 2003; Rampen et al., 2007) while C_{28} to C_{32} 1,14-diols (Rampen et al., 2011) have also been identified in *Apedinella radians*. C_{28} to C_{32} 1,13- and 1,15-diols are produced by Eustigmatophyte algae (Volkman et al., 1992; Gelin et al., 1997b, 1999; Rampen et al., 2012, 2014a; Balzano et al., 2017; Zhang and Volkman, 2017), although LCD distributions produced by these algae are dissimilar to those in the marine environment (Volkman et al., 1992; Versteegh et al., 1997; Rampen et al., 2012, 2014a). LCDs produced by Eustigmatophytes have been shown to occur as part of the insoluble, non-hydrolysable biopolymer algaenan (de Leeuw et al., 1981; Tegelaar et al., 1989b; Gelin et al., 1997b; Volkman et al., 1998; Scholz et al., 2014; Zhang and Volkman, 2017).

Several indices based on LCD distribution have been proposed for use in paleo-environmental reconstructions and have since been applied in a variety of marine environments (Pancost et al., 2009; Willmott et al., 2010; Rampen et al., 2012, 2014b; Seki et al., 2012; Lopes dos Santos et al., 2013; Rodrigo-Gámiz et al., 2014, 2015, 2016; Nieto-Moreno et al., 2015; Plancq et al., 2015). The Long chain Diol Index (LDI) uses the fractional abundances of the C_{28} 1,13-, C_{30} 1,13- and C_{30} 1,15-diols (Rampen et al., 2012) to determine past sea surface temperatures (SST). The Diol Index I and Diol Index II reconstruct upwelling intensities/ high nutrient conditions by use of the abundances of C_{28} and C_{30} 1,14-diols relative to C_{28} and C_{30} 1,13-diols

(Willmott et al., 2010) or to C_{30} 1,15-diols (Rampen et al., 2008), respectively. More recently, the fractional abundance of the C_{32} 1,15-diol (FC_{32} 1,15-diol) has been proposed as a proxy for the reconstruction of riverine input into the marine environment (Lattaud et al., 2017b, 2017a; He et al., 2020). Additionally, the Diol Oxidation Index (DOXI) has been proposed to trace the occurrence of post-depositional oxidation (Ferreira et al., 2001). It is based on the ratio of LCDs and structurally similar mid-chain keto-ols (keto-ols) of identical chain length and mid-chain position of the functional group. Keto-ols are lipids occurring in a wide range of environments (Versteegh et al., 1997, 2000; Xu et al., 2007; Bogus et al., 2012) and because of their similar chemical structure and more oxidized state, have been hypothesized to represent oxidative products of LCDs (Ferreira et al., 2001; Sinninghe Damsté et al., 2003). Indeed, they have only been identified in trace amounts in one alga, i.e. *Nannochloropsis gaditana* (Méjanelle et al., 2003). However, differences in carbon chain lengths and position of functional moieties of LCDs and keto-ols have cast doubt on this hypothesis (Versteegh, 1997, 2019; Méjanelle et al., 2003).

Most studies using LCDs for paleoclimate reconstructions use a straightforward extraction procedure such as accelerated solvent extraction (ASE) or ultrasonic extraction. Consequently, they only take freely occurring LCDs into account. However, as shown by various studies (Ten Haven et al., 1987a; Ahmed et al., 2000; Grossi et al., 2001; Shimokawara et al., 2010), LCDs can occur not only as free lipids, but also bound in the extract and in the residue left after extraction. Typically, these LCDs are released by application of base and acid hydrolysis of the extract or residue (Volkman et al., 1992; Gelin et al., 1997b; Reiche et al., 2018). Therefore, most studies may have underestimated the amount of LCDs present in sediments, by not considering LCDs that are bound to organic matter by ester and glycosidic ether or amide bonds. Only few studies have examined LCDs bound in sediments. Ahmed et al. (2000) analyzed bound lipids from sediments of the Monterrey Formation, identifying C_{30}- and C_{32} 1,15-diols and keto-ols as ester-bound lipids. Shimokawara et al. (2010) analyzed LCDs in a sediment core from Lake Baikal, focusing on how LCDs are bound to other lipids. Freely occurring LCDs accounted for 70-100 % of total LCDs throughout the core while LCDs that were ether linked to long chain compounds accounted for 0-30 %. Additionally, small amounts of ester-bound LCDs linked to more polar compounds, e.g. hydroxy fatty acids, were detected. The C_{32} 1,15-diol was the most abundant freely occurring LCD, while the C_{30} 1,13-diol was the most abundant ester- and ether-bound LCD. Ten Haven et al. (1987a) analyzed LCDs and keto-ols in sediments of an S7 sapropel, finding free-extractable and extractable-bound C_{30} and C_{32} 1,15-diols as well as C_{30} 1,15-keto-ols.

Here, we studied the impact of mode of occurrence on LCDs and keto-ols in an S5 sapropel from the Eastern Mediterranean by analyzing not only freely occurring lipids, but also LCDs and keto-ols released by base and acid hydrolysis from the extract and extracted sediment residue. We use these results to evaluate the impact of the mode of occurrence of LCDs on the different proxies, i.e. the LDI, Diol Index I, FC_{32} 1,15-diol and DOXI.

2. Material and methods

2.1. Sampling

The piston core studied here was collected during the NESSC 64PE406 cruise on board of R/V Pelagia at station 1 (33° 18.14898' N, 33° 23.71998' E, 1760 m water depth) in January 2016 (cf. Bale et al., 2019). The core, 9.2 m in length, was split into several sections, each measuring 1 m, which were subsequently analyzed for its bulk inorganic geochemistry using X-Ray Fluorescence (XRF) and inductively coupled plasma mass spectrometry (ICP-MS) as described in Bale et al. (2019). Section 6 was selected for this study, displaying a well preserved S5

sapropel lithostratigraphy in a core depth of 371 – 337 cm. Due to the focus on the S5 sapropel, 30 samples over a depth range of 49 cm were chosen with a resolution of 1 cm around the visually identified upper and lower boundaries of the sapropel (11 samples) and a resolution of 2 – 3 cm within the sapropel (19 samples). Samples were subsequently freeze dried.

2.2. Lipid analysis

Lipids were analyzed following a modified approached described by Gelin et al. (1997) and Goossens et al. (1986) (Fig. 1) . Freeze-dried sediments were extracted by modified Bligh-Dyer extraction (Pitcher et al., 2011; Bale et al., 2015). After addition of a known volume of methanol (MeOH): dichloromethane (DCM): phosphate buffer (2:1:0.8; v,v,v), sediments were ultrasonically extracted for 10 min. The solvent mixture was separated from the residues by centrifugation, collected into a round bottom flask and the process was repeated three times. Subsequently, DCM and phosphate buffer were added to the collected solvents to induce phase separation, producing a new ratio of MeOH: DCM: phosphate buffer (1:1:0.9: v,v,v). After centrifugation, the DCM phase was collected into a round bottom flask and the remaining MeOH: phosphate buffer mixture was washed three times using DCM. The collected DCM phase and the residue were dried using rotary evaporation and drying under N_2. The extract produced by this work-up step was labelled as the free-extractable fraction.

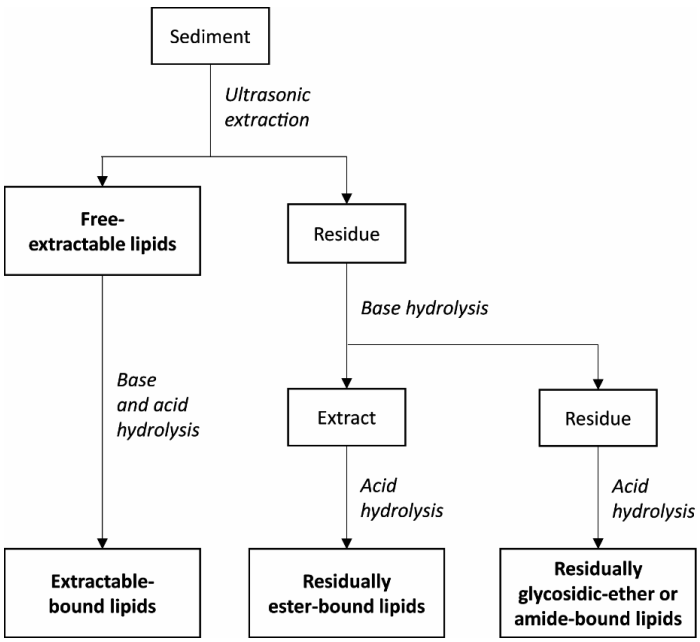

Fig. 1: Analytical scheme representing the work up for the analysis of free and bound LCDs in S5 sapropel sediments, as described in Section 2.2.

An aliquot of the Bligh-Dyer extract was subsequently base and acid hydrolyzed. In the first step of this procedure, the Bligh-Dyer extract was base hydrolyzed by refluxing with 1 M KOH in MeOH. After cooling, the extract was acidified to a pH of 3 using 2 N HCl in MeOH and furthermore extracted with DCM/ H_20 (1:1; v,v: 3x). The DCM phase was separated from the H_20/ MeOH phase, subsequently combined and dried under N_2. In the second step, the base hydrolyzed extract was acid hydrolyzed using 1,5 M HCl in MeOH. After cooling, the extract was neutralized using 2 N KOH in MeOH and extracted with DCM/H_2O (1:1 v,v, 3x). The DCM phases were separated from the H_20/ MeOH phase, the DCM phase was combined and dried under N_2. The extract resulting from the base and acid hydrolysis of the Bligh-Dyer extract was labelled as the extractable-bound and contained freely occurring as well as bound lipids present in the extract (Fig. 1).

The sediment residue left after the Bligh-Dyer extraction was also base and acid hydrolyzed. After base hydrolysis of the residue using 1 M KOH in MeOH, solvents were collected into a separatory funnel and acidified to a pH of 3 using 2 N HCl in MeOH. Residues were subsequently extracted using H_2O/ MeOH (1:1 v,v), MeOH (2x) and DCM (3x). The DCM layer was separated from the MeOH/ H_2O layer and collected, the MeOH/ H_2O layer was extracted with DCM (3x) and the combined DCM phases were dried under N_2. The extract resulting from the base hydrolysis of the residues was subsequently acid hydrolyzed following the procedure as outlined above. The extract resulting from the base hydrolysis of the residue and the subsequent acid hydrolysis of the resulting base hydrolyzed extract, was labelled as the residually ester-bound fraction, i.e. containing lipids bound via an ester bond to the organic matrix t (Fig. 1).

In a last step, the sediment residue resulting from the base hydrolysis of the Bligh-Dyer was acid hydrolyzed by refluxing with 1.5 M HCl in MeOH. After cooling, solvents were collected into a separatory funnel and neutralized using 2 N KOH in MeOH. Residues were subsequently extracted using H_2O/ MeOH (1:1 v,v), MeOH (2x) and DCM (3x) and solvents were collected into the separatory funnel. The DCM layer was separated from the MeOH/ H_2O layer and collected, the MeOH/ H_2O layer was extracted with DCM (3x) and the combined DCM phases were dried under N_2. The extract resulting from this last step was labelled as the residually glycosidic ether- or amide-bound fraction (Fig. 1).

All resulting extracts were eluted with DCM over a small Pasteur pipette containing Na_2SO_4 to remove remaining salts. A known amount of the C_{22} 7,16- diol internal standard was added to aliquots which were subsequently methylated with diazomethane in diethylether. Very polar components were removed by eluting in ethyl acetate over a small pasteur pipette containing silica gel.

Prior to analysis by GC and GC/MS, extracts were silylated by adding BSTFA [N,O-bis(trimethyl-silyl)trifluoroacetamine] and pyridine and heated up to 60 °C for 20 min. Subsequently, samples were dissolved in ethyl acetate. Samples were analyzed for LCDs and keto-ols on an Agilent 7890B gas chromatograph coupled to an Agilent 5977A mass spectrometer, equipped with a fused silica capillary column (25 m x 0.32 mm) coated with CP Sil-5 (film thickness 0.12 µm) with a helium flow of 2mL/ min. Samples were injected at 70 °C oven temperature, increasing to 130 °C at 20 °C/min and then 320 °C at 4°/min which was held for 25 min. The mass spectrometer operated with an ionization energy of 70 eV. LCDs and keto-ols were quantified in selective ion monitoring (SIM) of *m/z* 187, 313, 339 and 341 for the different LCDs and *m/z* 300, 314 and 328 characteristic for the different keto-ols (Versteegh et al., 1997; Rodrigo-Gámiz et al., 2015, 2016).

Concentrations of LCDs and keto-ols were normalized on the total organic carbon (TOC) content, which has been determined by Bale et al. (2019). Residually ester-bound and residually

glycosidic ether- or amide-bound lipids were analyzed in a lower resolution (12 out of 30 samples) than free-extractable and free- and extractable-bound lipids.

The LDI was calculated and converted to SST as follows (Rampen et al., 2012):

$$\mathrm{LDI} = \frac{[\mathrm{C_{30}}1,15\mathrm{-diol}]}{[\mathrm{C_{28}}1,13\mathrm{-diol}]+[\mathrm{C_{30}}1,13\mathrm{-diol}]+[\mathrm{C_{30}}1,15\mathrm{-diol}]} \quad [1]$$

$$SST = \frac{LDI-0.095}{0.033} \quad [2]$$

The Index I was calculated as follows (Rampen et al., 2008):

$$\text{Diol Index I} = \frac{[\mathrm{C_{28}}1,14\mathrm{-diol}]+[\mathrm{C_{30}}1,14\mathrm{-diol}]}{[\mathrm{C_{28}}1,14\mathrm{-diol}]+[\mathrm{C_{30}}1,14\mathrm{-diol}]+[\mathrm{C_{30}}1,15\mathrm{-diol}]} \quad [3]$$

The FC_{32} 1,15-diol was calculated as follows (Lattaud et al., 2017b):

$$\mathrm{FC_{32}}1,15-\mathrm{diol} = \frac{[\mathrm{C_{32}}1,15\mathrm{-diol}]}{[\mathrm{C_{28}}1,13\mathrm{-diol}]+[\mathrm{C_{30}}1,13\mathrm{-diol}]+[\mathrm{C_{30}}1,15\mathrm{-diol}]+[\mathrm{C_{32}}1,15\mathrm{-diol}]}\mathrm{x100} \quad [4]$$

The DOXI was calculated for LCDs and keto-ols showing identical carbon lengths and mid-chain functional groups (Ferreira et al., 2001):

$$\mathrm{DOXI} = \frac{[\mathrm{keto-ol}]}{[\mathrm{keto-ol}]+[\mathrm{diol}]} \quad [5]$$

3. Results

The boundaries of the S5 sapropel were based on the Ba/Al increase and decrease associated to the sapropel initiation and termination, respectively, following Bale et al. (2019). An influence of post-depositional oxidation, the oxidation of organic matter after deposition by a downward moving oxygen front (de Lange et al., 1989; Higgs et al., 1994; Thomson et al., 1995), could not be distinguished in the present S5 sapropel. Comparison of the TOC and Ba/Al profiles shows this absence of post-depositional diagenesis, as Ba/Al shows a similar profile to TOC while being resistant to post-depositional oxidation (Bale et al., 2019).

3.1. LCD and keto-ol concentration profiles

In order to assess the impact of mode of occurrence on the different LCDs and keto-ols, the sediment samples were worked up in a comprehensive approach following the methods described by Gelin et al. (1997) and Goossens et al. (1986) (Fig. 1). Ultrasonic extraction of the sediments resulted in free-extractable lipids, while a subsequent base and acid hydrolysis of the ultrasonic extract represented extractable-bound lipids. Residually ester-bound lipids were obtained after base hydrolysis of the ultrasonically extracted sediment, followed by acid hydrolysis of the base hydrolyzed extract. The residue left after base hydrolysis of the ultrasonically extracted sediment was finally acid hydrolyzed and yielded the residually glycosidic ether or amide-bound lipids. Since extractable-bound lipids represent both freely occurring lipids as well as lipids released by base and acid hydrolysis, extractable-bound LCDs and keto-ols were corrected for free-extractable lipids. However, correction of extractable-bound keto-ols resulted in a series of negative numbers and these were therefore excluded from our discussion. While work-up losses or a potential artifact formation by condensation reactions in alkaline or acidic conditions (Allard et al., 1997, 1998), have been discussed previously to account for minor losses during consecutive hydrolyses (Reiche et al., 2018), it is unclear, why extractable-bound keto-ols were as labile during work-up here.

Several LCDs were identified in the different extract fractions, i.e. the C_{28} 1,12-, C_{28} 1,13-, C_{28} 1,14-, $C_{28:1}$ 1,14-, C_{30} 1,13-, C_{30} 1,14-, C_{30} 1,15- and C_{32} 1,15-diols. The C_{30} 1,15-diol was present in highest concentrations, followed by the C_{32} 1,15-diol, while other LCDs were generally in low abundance. Of the two 1,14-diols identified, the C_{30} 1,14-diol was generally the most abundant, while the $C_{28:1}$ 1,14-diol was only present in trace amounts.

The free-extractable C_{30} 1,15-diol (Fig. 2B) was present in low abundance below and above the S5 sapropel with concentrations of 0 to 4 µg/g TOC, while concentrations increased to maximum concentrations of 300 µg/g TOC at 345 cm core depth inside the sapropel. The extractable-bound C_{30} 1,15-diol was present in lower concentrations of 6 to 64 µg/g TOC, except for a high value of 340 µg/g TOC at 345 cm core depth (Fig. 2B). The residually ester-bound (40 µg/g TOC at 360 cm core depth) and residually glycosidic ether- or amide-bound C_{30} 1,15-diol (39 µg/g TOC at 358 cm core depth) showed lowest concentrations (Fig. 2B). The free-extractable C_{32} 1,15-diol was present with concentrations of 0 to 2 µg/g TOC below and above the sapropel and inside the sapropel with maximum concentrations up to 30 µg/g TOC at 363 cm core depth (Fig. 2C), which represents an earlier concentration maximum in contrast to the C_{30} 1,15-diol. Concentrations of the extractable-bound C_{32} 1,15-diols were slightly lower with maximum values of 20 µg/g TOC at 345 cm core depth (Fig. 2C). The concentration for residually ester-bound and residually glycosidic ether or amide-bound C_{32} 1,15-diol showed similar profiles but were lower in concentration than the free-extractable LCDs, i.e. maximizing at 15 µg/g TOC at 360 cm core depth and 12 µg/g TOC at 358 cm core depth respectively (Fig. 2C). The sum of 1,14-diols showed maximum concentrations up to 30 µg/g TOC at 338 cm core depth as free-extractable LCDs. These LCDs could not be detected in sediments below the sapropel and only in trace amounts above the sapropel. The maximum concentration was higher up in the sapropel than that of the 1,15-diols (Fig. 2A). Extractable-bound 1,14-diols were in higher maximum abundance (i.e. 50 µg/g TOC at 345 cm core depth) than free-extractable 1,14-diols (Fig. 2A). In comparison, residually ester-bound and residually glycosidic ether- or amide-bound 1,14-diols were in much lower abundances with maximum concentration at 6 µg/g TOC at 337 cm core depth and 2 µg/g TOC at 342 cm core depth, respectively (Fig. 2A).

The C_{30} and C_{32} 1,15-keto-ol are the two major keto-ols identified in the S5 sapropel. Both keto-ols were only detected in the sapropel and not in the sediments below or above it. Additionally, the keto-ols were only identified from 366 cm core depth onwards, therefore showing a slower onset in increasing abundances than the corresponding LCDs. The free-extractable C_{30} 1,15-keto-ol was present in highest concentrations with maximum concentrations of 210 µg/g TOC at 353 cm core depth, whereas the free-extractable C_{32} 1,15-keto-ol had maximum concentrations of 60 µg/g TOC at 353 cm core depth (Fig. 2D, E). Both keto-ols showed increasing concentrations towards a mid-sapropel maximum at 353 cm depth and decreasing concentrations thereafter. Concentrations for residually ester-bound C_{30} 1,15- and C_{32} 1,15-keto-ols were substantially lower at ca. 20 µg/g TOC at 360 cm core depth. Similarly, residually glycosidic ether- or amide bound C_{30} 1,15- and C_{32} 1,15-keto-ols reached similar concentrations at 358 cm core depth (Figs. 2D, E). As indicated above, the extractable-bound C_{30} and C_{32} 1,15-keto-ols were excluded from discussion.

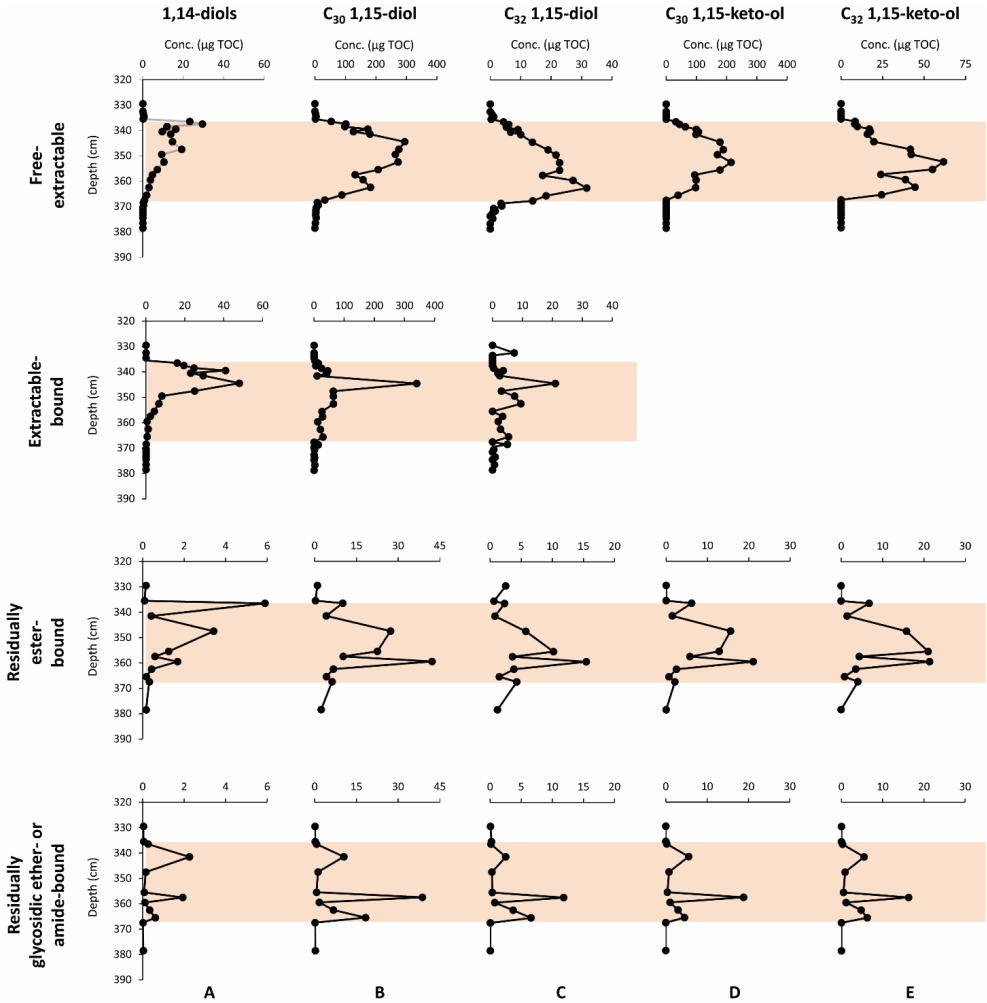

Fig. 2: Trends of 1,14- (A), C_{30} 1,15- (B) and C_{32} 1,15-diols (C), as well C_{30} 1,15- (D) and C_{32} 1,15-keto-ol (E) through the S5 sapropel as free-extractable, extractable-bound, residually ester-bound and residually glycosidic ether or amide-bound lipids. Shading indicates S5 sapropel.

3.2. LCD and keto-ol indices

A variety of LCD indices, i.e. the LDI, the Diol Index I, the FC_{32} 1,15-diol and the DOXI, were calculated using these data. Since most LCDs and keto-ols used for their calculation were not detected outside of the sapropel, these indices could only be calculated for the sapropel sediments.

The LDI for the different modes of occurrences yielded SST estimates ranging from 25.2 to 27.0 °C. These values are 2 to 5 °C higher than previously reported SST for the S5 sapropel calculated using different calibrations of the $U^{k'}_{37}$ index (Emeis et al., 1998, 2003) and also up to 10 °C higher for calculated $U^{k'}_{37}$ SST for the same S5 sapropel that was studied here (Witkowski et al. (submitted)).

The LDI calculated from free-extractable LCDs stayed relatively constant throughout the sapropel with SSTs of 26.8 to 27.0 °C (Fig. 3B). A slight decrease in the LDI can be discerned for the upper 1 cm of the sapropel. The absolute values and trends for the LDI calculated from extractable-bound, residually ester-bound and residually glycosidic ether- or amide-bound LCDs were similar to those of the LDI calculated from free-extractable LCDs (Fig. 3B). A slight shift to lower values of 25.2 to 26.6 °C was visible in the LDI calculated from residually ester-bound and residually glycosidic ether- or amide-bound LCDs, respectively.

The Diol Index I, used here rather than Diol Index II due to the predominance of the C_{30} 1,15-diol and calculated from free-extractable LCDs, increased over the sapropel from 0.02 at 366 cm core depth to 0.30 at 337 cm core depth (Fig. 3A). The same trend and values were also visible for the Diol Index I calculated from extractable-bound, residually ester-bound and residually glycosidic ether- or amide-bound LCDs (Fig. 3A).

The FC_{32} 1,15-diol calculated for free-extractable LCDs had an early maximum of 18% at 366 cm core depth gradually decreasing thereafter to 345 cm core depth reaching 5% (Fig. 3C). A slight increase to 8% was apparent at 337 cm core depth. A general decreasing trend over the sapropel was apparent for the FC_{32} 1,15-diol of extractable-bound and residually ester-bound and residually glycosidic ether- or amide-bound LCDs (Fig. 3C). Values were slightly higher for the FC_{32} 1,15-diol calculated from residually ester-bound and residually glycosidic ether- or amide-bound LCDs compared to the FC_{32} 1,15-diol calculated from free-extractable LCDs.

The C_{30} 1,15-DOXI calculated from free-extractable LCDs and keto-ols was approximately constant throughout the sapropel with values between 0.30 to 0.46 and maxima at 356 and 341 cm core depth (Fig. 3D). Similar trends were apparent in the C_{32} 1,15-DOXI profile calculated from free-extractable LCDs and keto-ols, but values were slightly higher between 0.57 to 0.73. The C_{30} 1,15-DOXI calculated from residually ester-bound and residually glycosidic ether- or amide-bound LCDs and keto-ols stayed approximately constant throughout the sapropel at values of 0.25 to 0.38 and 0.20 to 0.40, respectively (Fig. 3D). The C_{32} 1,15-DOXI calculated from residually ester-bound and residually glycosidic ether- or amide-bound LCDs and keto-ols showed gradually increasing values throughout the sapropel with slight decreases in the upper sapropel. Values ranged between 0.48 to 0.74 for the C_{32} 1,15-DOXI calculated from residually ester-bound and between 0.49 to 0.75 for residually glycosidic ether- or amide-bound LCDs and keto-ols (Fig. 3D). The DOXI calculated from extractable-bound LCDs and keto-ols could not be calculated, since the latter were excluded from the discussion.

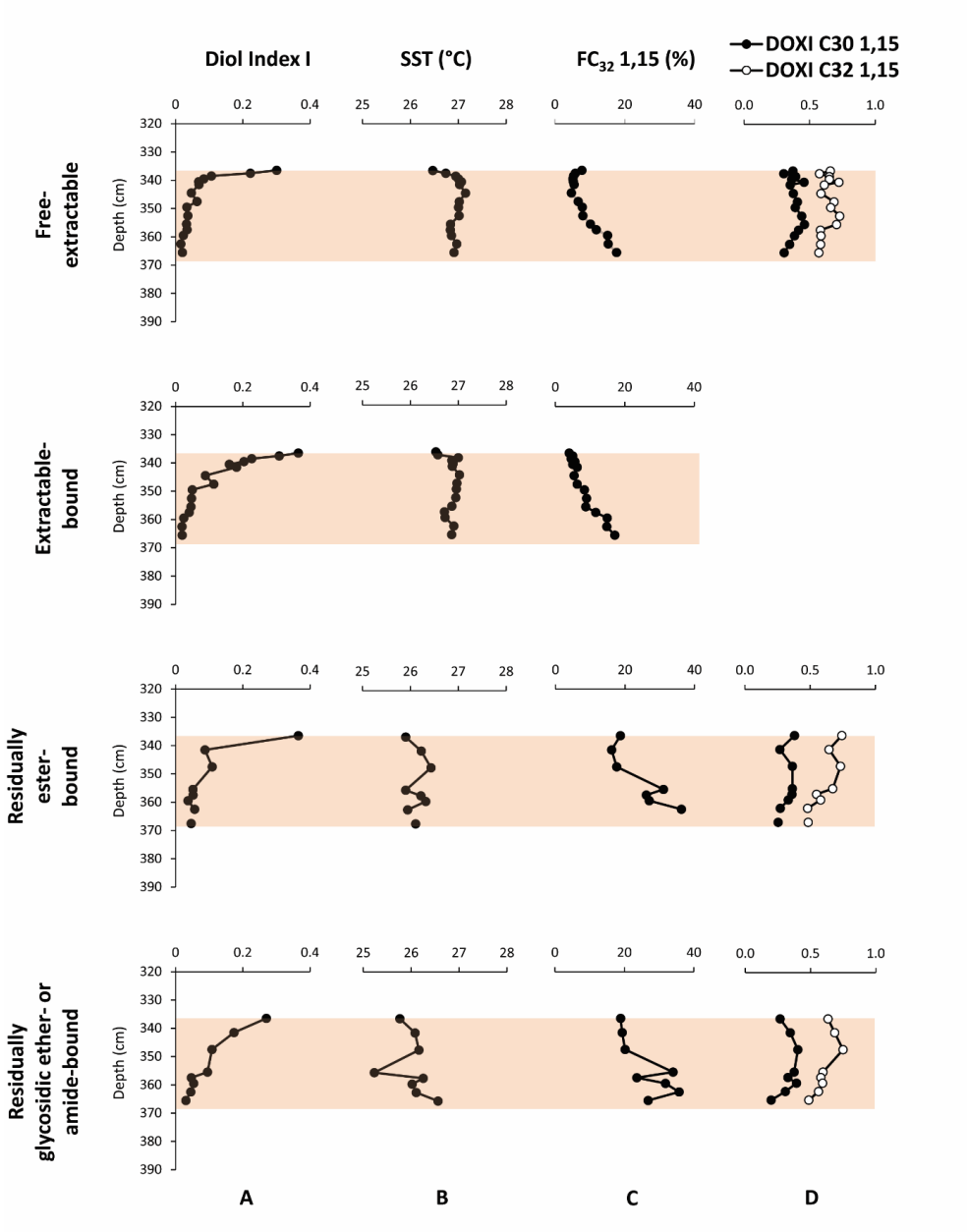

Fig. 3: Trends of Diol Index I (A), LDI SSTs (B), FC_{32} 1,15-diol (C) and C_{30} and C_{32} 1,15-DOXI (D) through the S5 sapropel calculated from free-extractable, extractable-bound, residually ester-bound and residually glycosidic ether or amide-bound lipids. Shading indicates S5 sapropel.

4. Discussion

4.1. Impact of the mode of occurrence of LCDs on LCD profiles and indices

Most studies which analyzed LCDs in sediments, only report freely occurring LCDs extracted using common extraction techniques. Here, in addition, we studied bound LCDs released by hydrolysis of the extract as well as the sediment residue, both within and outside of the S5 sapropel. With respect to LCDs, it is apparent that extractable-bound 1,14-diols show higher concentrations than free-extractable 1,14-diols, suggesting some LCDs are bound to other molecules in the extract. The mode of occurrence of 1,14-diols has not been studied comprehensively to our knowledge. Rampen et al. (2007) applied a base hydrolysis to ultrasonic extracts of *Proboscia indica*, *Proboscia alata* and *Proboscia inermis*, thereby analyzing extractable-bound 1,14-diols, but did not study free-extractable LCDs released by direct extraction. Rampen et al. (2014) compared LCDs in ASE-extracted sediments with LCDs in ASE-extracted and subsequently base hydrolyzed sediments and found higher abundances of mono-unsaturated 1,14-diols after base hydrolysis, but did not discuss other LCD-isomers. Here, the $C_{28:1}$ 1,14-diol was only present in trace amounts as a free-extractable lipid and could not be detected as a bound lipid.

In order to analyze the impact of the mode of occurrence on the different LCDs over depth of the S5 sapropel, we calculated the fractional abundances of 1,14-diols and 1,13- and 1,15-diols as free-extractable, extractable-bound, residually ester-bound and residually glycosidic ether- or amide-bound lipids below, inside and above the S5 sapropel (Fig. 4). Our results show that within the sapropel, the free-extractable and extractable-bound 1,14-diols (Fig. 4A) and 1,13- and 1,15-diols (Fig. 4B) represent 71 – 94 % and 74 – 92 %, respectively, making them the most dominant pool of LCDs within in the sapropel. 1,13- and 1,15-diols were predominantly present as free-extractable lipids (57 – 86 %) and in lower abundances as extractable-bound LCDs (6 – 30%), except in the sediments of 336 cm core depth (20 % free-extractable 1,13- and 1,15-diols and 60 % extractable-bound 1,13- and 1,15-diols). In contrast, 1,14-diols were present as both free-extractable and extractable-bound lipids, e.g. 30 – 62 % for free-extractable 1,14-diols and 9- 64 % for extractable-bound 1,14-diols. Residually bound LCDs may still represent a substantial portion of total LCDs within the sapropel; they vary from 6 – 29 % for 1,14-diols and 8 – 26 % for 1,13- and 1,15-diols.

In contrast, outside of the sapropel, freely occurring 1,14- and 1,13- and 1,15-diols are not detected and LCDs occur solely as bound lipids, predominantly bound as residually ester-bound lipids (83 – 89 % for 1,14-diols and 93 – 95 % for 1,13- and 1,15-diols) and in low abundances as residually glycosidic ether- or amide-bound lipids (11 – 17 % for 1,14-diols and 5 – 7 % for 1,13- and 1,15-diols) (Fig. 4). These residually bound LCDs may be predominant due to their recalcitrant and resistant nature as lipids are bound to the sedimentary matrix (Wakeham and Canuel, 2006) and therefore protected against microbial oxic degradation during deposition of the non-sapropel sediments in oxic bottom water. An impact of oxic degradation on LCDs and related proxies has been indeed been shown by a few studies, which mostly analyzed freely occurring LCDs (Ferreira et al., 2001; Hoefs et al., 2002; Sinninghe Damsté et al., 2002a; Bogus et al., 2012; Rodrigo-Gámiz et al., 2016) and have described decreasing concentrations of the individual LCDs upon oxygen exposure as well as decreasing LDI temperatures (Sinninghe Damsté et al., 2002a; Rodrigo-Gámiz et al., 2016). While Hoefs et al. (2002) have also shown decreasing concentrations of LCDs upon oxic degradation in Madeira Abyssal Plain turbidites, they also showed higher preservation efficiencies of residually ester-bound LCDs compared to free-extractable LCDs.

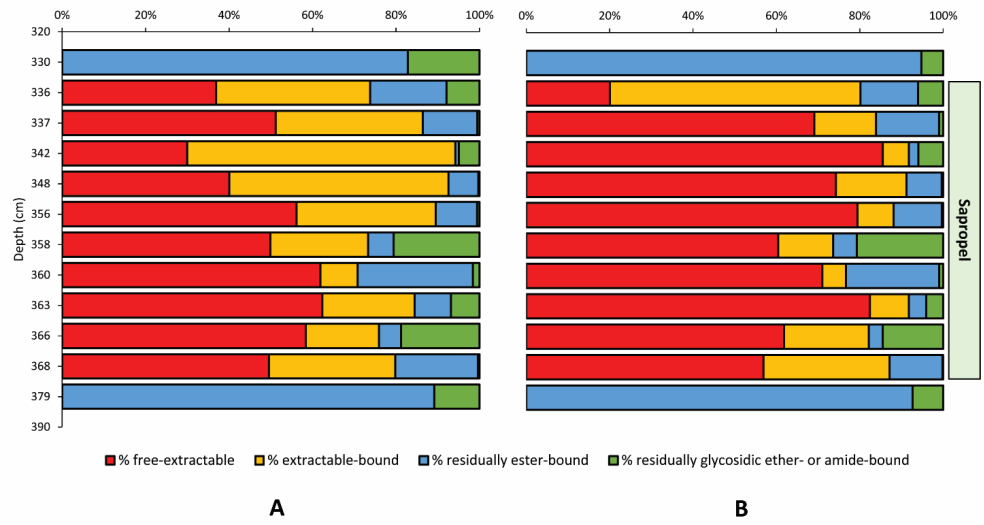

Fig. 4: Fractional abundances of A: 1,14-diols and B: 1,13- and 1,15-diols as free-extractable, extractable-bound, residually ester-bound and residually glycosidic ether or amide-bound LCDs over depth of sapropel.

Despite these substantial differences in the mode of occurrence, little difference is apparent in the various LCD indices, i.e. Diol Index I, LDI and FC_{32} 1,15-diol, calculated from either freely occurring or bound LCDs show similar trends and values (Fig. 3), indicating that the mode of occurrence does not have a large impact on the application of LCD indices in paleoenvironmental reconstructions. These results are somewhat different to the results of an aerobic incubation of *Nannochloropsis oculata* biomass, where the LDI varied strongly when calculated from free- extractable, bound LCDs and residually bound LCDs (Reiche et al., 2018). Possibly, the sedimentary LCDs are sourced from multiple species of algae with different LCD distributions as well as different amounts of free-extractable, bound LCDs and residually bound LCDs.

4.2. Paleo-environmentally significant trends in LCD concentration profiles

The presence of 1,14-diols, the C_{32} 1,15- and the C_{30} 1,15-diols has also been shown in previous studies of sapropels (Ten Haven et al., 1987a, 1987b, 1987c; Ferreira et al., 2001; Menzel et al., 2003; Plancq et al., 2015). All three LCDs showed different trends throughout the sapropel studied here, e.g. different maximum concentrations as free-extractable lipids at different depths. The concentration of the C_{32} 1,15-diol maximizes at the base of the sapropel, i.e. their production/delivery maximized during the early phase of sapropel deposition. In contrast the C_{30} 1,15-diol has a mid-sapropel maximum and the 1,14-diols showing late sapropel maxima. The C_{30} 1,15-diol follows the trend of TOC and the general productivity trends as indicated by Ba/Al (cf. Bale et al., 2019), suggesting that its producer bloomed in concert with the majority of phytoplankton. In contrast, the concentration maximum of 1,14-diols in the upper sapropel (Fig. 2A) indicates that its producers, i.e. *Proboscia* diatoms (Sinninghe Damsté et al., 2003; Rampen et al., 2007), did not follow general productivity trends and proliferated at a later stage. It has been suggested that rhizosolenid diatoms are important contributors to the phytoplankton

community at the time of the sapropel deposition (Kemp et al., 1999). Potentially, *Proboscia* diatoms were outcompeted by other diatoms and could only proliferate, when certain nutrient conditions were more favorable. Lower silica concentrations have been discussed to favor the growth of *Proboscia* diatoms, i.e. *Proboscia alata*, as due to their weakly silicified frustule, less silica may be required for growth than for heavily silicified diatom species (Sakka et al., 1999; Sinninghe Damsté et al., 2003). Indeed, higher concentrations of lightly silicified diatoms were shown at the end of sapropel deposition of an S5 sapropel in a core collected south of Crete (Sangiorgi et al., 2006). Additionally, increased abundances of *Proboscia* following periods of elevated diatom abundances have been shown for a sedimentary record of the Peru upwelling region (de Bar et al., 2018). Thus, the late maximum in the 1,14-diols may be due to more favorable nutrient conditions for *Proboscia* diatoms.

The early sapropel concentration maximum of the C_{32} 1,15-diol can be linked to the conditions leading to the formation of the sapropel itself. Sapropels in the Eastern Mediterranean are generally thought to result from a combination of surface water freshening, reducing deep water ventilation, and an increased export production, increasing oxygen consumption at depth. The reduced ventilation is probably intimately linked to an intensification of the summer monsoon and therefore an increased input of freshwater into the Mediterranean basin by drainage from large river catchments like the river Nile during precession minima (Rossignol-Strick, 1983, 1985; Rohling et al., 2015). Indeed, several studies using e.g. δD of alkenones (van der Meer et al., 2007), $\delta^{18}O$ of foraminifera carbonate tests (Rossignol-Strick et al., 1982, 1985; Rohling et al., 2002) and biomarkers for freshwater cyanobacteria (Bale et al., 2019) have shown large freshwater inputs into the Mediterranean basin at the onset of sapropels in general, and sapropel S5 specifically. The C_{32} 1,15-diol can be derived from riverine sources in coastal regions as it is a dominant LCD in rivers (de Bar et al., 2016; Lattaud et al., 2017a, 2017b). The relatively high levels of the C_{32} 1,15-diol (19%) at the onset of the sapropel are therefore a strong indication for the input of Nile freshwater and the following decrease suggest a reduced input of riverine freshwater, as evidenced by other proxies in other S5 sapropels (Rohling et al., 2002; van der Meer et al., 2007)

4.3. Keto-ols as potential oxidation products of LCDs

Two major keto-ols were identified in this sapropel, the C_{30} and C_{32} 1,15-keto-ol, with the C_{30} 1,15-keto-ol being the more abundant one. Both were not detected outside of the sapropel. The occurrences of keto-ols agree with previously published results on keto-ols in different sapropels from the Mediterranean (Smith et al., 1983; Ten Haven et al., 1987a, 1987b, 1987c; Versteegh et al., 1997; Ferreira et al., 2001) and similar trends of keto-ols over sapropel depth have also been shown in S1 sapropel sediments (Ferreira et al., 2001).

Since keto-ols are structurally related to LCDs, their formation by oxidation of LCDs (Ferreira et al., 2001; Sinninghe Damsté et al., 2003) has been proposed. Analysis of an S1 sapropel, heavily impacted by post-depositional oxidation as indicated by profiles of TOC and Ba/Ti (Ferreira et al., 2001), showed an enrichment of keto-ols relative to LCDs, expressed in the DOXI, at the base of the oxidized part of the sapropel, indicating a potential formation of keto-ols as oxidative intermediate products from LCDs. Here, in comparison, profiles of TOC and Ba/Al do not indicate a strong impact of post-depositional oxidation, i.e. at the top of the sapropel TOC levels drop in concert with Ba/Al levels (cf. Bale et al. (2019)). Indeed, the DOXI did not show any significant trends in contrast to those of Ferreira et al. (2001) while values were on average higher here compared to the C_{30} and C_{32} 1,15-DOXI in the unoxidized interval of S1 sapropel sediments, reported by Ferreira et al. (2001). Differences in DOXI values between both sapropels may be related to the extent of photic zone euxinia in the water column.

While the S5 sapropel has been discussed to be deposited from a fully anoxic water column (Rohling et al., 2006; Sinninghe and Hopmans, 2008), this was likely not the case during the S1 sapropel (Ferreira et al., 2001).

While the DOXIs for both chain lengths show similar trends when calculated from free-extractable LCDs and keto-ols, a alight diverging trend is visible for the C_{32} 1,15-DOXI calculated from residually ester-bound and residually glycosidic ether- or amide-bound LCDs and keto-ols indicating a higher preservation of the C_{32} 1,15-keto-ol versus C_{32} 1,15-diol. If a formation of keto-ols by oxidation of LCDs is assumed, the high riverine input of the C_{32} 1,15-diol likely led to an increased formation of the respective keto-ol due to a longer transport and therefore increased impact of oxic degradation. Since the subsequently decreasing concentration of the C_{32} 1,15-diol indicate an increased degradation of this LCD and likely its derived keto-ol, residually ester-bound and residually glycosidic ether- or amide-bound keto-ols might be better preserved due to their more recalcitrant bonds to the sedimentary matrix. Finally, no 1,14-keto-ols were detected in this study. This agrees with previous studies and has been suggested to be due to the rapid sinking through the water column due to the larger size of the diatoms, in comparison to keto-ols potentially produced by the Eustigmatophytes, thereby reducing the time to oxygen exposure (Sinninghe Damsté et al., 2003).

5. Conclusions

In order to elucidate the impact of the mode of occurrence on long chain LCDs, keto-ols and related indices, we analyzed freely occurring as well as extractable-bound, residually ester-bound and residually glycosidic ether or amide-bound LCDs and keto-ols in an S5 sapropel from the Eastern Mediterranean. The C_{30} 1,15-diol as the most abundant LCD identified, showing a mid-sapropel maximum in concentration while the C_{32} 1,15-diol showed a maximum at the base of the sapropel. The latter is in line with an increased riverine freshwater input during sapropel onset into the Mediterranean basin. The 1,14-diols showed a late maximum in the sapropel, indicating a late establishment of the *Proboscia* diatom community. In the sapropel, freely occurring and extractable-bound LCDs were predominant, whereas above and below the sapropel LCDs were present as residually ester-bound and residually glycosidic ether or amide-bound LCDs. The LDI, LCD Index I and FC_{32} 1,15-diol calculated from freely occurring and bound LCDs showed similar values and trends irrespective of the bond of LCDs used to calculate the indices, indicating that matrix sequestration does not have an impact on LCD indices in paleoenvironmental reconstructions. Keto-ols were only present in the sapropel and calculated DOXIs did not show significant trends throughout this S5 sapropel, indicating a lack of post-depositional oxidation.

Acknowledgements

We thank Denise Dorhout for analytical support. This research has been funded by the European Research Council (ERC) under the European Union's Seventh Framework Program (FP7/2007-2013) ERC grant agreement [339206] to S.S. S.S and J.S.S.D. receive financial support from the Netherlands Earth System Science Centre (NESSC).

Chapter 6

The effect of post-depositional oxidation on long-chain diol proxies in the f-turbidite of the Madeira Abyssal Plain

Sophie Reiche[1], Cindy Schrader[2], Sebastiaan W. Rampen[1,3], Jaap S. Sinninghe Damsté[1,2], Stefan Schouten[1,2]

[1]*NIOZ Royal Netherlands Institute for Sea Research, Department of Marine Microbiology and Biogeochemistry, and Utrecht University, PO Box 59, 1790 AB Den Burg, The Netherlands.*

[2]*Utrecht University, Department of Earth Sciences, Faculty of Geosciences, P.O. Box 80.021, 3508 TA Utrecht, The Netherlands.*

[3]*present address: Universität Göttingen, Geoscience Center, Geobiology Group, Goldschmidtstrasse 3, 37073 Göttingen, Germany.*

To be submitted to Biogeosciences

Abstract

Long-chain diols (LCDs) are increasingly used in paleo-environmental reconstructions. However, few studies have considered the impact of diagenesis on the application of LCD proxies. Here, the impact of post-depositional oxidation on the abundance and distribution of LCDs and mid chain keto-ols (keto-ols) as well as LCD proxies are studied in the f-turbidite of the Madeira Abyssal Plain. Comparison of the upper part, which is affected by post-depositional oxidation, with the lower part that remained anoxic showed that the C_{28} 1,13-diol, C_{30} 1,15-diol and the C_{30} 1,15-keto-ol were better preserved than other LCDs and keto-ols. The Diol Index I (an indicator of upwelling) and the FC_{32} 1,15-diol (an indicator for river influence on the marine environment) showed decreasing values with increased oxygen exposure, while the LDI (a proxy for sea surface temperature reconstruction) showed slightly increasing values. This impact of post-depositional oxidation likely resulted from preferential preservation of the C_{30} 1,15- and C_{32} 1,15-diol over 1,13- and 1,14-diols. A significant increase of the C_{30} 1,15-keto-ols relative to the 1,15-diols was apparent in the upper part of the turbidite impacted by post-depositional oxidation, suggesting that keto-ols may be intermediate products in the oxidation of LCDs. Our results show that care has to be taken in interpreting LCD proxies from sediments deposited under changing oxygen conditions.

1. Introduction

In order to reconstruct past environmental changes, such as sea surface temperatures (SST), several organic proxies are used in paleoclimate studies. For example, SST reconstructions using the $U^{K'}_{37}$ index are based on the degree of unsaturation of long-chain alkenones, produced by haptophyte algae (Brassell et al., 1986; Prahl and Wakeham, 1987), while SST reconstructions using the TEX_{86} proxy are based on the number of cyclopentane moieties in glycerol dialkyl glycerol tetraether lipids (GDGTs) (Schouten et al., 2002), which in the marine environment are produced by Thaumarchaeota (Schouten et al., 2000; Sinninghe Damsté et al., 2002b; Besseling et al., 2019; Zeng et al., 2019).

More recently, proxies based on long-chain alkyl diols (LCDs) have been developed for palaeoceanographic reconstructions. LCDs occur in a large variety of marine and freshwater environments (Versteegh et al., 1997; Sinninghe Damsté et al., 2003; Zhang et al., 2011; Romero-Viana et al., 2012; Rampen et al., 2014a, 2014b; de Bar et al., 2016, 2020; Lattaud et al., 2017b) and are generally composed of C_{28} to C_{32} *n*-alkyl carbon chains with alcohol moieties at the first carbon atom and at a mid-chain position (i.e. at C_{12} to C_{15}). Saturated and mono-unsaturated C_{28} and C_{30} 1,14 diols have been shown to be predominantly produced by *Proboscia* diatoms (Sinninghe Damsté et al., 2003; Rampen et al., 2007) and saturated C_{28} to C_{32} 1,14-diols have been identified in *Apedinella radians* (Rampen et al., 2011). LCDs with the mid-chain moiety at an odd numbered carbon atom, i.e. 1,13- and 1,15-diols, have been identified in cultures of marine and freshwater Eustigmatophyte alga and range in chain length from C_{24} to C_{36} (Volkman et al., 1992, 1999; Gelin et al., 1997b; Versteegh et al., 1997; Méjanelle et al., 2003; Shimokawara et al., 2010; Rampen et al., 2014a; Balzano et al., 2017). However, LCD distributions of 1,13- and 1,15 diols in marine environments differ from LCD distributions in marine Eustigmatophyte cultures, suggesting unknown marine sources (Volkman et al., 1992; Versteegh et al., 1997; Rampen et al., 2012, 2014a; Balzano et al., 2018; Reiche et al., 2018).

Several indices based on LCD distributions have been proposed to reconstruct paleo-environmental conditions. The Long-chain Diol Index (LDI), based on the fractional abundances of C_{28} 1,13-, C_{30} 1,13- and C_{30} 1,15-diols, has been proposed as an SST proxy (Rampen et al., 2012), while the Diol Indices using the abundances of C_{28} and C_{30} 1,14-diols

relative to C_{28} and C_{30} 1,13-diols (Willmott et al., 2010) or to C_{30} 1,15-diols (Rampen et al., 2008), have been used to reconstruct upwelling/nutrients and productivity (de Bar et al., 2018; Zhu et al., 2018; 2020). More recently, the fractional abundance of the C_{32} 1,15-diol (FC_{32} 1,15-diol) has been used to study riverine inputs into marine environments (de Bar et al., 2016; Lattaud et al., 2017a, 2017b; Häggi et al., 2019). These indices have since their development been applied in paleo-environmental reconstructions of different marine environments (Pancost et al., 2009; Rampen et al., 2012; Seki et al., 2012; Lopes dos Santos et al., 2013; Rodrigo-Gámiz et al., 2014; Plancq et al., 2015; Jonas et al., 2017; Dauner et al., 2019; de Bar et al., 2019; Lattaud et al., 2019a; Zhu et al., 2020). Additionally, the Diol Oxidation Index (DOXI), based on the ratio of LCDs and structurally related mid-chain keto-ols (keto-ols) of identical chain length and position of functional groups, has been proposed as a tool to assess the impact of post-depositional oxidation (Ferreira et al., 2001), although this has been questioned (Versteegh and Lipp, 2019).

Although LCD indices are now regularly used in paleo-environmental reconstructions, only few studies consider the impact of diagenesis on the distribution and abundance of LCDs and the application of LCD indices. In general, oxic degradation has been shown to have a profound effect on the distribution of biomarkers (Sun and Wakeham, 1994; Hoefs et al., 1998a; Prahl et al., 2003; Rontani et al., 2009, 2013), including paleoclimate proxies such as the $U^{K'}_{37}$ proxy (Gong and Hollander, 1999; Hoefs et al., 2002; Huguet et al., 2009; Kim et al., 2009a). Several studies have analyzed the impact of oxic degradation on LCDs and LCD indices (Ferreira et al., 2001; Hoefs et al., 2002; Sinninghe Damsté et al., 2002a; Rampen et al., 2007; Bogus et al., 2012; Rodrigo-Gámiz et al., 2016; Reiche et al., 2018). Sinninghe Damsté et al. (2002) analyzed LCDs in sediment cores from the Arabian Sea finding relatively high preservation efficiencies of LCDs compared to steroids and alkenones. Hoefs et al. (2002) studied the impact of oxygen exposure on the distribution of LCDs in Madeira Abyssal Plain turbidites, which consist of anoxic shelf sediments deposited in oxic waters thereby creating an oxidation front. By comparing the oxidized part with the unoxidized part of the turbidite, a higher preservation of residually ester-bound LCDs compared to freely extractable LCDs was shown. Rodrigo-Gámiz et al. (2016) showed a decrease in LCD abundances with increasing oxygen exposure in Arabian Sea surface sediments under contrasting redox conditions and a higher preservation of 1,14- and 1,13-diols compared to 1,15-diols, which resulted in a decrease in LDI with increasing oxygen exposure time. The latter result is in contrast to a laboratory incubation study by Reiche et al. (2018), investigating the impact of oxygen exposure on LCD-containing biomass, which showed a negligible effect of oxic degradation on the LDI.

Here, we analyze the impact of post-depositional oxic degradation on LCD and keto-ol proxies by analyzing sediments from a turbidite from the Madeira Abyssal Plain (MAP), which was previously investigated for GDGTs and associated proxies (Lengger et al., 2013). The results are compared with those of previous studies investigating the impact of post-depositional oxidation on LCDs and LCD indices.

2. Material and methods

2.1. Study sites and sampling

A piston core was retrieved from the Madeira Abyssal Plain (MAP) in the eastern North Atlantic at 31°26.8′N 024°48.8′W during cruise JCR209 onboard R/V James Clark Ross in September 2007 and the f-turbidite was sub-sampled directly after retrieval of the core (see Lengger et al., 2013 for details). Its location is in the area of well-studied turbidite deposits which in previous studies have been analyzed to ascertain oxic degradation effects on various biomarkers (de Lange et al., 1987, 1998; Cowie and Hedges, 1994, 1995; Prahl et al., 1997,

Hoefs et al., 1998a, 2002; Sinninghe Damsté et al., 1998; Huguet et al., 2008, 2009; Lengger et al., 2013).

2.2. Lipid analysis and quantification

Aliquots of the sediment layers of core MAP-1 stored frozen, were extracted specifically for this study. Freeze dried sediment samples were extracted by accelerated solvent extraction (ASE 200, DIONEX) with a mixture of dichloromethane (DCM) and methanol (MeOH) (9:1; v/v). A known amount of the internal standard (C_{22} 7,16 – diol, MolPort SIA, Latvia) was added to the extracts, which were subsequently separated into apolar, ketone and polar fractions by elution over an Al_20_3 column using hexane: DCM (9:1, v/v), hexane: DCM (1:1, v/v) and DCM: MeOH (1:1, v/v). Prior to analysis by gas chromatography/mass spectrometry (GC/MS), polar fractions were silylated by adding BSTFA [N,O-bis(trimethyl-silyl)trifluoroacetamide] and pyridine and heated up to 60 °C for 20 min. Subsequently, samples were dissolved in ethyl acetate.

Samples were analyzed for LCDs and keto-ols on an Agilent 7890B gas chromatograph coupled to an Agilent 5977A mass spectrometer, equipped with a fused silica capillary column (25 m x 0.32 mm) coated with CP Sil-5 (film thickness 0.12 µm) with a helium flow of 2mL/ min. Samples were injected at 70 °C oven temperature, increasing to 130 °C at 20 °C/min and then programmed at 4°/ min 320 °C which was held for 25 min with a helium flow of 2 mL/min. The mass spectrometer operated with an ionization energy of 70 eV. Lipids were quantified in selective ion monitoring (SIM) of *m/z* 187, 299, 313, 327 and 341 characteristic for the different LCDs and the diol standard and *m/z* 300, 314, 328 for the different keto-ols (Versteegh et al., 1997; Rodrigo-Gámiz et al., 2015; 2016).

LCD and keto-ol concentrations in the sediments of the MAP-1 f-turbidite were normalized on dry weight of the sediment (µg/g dry sediment).

The LDI was calculated according to Rampen et al. (2012):

$$\mathrm{LDI} = \frac{[\mathrm{C_{30}}1,15\mathrm{-diol}]}{[\mathrm{C_{28}}1,13\mathrm{-diol}]+[\mathrm{C_{30}}1,13\mathrm{-diol}]+[\mathrm{C_{30}}1,15\mathrm{-diol}]} \quad [1]$$

using the calibration of de Bar et al. (2020):

$$\mathrm{SST} = \frac{\mathrm{LDI} - 0.1082}{0.0325} \quad [2]$$

The Diol Index I was calculated according to Rampen et al. (2008):

$$\text{Diol Index I} = \frac{[\mathrm{C_{28}}1,14\mathrm{-diol}] + [\mathrm{C_{30}}1,14\mathrm{-diol}]}{[\mathrm{C_{28}}1,14\mathrm{-diol}]+[\mathrm{C_{30}}1,14\mathrm{-diol}]+[\mathrm{C_{30}}1,15\mathrm{-diol}]} \quad [3]$$

The fractional abundance of the C_{32} 1,15-diol was calculated according to Lattaud et al. (2017a):

$$\mathrm{FC_{32}}1,15-\mathrm{diol} = \frac{[\mathrm{C_{32}}1,15\mathrm{-diol}]}{[\mathrm{C_{28}}1,13\mathrm{-diol}]+[\mathrm{C_{30}}1,13\mathrm{-diol}]+[\mathrm{C_{30}}1,15\mathrm{-diol}]+[\mathrm{C_{32}}1,15\mathrm{-diol}]} \mathrm{x100} \quad [4]$$

The DOXI was calculated as proposed by Ferreira et al. (2001):

$$\mathrm{DOXI} = \frac{[\mathrm{keto-ol}]}{[\mathrm{keto-ol}]+[\mathrm{diol}]} \quad [5]$$

3. Result and discussion

3.1. Impact of post-depositional oxic degradation on LCDs

We used sedimentary intervals of the MAP f-turbidite which have previously been studied by Lengger et al. (2013) to study the impact of post-depositional oxidation on GDGT- based proxies, i.e. TEX_{86} and the BIT index. Since MAP turbidites represent organic-matter rich homogenous turbidites (Buckley and Cranston, 1988) that are subsequently exposed to downward diffusing oxygen from the oxygen rich deep abyssal waters (de Lange, 1992), they are ideal to study the impact of oxidation on lipid distribution and abundance (Cowie et al., 1995, 1998; Prahl et al., 1997; Hoefs et al., 2002). The stratigraphic boundary between the oxidized and unoxidized f-turbidite was set at 1105 cmbsf, following Lengger et al. (2013) and was based on statistical clustering of XRF data, organic carbon content and grain size distribution.

3.1.1. LCD and keto-ol distributions

A suite of LCDs and keto-ols were identified in the MAP turbidite, in varying concentrations (Table 1). Of all LCDs, the C_{30} 1,15-diol (Fig. 1B) was present in highest abundance with concentrations of 39 ± 15 µg/g in the oxidized zone and tenfold higher concentrations (i.e. 390 ± 60 µg/g) in the unoxidized zone. Other abundant LCDs were the C_{28} 1,14-, the C_{30} 1,14- (Fig. 1A) and the C_{32} 1,15-diols (Fig. 1C) with concentrations of 10 ± 4 µg/g, 9 ± 3 µg/g and 8 ± 3 µg/g in the oxidized zone and 128 ± 11 µg/g, 137 ± 30 µg/g and 106 ± 24 µg/g in the unoxidized zone, respectively. The C_{28} 1,13-, C_{28} 1,12- and C_{30} 1,13-diols were present in lower concentrations, while the $C_{28:1}$ 1,14-diol was only present in trace amounts. Four different keto-ols were identified, of which the C_{30} 1,15- (Fig. 1D) and C_{32} 1,15-keto-ols (Fig. 1E) were most abundant with concentrations of 32 ± 20 µg/g and 17 ± 12 µg/g in the oxidized zone and 171 ± 147 µg/g and 210 ± 187 µg/g in the unoxidized zone, respectively. The C_{30} 1,13- and C_{30} 1,14-keto-ols were present in lower concentrations at 13 ± 8 µg/g and 5 ± 3 µg/g in the oxidized zone and 104 ± 92 µg/g and 32 ± 26 µg/g in the unoxidized zone, respectively (Table 1). No C_{28} keto-ols were detected. Keto-ols showed slightly different trends in the unoxidized zone, when compared to LCDs, with lower values at the top and the deepest part of the unoxidized zone.

With these data, the relative preservation efficiency (RPE) between lipids in the oxidized and unoxidized zone was calculated (cf. Lengger et al., 2013):

$$RPE\ (\%) = 100\ x\ \frac{average\ lipid\ concentration\ in\ oxidized\ zone}{average\ lipid\ concentration\ in\ unoxidized\ zone} \quad [6]$$

For LCDs, RPEs varied between 6.4 to 10.8 %, with lowest RPEs for the C_{28} 1,12-diol, C_{30} 1,13- and 1,14-diols with 7.1 %, 7.1 % and 6.4 %, respectively, and highest RPEs with 10.8 % and 10.2 % for the C_{28} 1,13-diol and C_{30} 1,15-diols, respectively (Table 1, Fig. 2). A much wider range of RPEs was apparent for keto-ols, with a RPE of 8.0 % for the C_{32} 1,15-keto-ol and 18.9 % for the C_{30} 1,15-keto-ol. The C_{30} 1,13- and C_{30} 1,14-keto-ols showed RPEs of 12.3 % and 15.5 %, respectively.

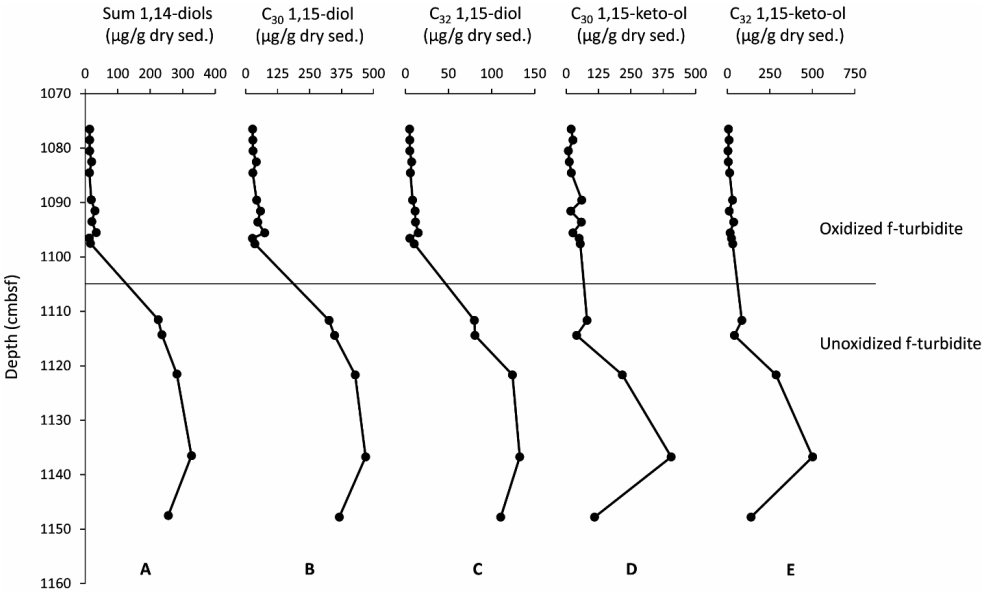

Fig. 1: Concentrations of LCDs and keto-ols with depth in the f-turbidite of the MAP-1 core. A: Sum of 1,14-diols, B: C_{30} 1,15-diol, C: C_{32} 1,15-diol, D: C_{30} 1,15 keto-ol and E: C_{32} 1,15 keto-ol. Horizontal line marks stratigraphic boundary of the oxidized f-turbidite and the unoxidized f-turbidite (*cf.* Lengger et al., 2013).

Our results indicate that the C_{28} 1,13-diol, C_{30} 1,15-diol and C_{30} 1,15-keto-ol are, among LCDs and keto-ols, potentially least affected by oxic degradation, while the C_{28} 1,12-diol, C_{30} 1,13- and C_{30} 1,14-diols and the C_{32} 1,15-keto-ol are more affected. Since 1,14-diols and 1,13-/ 1,15-diols are produced by different biological source organisms (Volkman et al., 1992; Gelin et al., 1997b; Versteegh et al., 1997; Sinninghe Damsté et al., 2003; Rampen et al., 2007), a difference in degradation behavior under oxic conditions between both groups might be expected. However, differences between 1,13-diols and 1,15-diols, which presumably have the same biological source as they are often found together in cultured algae (Volkman et al., 1992; Gelin et al., 1997b; Rampen et al., 2012; Reiche et al., 2018), and show a strong temperature correlation in marine sediments (Rampen et al., 2012), are harder to explain. Our results are also in contrast to Rodrigo-Gámiz et al. (2016), who analyzed Arabian Sea sediments and showed a better preservation of 1,13-diols (RPE of 11 %) over 1,14-diols (RPE of 6 %) and 1,15-diols (RPE of 4 %), irrespective of chain length. This difference in degradation behavior among different LCDs has been explained by potentially higher abundances of certain LCDs occurring as bound lipids in contrast to free lipids (Rodrigo-Gámiz et al., 2016), i.e. implying that LCDs bound to organic matter by e.g. ester-bonds were released during oxic degradation. However, more recent results by Reiche et al. (2018) showed that oxic degradation did not alter the composition of both free and bound LCDs. The major differences between our results and the study of Rodrigo-Gámiz et al. (2016) are the study area and different oxygen exposure times. Whereas Buckley and Cranston (1986) estimated an oxygen exposure time of 10 kyr for the MAP f-turbidite, Lengger et al. (2014) reported an oxygen exposure time of just up to 200 years for Arabian Sea surface sediments. However, it is unclear how the difference in oxygen exposure time would lead to different RPEs for different LCDs.

Hoefs et al. (2002) studied LCDs in older turbidites of the Madeira Abyssal Plain of Pliocene age and showed much lower RPEs for both freely extractable LCDs ($C_{28,}$ C_{30} and C_{32} 1,15-diols) and keto-ols (C_{30} and C_{32} 1,15-keto-ols) than found here, i.e. for LCDs RPEs of < 0.5 to 2.5 % (vs. 7.1 % to 10.2 % reported here for the f-turbidite) and keto-ols 1.7 to 3.1 % (vs. 8.0 to 18.9 % for the f-turbidite). However, residual ester-bound LCDs and keto-ols (not studied here) showed significantly higher RPEs (Hoefs et al., 2002). The reason for the difference between the RPEs of extractable LCDs and keto-ols in the f-turbidite and the Pliocene turbidites is not clear and may be related to the older age and/or different oxygen exposure times.

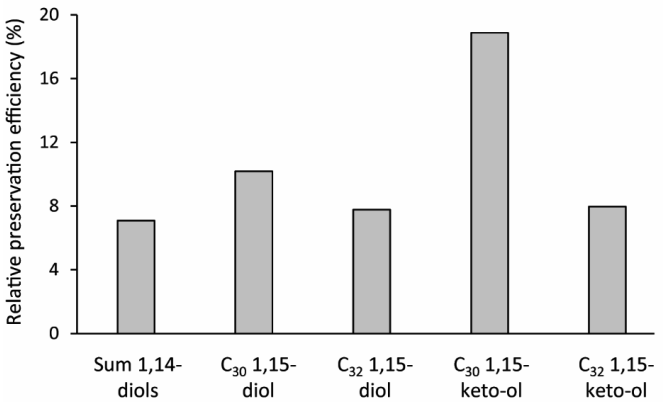

Fig. 2: Relative preservation efficiency (%) of LCDs and keto-ols in f-turbidite of MAP-1 core.

3.1.2. LCD and keto-ol indices

Commonly used LCD and keto-ol indices were calculated for the f-turbidite, i.e. the Diol Index I (Eq. 2) (Rampen et al., 2008), the LDI (Eq. 1) (Rampen et al., 2012), the fractional abundance of the C_{32} 1,15 LCD (Eq. 4) (Lattaud et al., 2017b) and various DOXIs (Eq. 5) (Ferreira et al., 2001). The Diol Index I, used here due to the predominance of the C_{30} 1,15-diol, showed a lower average value of 0.32 ± 0.01 in the oxidized zone than in the unoxidized zone (0.41 ± 0.01, Fig. 3A). The LDI showed similar, slightly higher values (0.84 ± 0.04) in the oxidized zone than in the unoxidized zone (0.81 ± 0.03. Fig. 3B). This would translate into reconstructed SSTs of 22.4 ± 1.3 °C in the oxidized zone and 21.7 ± 1.1 °C in the unoxidized zone of the turbidite using the SST calibration of de Bar et al. (2020). The FC_{32} 1,15-diol (Fig. 3C) decreased somewhat with increased oxygen exposure time with average values of 14.7 ± 1.6 % in the oxidized zone and 18.0 ± 1.6 % in the unoxidized zone. These indices, therefore, show an effect of post-depositional oxidation, which likely results from preferential preservation of the C_{30} 1,15-diol over 1,13- and 1,14-diols (Fig. 1).

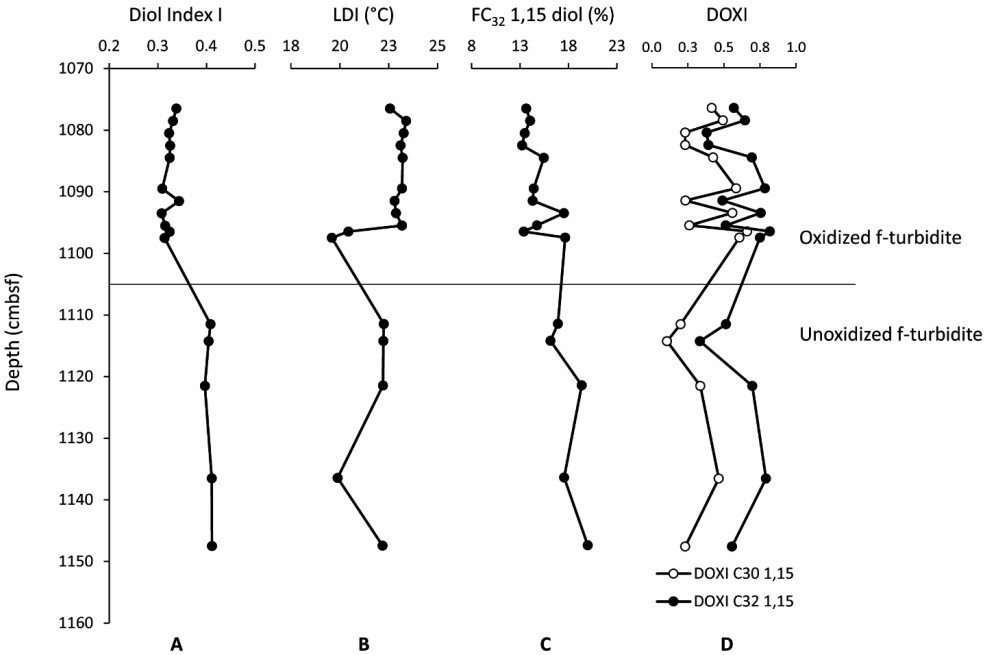

Fig. 3: Comparison of LCD and keto-ol indices over depth in f-turbidite of MAP-1 core. A: Diol Index I, B: LDI in °C, C: FC_{32} 1,15-diol in %, D: DOXI C_{30} 1,15 (depicted with open circles) and DOXI C_{32} 1,15 (depicted with black circles). Horizontal line marks stratigraphic boundary of the oxidized f-turbidite and the unoxidized f-turbidite (*cf.* Lengger et al. (2013).

This impact of post-depositional oxidation on the LDI differs from results reported for Arabian Sea surface sediments (Rodrigo-Gámiz et al., 2016). The latter study showed a decrease for the LDI, showing differences of 2.0 – 3.5 °C, due to a better preservation of the 1,13-diols. Furthermore, no impact of oxygen exposure was noted in that study for the Diol Index I as 1,15- and 1,14-diols were equally well preserved. As discussed above, the main differences are the different study regions, and possibly therefore different marine sources of diols, as well as the quite different oxygen exposure times of the turbidites versus the Arabian Sea sediments but it remains unclear how this would impact the different RPEs of LCDs. In any case, it suggests that oxic degradation can have variable effects on the different LCD indices.

The DOXI index has been applied to study paleo-oxicity and post-depositional oxidation (Ferreira et al., 2001; Bogus et al., 2012; Rodrigo-Gámiz et al., 2016), which is based on the idea that keto-ols are likely intermediate products formed by oxidation of LCDs as, for example, has been demonstrated by the study of post-depositional oxidation of sapropels (Ferreira et al., 2001). Indeed, a biological source of keto-ols is still unknown (Volkman et al., 1992; Versteegh et al., 1997; Méjanelle et al., 2003; Sinninghe Damsté et al., 2003; Versteegh and Lipp, 2019). The C_{30} 1,15-DOXI (Fig. 3D) showed higher average values in the oxidized turbidite, i.e. 0.43 ± 0.17 in the oxidized zone vs. 0.27 ± 0.14 in the unoxidized zone. The C_{32} 1,15-DOXI (Fig. 3D) also showed higher average values (0.62 ± 0.16 in the oxidized zone vs. 0.58 ± 0.18 in the unoxidized zone) but the difference is not significant. Therefore, especially the C_{30} 1,15-DOXI showed the impact of post-depositional oxidation. While the DOXI values in the unoxidized

zone likely reflect oxidation of LCDs during water column settling, deposition in the surface shelf sediments and transport to the abyssal plain during turbidite deposition, the higher DOXI values in the oxidized zone may be the result of additional formation of keto-ols from LCDs by post-depositional oxidation of the turbidite. The higher overall values for the C_{32} 1,15-DOXI, in comparison to C_{30} 1,15-DOXI, may be due to the different origin of the C_{32} 1,15-diols, i.e. they can be derived from an input of distant riverine sources (Lattaud et al., 2017b, 2018) and thus be oxidized to keto-ols already during transport from the river mouth to the shelf sediment. The C_{30} 1,14-DOXI also showed higher values of 0.35 ± 0.15 in the oxidized turbidite than in the unoxidized zone (0.17 ± 0.08). If the keto-ols are formed by post-depositional oxidation of LCDs, then the somewhat lower overall values for the 1,14-DOXI, compared to the C_{30} and C_{32} 1,15-DOXI may be the result of a different matrix preservation of 1,14-diols over 1,13- and 1,15-diols. 1,14-diols are hypothesized to being initially less exposed to oxygen during settling through the water column due to the initially protective silica skeleton and generally heavier cells of *Proboscia* diatoms and therefore less production of corresponding keto-ols, as previously discussed by Rampen et al. (2007) and Sinninghe Damsté et al. (2003). Small changes in DOXI trends are visible in the unoxidized zone, similar to the trends of LCDs, keto-ols and the other LCD indices, and suggest some inhomogeneity in the unoxidized turbidite.

Our data therefore are in contrast with another study which showed only a weak relationship of DOXI with oxygen exposure time in the Arabian Sea (Rodrigo-Gámiz et al., 2016). In other studies, differences between LCD and keto-ol carbon chain lengths, i.e. C_{26} to C_{34} for LCDs and C_{28} to C_{36} for keto-ols, and mismatches between LCDs and keto-ols, i.e. an unsaturated $C_{32:1}$ keto-ols without matching parent diol or $C_{30:1}$ 1,14-diols without matching keto-ols, as evidenced by HPLC-APCI-MS analyses (Versteegh and Lipp, 2019) have also been reported.

3.1.3. Comparison of LCDs with GDGTs and GDGT proxies

RPE values for GDGTs were measured for the same f-turbidite, with RPE values of 3.5 % and 4.4 % for core lipid derived and intact polar lipid derived branched GDGTs, respectively, and RPEs of 0.25 to 0.31 % and 0.49 to 2.2 % for core lipid and intact polar lipid isoprenoid GDGTs, respectively (Lengger et al., 2013). The higher RPEs for branched GDGTs have been suggested to be the result of enhanced preservation of terrigenous derived GDGTs in contrast to marine derived GDGTs in combination with some minor contributions by in-situ production (Huguet et al., 2008; Lengger et al., 2013). In comparison, LCDs and keto-ols (RPE from 6.4 % to 18.9 %) seem to be better preserved than branched and isoprenoid GDGTs in the f-turbidite. This mirrors results on post-depositional oxidation studies of Arabian Sea sediments, which also showed a better preservation of LCDs and keto-ols over GDGTs (Sinninghe Damsté et al., 2002a).

Our analysis of the f-turbidite of the Madeira Abyssal Plain showed an impact of oxic degradation on the different LCD indices. An impact of post-depositional oxidation of the turbidite was also apparent for the BIT index (Huguet et al., 2008; Lengger et al., 2013), a proxy for the river- and soil contribution to marine environments based on branched GDGTs and crenarchaeol (Hopmans et al., 2004; Walsh et al., 2008). The preferential preservation of terrestrial-derived GDGTs over marine isoprenoid GDGTs resulted in an increase of BIT values upon post-depositional oxidation. In contrast, the FC_{32} 1,15-diol, a tracer for input of riverine organic matter (de Bar et al., 2016; Lattaud et al., 2017b), showed a decrease. This difference may be explained by the different origins of the branched GDGTs versus the C_{32} 1,15-diol, i.e. when derived from the continent it is mainly originating from rivers and lakes (Rampen et al., 2014a; Lattaud et al., 2017b, 2018, 2019b), while the former is, when derived from land, also sourced from soil run-off (Hopmans et al., 2004). Irrespective of the cause, our results suggest

that changes in oxygen exposure time may cause a difference between these two terrestrial proxies, i.e. the BIT index might increase, while the FC_{32} 1,15-diol would decrease upon post-depositional oxidation, although the latter decrease is relatively minor.

With respect to the temperature proxies, the effect of oxic degradation on the TEX_{86} was negligible in the f-turbidite (Lengger et al., 2013), which is partly in agreement with Huguet et al. (2009), who showed only small increases of TEX_{86} in the Madeira Abyssal Plain f-turbidite with increased oxygen exposure. The small increase in the study of Huguet et al. (2009) was explained by preferential preservation of soil-derived isoprenoid GDGTs suggesting that oxic degradation may lead to small changes in the TEX_{86}. In the same study, a slight preferential degradation of the $C_{37:3}$ alkenone upon oxygen exposure was reported, resulting in a small increase in the $U^{K'}_{37}$ index, previously also shown by Hoefs et al. (1998b). These changes of the $U^{K'}_{37}$ index translated to changes in reconstructed SST < 0.5 °C, while for the LDI we show changes of ca. <1 °C with post-depositional oxidation, which are just slightly larger. In contrast, Rodrigo-Gámiz et al. (2016) indicated a decrease in the LDI, equivalent to 2.0–3.5 °C, in sediments from the Arabian Sea. Together, these results suggest that oxic exposure may result in unpredictable changes in LDI, although mostly within the calibration error of the proxy (de Bar et al., 2020). Overall, a change in oxygen exposure time in sediments will therefore cause (mostly small) changes in different organic temperature proxies, i.e. LDI, TEX_{86} and $U^{K'}_{37}$, but not always in a uniform direction. This may partly explain observed mismatches between LDI, TEX_{86} and $U^{K'}_{37}$ SST records (Lopes dos Santos et al., 2013; Jonas et al., 2017; de Bar et al., 2018).

4. Conclusions

The impact of post-depositional oxidation on the abundances and distributions of LCDs and LCD proxies were determined by analysis of a turbidite from the Madeira Abyssal Plain. The C_{28} 1,13-diol, C_{30} 1,15-diol and the C_{30} 1,15-keto-ol showed the highest preservation. The Diol Index I, the LDI and the fractional abundance of the C_{32} 1,15-diol were all impacted by post-depositional oxidation to some degree, likely due to a preferential preservation of the C_{30} 1,15-diol over 1,13- and 1,14-diol, suggesting that care has to be taken in applying these proxies in sediment cores deposited under changing oxygen exposure time. The DOXI indices showed increases in varying degrees with post-depositional oxidation, depending on the LCD chain length and mid-chain functional position, suggesting immediate formation of keto-ols.

Acknowledgments

This research has been funded by the European Research Council (ERC) under the European Union's Seventh Framework Program (FP7/2007-2013) ERC grant agreement [339206] to S.S. S.S and J.S.S.D. receive financial support from the Netherlands Earth System Science Centre (NESSC) through a gravitation grant (NWO 024.002.001) from the Dutch Ministry for Education, Culture and Science.

Table 1: Average LCD and keto-ol concentrations (variation indicated by standard deviation, n = 11 for oxidized turbidite, n = 5 for unoxidized turbidite), their derived relative preservation efficiency (RPE) and values for LCD indices in the oxidized and unoxidized zones of the f-turbidite.

Parameter	Oxidized Zone	Unoxidized zone	RPE (%)
Concentrations (μg/g dry sed.)			
C_{28} 1,12-diol	3 ± 1	37 ± 3	7.1
C_{28} 1,13-diol	3 ± 1	28 ± 9	10.8
C_{28} 1,14-diol	10 ± 4	128 ± 11	7.8
C_{30} 1,13-diol	4 ± 2	64 ± 27	7.1
C_{30} 1,14-diol	9 ± 3	137 ± 30	6.4
C_{30} 1,15-diol	39 ± 15	387 ± 60	10.2
C_{32} 1,15-diol	8 ± 3	106 ± 24	7.8
C_{30} 1,13-keto-ol	13 ± 8	104 ± 92	12.3
C_{30} 1,14-keto-ol	5 ± 3	32 ± 26	15.5
C_{30} 1,15-keto-ol	32 ± 20	171 ± 147	18.9
C_{32} 1,15-keto-ol	17 ± 12	210 ± 187	8.0
LCD indices			
Diol Index I	0.32 ± 0.01	0.41 ± 0.01	
LDI	0.84 ± 0.04	0.81 ± 0.03	
LDI SST (°C)	22.4 ± 1.3	21.7 ± 1.1	
FC_{32} 1,15-diol (%)	14.7 ± 1.6	18.0 ± 1.6	
C_{30} 1,13 DOXI	0.69 ± 0.14	0.56 ± 0.14	
C_{30} 1,14 DOXI	0.35 ± 0.15	0.17 ± 0.08	
C_{30} 1,15 DOXI	0.43 ± 0.17	0.27 ± 0.14	
C_{32} 1,15 DOXI	0.62 ± 0.16	0.58 ± 0.18	

Chapter 7

Synthesis

Since their development as proxies for paleo-reconstructions, the long-chain diols (LCD) proxies, i.e. the LDI and the Diol Index as well as newly established proxies such as the FC_{32} 1,15-diol index, are increasingly used. The LDI has since the start of work described in this thesis been applied in a variety of regions to reconstruct SST, along with the UK'_{37} and TEX_{86} proxies (Nieto-Moreno et al., 2015; Plancq et al., 2015; Rodrigo-Gámiz et al., 2015; de Bar et al., 2016, 2018; Jonas et al., 2017; Warnock et al., 2018; Zhu et al., 2018, 2019; Dauner et al., 2019; Lattaud et al., 2019a; Crampton-Flood et al., 2020; García-Alix et al., 2020; He et al., 2020). Furthermore, the LDI calibration has been refined (de Bar et al., 2020) and regional calibrations have been applied (Lattaud et al., 2019a; Yang et al., 2020). The FC_{32} 1,15-diol index has been recently developed to ascertain the riverine input into marine environments and applied in a variety of regions (de Bar et al., 2016; Lattaud et al., 2017a, 2017b; 2018; Häggi et al., 2019; He et al., 2020). Additionally, a number of studies have analyzed upwelling, nutrient and productivity conditions using the Diol Index and the newly developed Nutrient Diol Index (de Bar et al., 2018; Gal et al., 2018, 2019; Zhu et al., 2020). However, a lack of studies analyzing the impact of diagenesis on the application of LCD proxies is apparent. While a development and refinement of new and existing proxies is necessary and application in paleoenvironmental studies leads to new insights when developing climate proxies, the level of confidence in the proxy can only be raised when targeted studies are employed to constrain possible biases and diagenetic effects. In this thesis, the impact of diagenesis and sequestration on LCDs and associated proxies was studied in an effort to ascertain possible biases in the application of LCD proxies in paleoclimate reconstructions. In particular, the impact of oxygen exposure and the mode of occurrence was analyzed in algal biomass and marine sediments.

Research described in chapter 2, 3 and 4 revealed a number of issues that represent some of the underlying problems in using LCDs in paleo-reconstructive studies. The large-scale aerobic degradation of *N. oculata* biomass showed that LCDs are in fact not degraded in the time span of the incubation (271 days), nor is the structure of the algaenan affected (chapter 2 and 3). This suggest that both are well preserved, at least in suspended particulate matter and settling particles in the water column. Recently, Balzano et al. (2018) used 18S rRNA amplicon sequencing in suspended particulate matter from the western tropical North Atlantic Ocean to identify potential sources of 1,13- and 1,15-diols. However, only weak relationships between the abundance of sequences and the concentrations of the C_{30} 1,15-diols were shown. This was attributed to the low degradability of the C_{30} 1,15-diol compared to DNA, in agreement with the observation of low degradability of LCDs on short times scales described in thesis (chapter 2). Additionally, this suggests that it will be difficult to determine the unknown producers of marine 1,13- and 1,15-diols by comparing LCD abundances with DNA abundance or even microscopic analysis as the degradability of the LCDs is much lower than that of DNA or intact cells.

LCDs are commonly considered to be the building blocks of the biopolymer algaenan (de Leeuw et al., 1981; Tegelaar et al., 1989b; Gelin et al., 1997b, 1999; Volkman et al., 1998; Scholz et al., 2014; Zhang and Volkman, 2017). Algaenan is thought to play a role in the cell protection due to its non-hydrolysable and highly resistant character (Tegelaar et al., 1989b; de Leeuw and Largeau, 1993; Largeau and de Leeuw, 1995; Blokker et al., 2000; van Bergen et al., 2004). Indeed, a significant structure change in the algaenan of *N. oculata* was not observed, although it could not be ruled out that the abundance of algaenan diminished (chapter 3). Furthermore, it is likely that outer parts of the algaenan were affected as indicated by the release of LCDs (chapter 2). While the pyrolysis GC-MS analysis represented a qualitative approach, a quantitative approach is required to ascertain if the actual abundance of algaenan decreased during oxic degradation. This could for example be achieved by relative quantitation using authentic standards (Hoefs et al., 1998b). Additionally, the application of additional pyrolysis GC-MS techniques might be advantageous, i.e. by tetramethylammonium hydroxide (TMAH)

pyrolysis (De Leeuw and Baas, 1993; Clifford et al., 1995; Nierop, 1998). TMAH pyrolysis might enable a more targeted breakdown of the algaenan and due to the additional methylation of more polar lipids, might lead to a more in-depth structural analysis of the algaenan. Furthermore, application of chemically degradative methods, i.e. by HI or RuO_4 degradation (Blokker et al., 1998b, 2000, 2006), could shed further light on the potentially aerobically degraded algaenan structure and composition.

Commonly, LCDs are thought to be extractable-bound in algal biomass and to only occur in low concentrations as freely extractable lipids (Volkman et al., 1992). However, as shown here, results indicate otherwise (chapter 4) as high concentrations of freely occurring LCDs were detected. Interestingly, analysis of different strains of *Nannochloropsis spp.* highlighted that application of a saponification and subsequent acid hydrolysis, which should in theory release additional lipids, in contrast led to a decrease in lipid concentration (chapter 2, 4, 5). While losses during the work-up might have led to a decrease, e.g. from shaking against water and subsequent dissolution or micelle formation, the formation of melanoidin-like polymers induced by harsh consecutive hydrolyses (Allard et al., 1997, 1998) could potentially lead to the binding of the LCDs to other compounds. The use of trifluoroacetic acid in hydrolyses (Allard et al., 1998) has been applied previously in the context of algaenan isolation as an alternative and may represent another methodological approach to be used in the analysis of bound LCDs both in biomass and sediment studies. Nevertheless, the lack of soluble macromolecules, equivalent to the algaenan (chapter 4), is somewhat surprising in that it would be expected that a less densely cross-polymerized algaenan would be soluble and degradable by chemical agents. Possibly, different approaches during the cultivation of the algal biomass, preparation of the biomass, i.e. freeze drying and storage until the work-up, and the eventual chemical work-up might lead to further insights if there are soluble parts of the algaenan.

Intriguingly, the results of the first chapters describing the analysis of LCDs in mostly aerobically degraded biomass of *Nannochloropsis spp.* (chapter 2, 3, 4) were often in contrast to the results from the natural environment (chapter 5 and 6). For example, in contrast to the results of the aerobic incubation experiment, LCDs were not only predominant as freely occurring lipids, but also occurred abundantly extractable-bound LCDs inside of the sapropel (chapter 5). In fact, above and below the sapropel, at low TOC values, LCDs occurred as residually ester-bound and residually glycosidic ether- or amide bound lipids only, although present in low concentrations. Interestingly, the finding of a higher abundance of extractable-bound 1,14-diols, compared to freely occurring 1,14-diols, in the S5 sapropel sediments is surprising as *Proboscia* diatoms represent a silica-based organism, which likely does not contain a biopolymer similar to the algaenan, in contrast to Eustigmatophyte alga. However, studies analyzing *Proboscia* biomass similarly to the approach outlined in chapters 2, 4 and 5, do not exist and could highlight how 1,14-diols are bound to the biomass.

While an impact of oxygen exposure could not be shown for the LDI in the aerobic incubation experiment (chapter 2), oxic degradation had a significant impact on LCD proxies in turbidites of the Madeira Abyssal Plain, which had been impacted by post-depositional oxidation (chapter 6). These results were furthermore mirrored by Rodrigo-Gámiz et al. (2016), who analyzed the impact of oxic degradation in Arabian Sea sediments and similarly showed an effect of oxygen exposure on LCD proxies. While both environmental studies indicated a potential preferential preservation of certain LCD isomers, the impact of oxic degradation affected the LCDs and LCD proxies differently in both studies and showed different preservation for the different isomers. Therefore, the change in values of LCD proxies upon oxygen exposure was not unidirectional nor consistent with the short-term aerobic degradation experiment (chapter 2). These differences may point to different modes of breakdown of LCDs in biomass and sediment. While the release of LCDs in the oxic degradation experiment (chapter 2) and therefore, the impact of oxygen exposure, was possibly governed by the external parts of the

algaenan, additional mechanisms of selective degradation seem to take place in the sediment. However, up to now, the knowledge of degradation mechanisms upon oxygen exposure is restricted to degradative time spans of under a year (chapter 2, 3), about 200 years (Rodrigo-Gámiz et al., 2016), and about 10 kyr (chapter 6). Therefore, further studies are needed to analyze the impact of oxygen exposure over time spans longer than 200 years and up to 10 kyr, i.e. by analysis of suitable sediments or further experimental studies. Furthermore, these studies comprise different regions with possibly different LCD producer compositions leading to a heterogeneity in the starting LCD pool prior to degradation. Possibly, the analysis of fossilized algaenan in sediments, could shed light on possible changes of algaenan structure upon longer oxygen exposure times. Pyrolysis GC-MS studies have shown a selective preservation of the aliphatic signatures, revealed by a series of *n*-alkene/ *n*-alkane pyrolysis products, likely pertaining to algaenans with increased oxygen exposure time (Hoefs et al., 1998b). A similar, targeted approach, analyzing and contrasting the LCD signatures of the algaenan of Eustigmatophytes, i.e. mid-chain ketones and n-alkan-1-ones, in sediments impacted by post-depositional oxidation could highlight possible changes over longer oxygen exposure times, but also further our knowledge of the algaenan of not only recent biomass but also fossilized biomass.

Overall, the application of LCDs and LCD proxies in paleoenvironmental proxies shows great promise and they will likely be increasingly used in future research, especially complimentary to already existing paleoclimate proxies. However, this thesis also highlighted that a number of issues need to be taken into consideration. An underlying problem of LCD proxy application remains the unidentified producer of 1,13- and 1,15-diols, since the mechanisms for their distribution and composition in biomass and the natural environment can only be properly understood when knowing the source organism. This also applies to gaining a better understanding of the biosynthetic pathways that are producing LCDs in the producer organism and comprehension of the nature of the biopolymer algaenan. However, this thesis especially highlighted the need for additional studies analyzing the impact of diagenesis. While open questions remain concerning the impact of oxygen exposure on LCD proxies, additional diagenetic processes have not yet been explored and need to be addressed, such as the impact of lateral transport on LCDs.

References

Ahmed, M., Schouten, S., Baas, M., de Leeuw, J.W., 2000. Bound lipids in kerogens from the Monterey formation, Naples Beach, California, in: Isaacs, C.M., Rullkötter, J. (Eds.), The Monterey Formation: From Rock to Molecules. Colombia University Press, New York, pp. 189-205.

Allard, B., Templier, J., Largeau, C., 1997. Artifactual origin of mycobacterial bacteran. Formation of melanoidin-like artifact macromolecular material during the usual isolation process. Organic Geochemistry 26, 691-703.

Allard, B., Templier, J., Largeau, C., 1998. An improved method for the isolation of artifact-free algaenans from microalgae. Organic Geochemistry 28, 543-548.

Bale, N.J., Hopmans, E.C., Zell, C., de Lima Sobrinho, R., Kim, J.H., Sinninghe Damsté, J.S., Villareal, T.A., Schouten, S., 2015. Long chain glycolipids with pentose head groups as biomarkers for marine endosymbiotic heterocystous cyanobacteria. Organic Geochemistry 81, 1-7.

Bale, N.J., Hennekam, R., Hopmans, E.C., Dorhout, D., Reichart, G.-J., van der Meer, M., Villareal, T.A., Sinninghe Damsté, J.S., Schouten, S., 2019. Biomarker evidence for nitrogen-fixing cyanobacterial blooms in a brackish surface layer in the Nile River plume during sapropel deposition. Geology 47, 1088-1092.

Balzano, S., Villanueva, L., de Bar, M., Sinninghe Damsté, J.S., Schouten, S., 2017. Impact of culturing conditions on the abundance and composition of long chain alkyl diols in species of the genus *Nannochloropsis*. Organic Geochemistry 108, 9-17.

Balzano, S., Lattaud, J., Villanueva, L., Rampen, S.W., Brussaard, C.P., Van Bleijswijk, J., Bale, N., Sinninghe Damsté, J.S., Schouten, S., 2018. A quest for the biological sources of long chain alkyl diols in the western tropical North Atlantic Ocean. Biogeosciences 15, 5951-5968.

Bauersachs, T., Hopmans, E.C., Compaoré, J., Stal, L.J., Schouten, S., Sinninghe Damsté, J.S., 2009. Rapid analysis of long-chain glycolipids in heterocystous cyanobacteria using high-performance liquid chromatography coupled to electrospray ionization tandem mass spectrometry. Rapid Communications in Mass Spectrometry 23, 1387-1394.

Bemis, B.E., Spero, H.J., Bijma, J., Lea, D.W., 1998. Reevaluation of the oxygen isotopic composition of planktonic foraminifera: Experimental results and revised paleotemperature equations. Paleoceanography 13, 150-160.

Besseling, M.A., Hopmans, E.C., Koenen, M., van der Meer, M.T., Vreugdenhil, S., Schouten, S., Sinninghe Damsté, J.S., Villanueva, L., 2019. Depth-related differences in archaeal populations impact the isoprenoid tetraether lipid composition of the Mediterranean Sea water column. Organic Geochemistry 135, 16-31.

Biller, P., Ross, A., 2014. Pyrolysis GC–MS as a novel analysis technique to determine the biochemical composition of microalgae. Algal Research 6, 91-97.

Blokker, P., Schouten, S., van den Ende, H., de Leeuw, J.W., Sinninghe Damsté, J.S., 1998a. Cell wall-specific ω-hydroxy fatty acids in some freshwater green microalgae. Phytochemistry 49, 691-695.

Blokker, P., Schouten, S., Van den Ende, H., de Leeuw, J.W., Hatcher, P.G., Sinninghe Damsté, J.S., 1998b. Chemical structure of algaenans from the fresh water algae *Tetraedron minimum*, *Scenedesmus communis* and *Pediastrum boryanum*. Organic Geochemistry 29, 1453-1468.

Blokker, P., Schouten, S., de Leeuw, J.W., Sinninghe Damsté, J.S., van den Ende, H., 2000. A comparative study of fossil and extant algaenans using ruthenium tetroxide degradation. Geochimica et Cosmochimica Acta 64, 2055-2065.

Blokker, P., van den Ende, H., de Leeuw, J.W., Versteegh, G.J.M., Sinninghe Damsté, J.S., 2006. Chemical fingerprinting of algaenans using RuO_4 degradation. Organic Geochemistry 37, 871-881.

Bogus, K.A., Zonneveld, K.A.F., Fischer, D., Kasten, S., Bohrmann, G., Versteegh, G.J.M., 2012. The effect of meter-scale lateral oxygen gradients at the sediment-water interface on selected organic matter based alteration, productivity and temperature proxies. Biogeosciences 9, 1553-1570.

Brassell, S., Eglinton, G., Marlowe, I., Pflaumann, U., Sarnthein, M., 1986. Molecular stratigraphy: a new tool for climatic assessment. Nature 320, 129-133.

Buckley, D., Cranston, R., 1988. Early diagenesis in deep sea turbidites: The imprint of paleo-oxidation zones. Geochimica et Cosmochimica Acta 52, 2925-2939.

Canuel, E.A., Martens, C.S., 1996. Reactivity of recently deposited organic matter: Degradation of lipid compounds near the sediment-water interface. Geochimica Et Cosmochimica Acta 60, 1793-1806.

Castañeda, I.S., Schouten, S., 2011. A review of molecular organic proxies for examining modern and ancient lacustrine environments. Quaternary Science Reviews 30, 2851-2891.

Clifford, D.J., Carson, D.M., McKinney, D.E., Bortiatynski, J.M., Hatcher, P.G., 1995. A new rapid technique for the characterization of lignin in vascular plants: thermochemolysis with tetramethylammonium hydroxide (TMAH). Organic Geochemistry 23, 169-175.

Contreras, S., Lange, C.B., Pantoja, S., Lavik, G., Rincón-Martínez, D., Kuypers, M.M., 2010. A rainy northern Atacama Desert during the last interglacial. Geophysical Research Letters 37.

Cowie, G., Calvert, S., de Lange, G., Keil, R., Hedges, J., 1998. Extents and implications of organic matter alteration at oxidation fronts in turbidites from the Madeira Abyssal Plain, in: Weaver, P.P.E., Schmincke, H.-U., Firth, J.V., Duffield, W. (Eds.), Proceedings of the Ocean Drilling Program, Scientific Results, 157: College Station, TX (Ocean Drilling Program), pp. 581-589.

Cowie, G.L., Hedges, J.I., 1994. Biochemical indicators of diagenetic alteration in natural organic matter mixtures. Nature 369, 304-307.

Cowie, G.L., Hedges, J.I., Prahl, F.G., de Lange, G.J., 1995. Elemental and major biochemical changes across an oxidation front in a relict turbidite: an oxygen effect. Geochimica et Cosmochimica Acta 59, 33-46.

Crampton-Flood, E.D., Noorbergen, L.J., Smits, D., Boschman, R.C., Donders, T.H., Munsterman, D.K., Ten Veen, J., Peterse, F., Lourens, L., Sinninghe Damsté, J.S., 2020. A new age model for the Pliocene of the southern North Sea basin: a multi-proxy climate reconstruction. Climate of the Past 16, 523-541.

Cranwell, P., 1981. Diagenesis of free and bound lipids in terrestrial detritus deposited in a lacustrine sediment. Organic Geochemistry 3, 79-89.

Cranwell, P., Eglinton, G., Robinson, N., 1987. Lipids of aquatic organisms as potential contributors to lacustrine sediments—II. Organic Geochemistry 11, 513-527.

Dauner, A.L.L., Mollenhauer, G., Bícego, M.C., de Souza, M.M., Nagai, R.H., Figueira, R.C.L., de Mahiques, M.M., e Sousa, S.H.d.M., Martins, C.C., 2019. Multi-proxy reconstruction of sea surface and subsurface temperatures in the western South Atlantic over the last~ 75 kyr. Quaternary Science Reviews 215, 22-34.

de Bar, M.W., Dorhout, D.J., Hopmans, E.C., Rampen, S.W., Sinninghe Damsté, J.S., Schouten, S., 2016. Constraints on the application of long chain diol proxies in the Iberian Atlantic margin. Organic Geochemistry 101, 184-195.

de Bar, M.W., Stolwijk, D.J., McManus, J.F., Sinninghe Damsté, J.S., Schouten, S., 2018. A Late Quaternary climate record based on long-chain diol proxies from the Chilean margin. Climate of the Past 14, 1783-1803.

de Bar, M.W., Rampen, S.W., Hopmans, E.C., Sinninghe Damsté, J.S., Schouten, S., 2019. Constraining the applicability of organic paleotemperature proxies for the last 90 Myrs. Organic Geochemistry 128, 122-136.

de Bar, M.W., Weiss, G., Rampen, S., Lattaud, J., Bale, N.J., Brummer, G.-J.A., Schulz, H., Rush, D., Kim, J.-H., Donner, B., Knies, J., Lückge, A., Stuut, J.-B., Sinninghe Damsté, J.S., Schouten, S., 2020. Global temperature calibration of the Long chain Diol Index in marine surface sediments. Organic Geochemistry 142, 103983.

de Lange, G., Middelburg, J., Pruysers, P., 1989. Middle and Late Quaternary depositional sequences and cycles in the eastern Mediterranean. Sedimentology 36, 151-156.

de Lange, G., 1992. Distribution of exchangeable, fixed, organic and total nitrogen in interbedded turbiditic/pelagic sediments of the Madeira Abyssal Plain, eastern North Atlantic. Mar Geol 109, 95-114.

de Lange, G.J., Jarvis, I., Kuijpers, A., 1987. Geochemical characteristics and provenance of late Quaternary sediments from the Madeira Abyssal Plain, N Atlantic. Geological Society, London, Special Publications 31, 147-165.

de Lange, G.J., 1998. Oxic vs.anoxic diagenetic alteration of Turbiditic sediments in the Madeira Abyssal Plain, Eastern North Atlantic. Proceedings of the Ocean Drilling Program, Scientific Results 157, 573-580.

de Leeuw, J., vd Meer, F., Rijpstra, W., Schenck, P., 1980. On the occurrence and structural identification of long chain unsaturated ketones and hydrocarbons in sediments. Physics and Chemistry of the Earth 12, 211-217.

De Leeuw, J., Baas, M., 1993. The behaviour of esters in the presence of tetramethylammonium salts at elevated temperatures; flash pyrolysis or flash chemolysis? Journal of Analytical and Applied Pyrolysis 26, 175-184.

de Leeuw, J.W., Rijpstra, W.I.C., Schenck, P.A., 1981. The occurrence and identification of C_{30}, C_{31} and C_{32} alkan-1,15-diols and alkan-15-one-1-ols in Unit I and Unit II Black Sea sediments. Geochimica et Cosmochimica Acta 45, 2281-2285.

de Leeuw, J.W., Rijpstra, W.I.C., Mur, L.R., 1992. The absence of long-chain alkyl diols and alkyl keto-1-ols in cultures of the cyanobacterium *Aphanizomenon flos-aquae*. Organic Geochemistry 18, 575-578.

de Leeuw, J.W., Largeau, C., 1993. A review of macromolecular organic compounds that comprise living organisms and their role in kerogen, coal and petroleum formation., in: Engel, M.H., Macko, S.A. (Eds.), Organic Geochemistry. Topics in Geobiology, Vol. 11. Springer, Boston, MA, pp. 23-63.

Derenne, S., Largeau, C., Casadevall, E., Berkaloff, C., 1989. Occurrence of a resistant biopolymer in the *L* race of *Botryococcus braunii*. Phytochemistry 28, 1137-1142.

Derenne, S., Largeau, C., Berkaloff, C., Rousseau, B., Wilhelm, C., Hatcher, P., 1992a. Non-hydrolysable macromolecular constituents from outer walls of *Chlorella fusca* and *Nanochlorum eucaryotum*. Phytochemistry 31, 1923-1929.

Derenne, S., Le Berre, F., Largeau, C., Hatcher, P., Connan, J., Raynaud, J., 1992b. Formation of ultralaminae in marine kerogens via selective preservation of thin resistant outer walls of microalgae. Organic Geochemistry 19, 345-350.

Durand, B., 1980. Kerogen: Insoluble organic matter from sedimentary rocks. Editions technip, Paris.

Emeis, K.C., Schulz, H.M., Struck, U., Sakamoto, T., Doose, H., 1998. Stable isotope and alkenone temperature records of sapropels from Sites 964 and 967: constraining the physical environment of sapropel formation in the Eastern Mediterranean Sea, in: Robertson, A.H.F., Emeis, K.-C., Richter, C., Camerlenghi, A. (Eds.), Proceedings of the Ocean Drilling Program. Scientific Results, 160: College Station, TX (Ocean Drilling Program), pp. 309-331.

Emeis, K.C., Schulz, H., Struck, U., Rossignol-Strick, M., Erlenkeuser, H., Howell, M., Kroon, D., Mackensen, A., Ishizuka, S., Oba, T., 2003. Eastern Mediterranean surface water temperatures and $\delta^{18}O$ composition during deposition of sapropels in the late Quaternary. Paleoceanography 18.

Emiliani, C., 1954. Depth habitats of some species of pelagic Foraminifera as indicated by oxygen isotope ratios. American Journal of Science 252, 149-158.

Epstein, S., Buchsbaum, R., Lowenstam, H.A., Urey, H.C., 1953. Revised carbonate-water isotopic temperature scale. Geological Society of America Bulletin 64, 1315-1326.

Farrington, J.W., Quinn, J.G., 1973. Biogeochemistry of Fatty-Acids in Recent Sediments from Narragansett-Bay, Rhode-Island. Geochimica Et Cosmochimica Acta 37, 259-268.

Farrington, J.W., Henrichs, S.M., Anderson, R., 1977. Fatty-Acids and Pb-210 Geochronology of a Sediment Core from Buzzards-Bay, Massachusetts. Geochimica et Cosmochimica Acta 41, 289-296.

Fawley, M.W., Jameson, I., Fawley, K.P., 2015. The phylogeny of the genus *Nannochloropsis* (Monodopsidaceae, Eustigmatophyceae), with descriptions of *N. australis sp. nov.* and *Microchloropsis gen. nov*. Phycologia 54, 545-552.

Ferreira, A.M., Miranda, A., Caetano, M., Baas, M., Vale, C., Sinninghe Damsté, J.S., 2001. Formation of mid-chain alkane keto-ols by post-depositional oxidation of mid-chain diols in Mediterranean sapropels. Organic Geochemistry 32, 271-276.

Gal, J.-K., Kim, J.-H., Shin, K.-H., 2018. Distribution of long chain alkyl diols along a south-north transect of the northwestern Pacific region: Insights into a paleo sea surface nutrient proxy. Organic Geochemistry 119, 80-90.

Gal, J.-K., Kim, J.-H., Kim, S., Lee, S.H., Yoo, K.-C., Shin, K.-H., 2019. Application of the newly developed nutrient diol index (NDI) as a sea surface nutrient proxy in the East Sea for the last 240 years. Quaternary International 503, 146-152.

García-Alix, A., Jiménez Moreno, G., Pérez Martínez, M.D.C., Jiménez, L., Rodrigo-Gámiz, M., 2020. Algal lipids reveal unprecedented warming rates in alpine areas of SW Europe during the industrial period. Climate of the Past 16, 245-263.

Gelin, F., Boogers, I., Noordeloos, A.A., Sinninghe Damsté, J., Hatcher, P.G., de Leeuw, J.W., 1996. Novel, resistant microalgal polyethers: An important sink of organic carbon in the marine environment? Geochimica et Cosmochimica Acta 60, 1275-1280.

Gelin, F., Volkman, J.K., de Leeuw, J.W., Sinninghe Damsté, J.S., 1997a. Mid-chain hydroxy long-chain fatty acids in microalgae from the genus *Nannochloropsis*. Phytochemistry 45, 641-646.

Gelin, F., Boogers, I., Noordeloos, A.A.M., Sinninghe Damsté, J.S., Riegman, R., de Leeuw, J.W., 1997b. Resistant biomacromolecules in marine microalgae of the classes Eustigmatophyceae and Chlorophyceae: Geochemical implications. Organic Geochemistry 26, 659-675.

Gelin, F., Volkman, J.K., Largeau, C., Derenne, S., Sinninghe Damsté, J.S., de Leeuw, J.W., 1999. Distribution of aliphatic, nonhydrolyzable biopolymers in marine microalgae. Organic Geochemistry 30, 147-159.

Gong, C., Hollander, D.J., 1999. Evidence for differential degradation of alkenones under contrasting bottom water oxygen conditions: Implication for paleotemperature reconstruction. Geochimica et Cosmochimica Acta 63, 405-411.

Goossens, H., Rijpstra, W.I.C., Düren, R.R., de Leeuw, J.W., Schenck, P.A., 1986. Bacterial contribution to sedimentary organic matter; a comparative study of lipid moieties in bacteria and recent sediments. Organic Geochemistry 10, 683-696.

Goossens, H., Düren, R.R., de Leeuw, J.W., Schenck, P.A., 1989a. Lipids and their mode of occurrence in bacteria and sediments - II. Lipids in the sediment of a stratified, freshwater lake. Organic Geochemistry 14, 27-41.

Goossens, H., De Leeuw, J., Irene, W., Rijpstra, C., Meyburg, G., Schenck, P., 1989b. Lipids and their mode of occurrence in bacteria and sediments—IA methodological study of the lipid composition of Acinetobacter calcoaceticus LMD 79-41. Organic Geochemistry 14, 15-25.

Goth, K., De Leeuw, J., Püttmann, W., Tegelaar, E., 1988. Origin of Messel oil shale kerogen. Nature 336, 759-761.

Grossi, V., Baas, M., Schogt, N., Breteler, W.K., de Leeuw, J., Rontani, J.-F., 1996. Formation of phytadienes in the water column: myth or reality? Organic Geochemistry 24, 833-839.

Grossi, V., Blokker, P., Sinninghe Damsté, J.S., 2001. Anaerobic biodegradation of lipids of the marine microalga *Nannochloropsis salina*. Organic Geochemistry 32, 795-808.

Guillard, R.R., 1975. Culture of phytoplankton for feeding marine invertebrates, Culture of marine invertebrate animals. Springer, pp. 29-60.

Häggi, C., Schefuß, E., Sawakuchi, A.O., Chiessi, C.M., Mulitza, S., Bertassoli Jr, D.J., Hefter, J., Zabel, M., Baker, P.A., Schouten, S., 2019. Modern and late Pleistocene particulate organic carbon transport by the Amazon River: Insights from long-chain alkyl diols. Geochimica et Cosmochimica Acta 262, 1-19.

Hartnett, H.E., Keil, R.G., Hedges, J.I., Devol, A.H., 1998. Influence of oxygen exposure time on organic carbon preservation in continental margin sediments. Nature 391, 572-575.

Harvey, H.R., Macko, S.A., 1997a. Kinetics of phytoplankton decay during simulated sedimentation: changes in lipids under oxic and anoxic conditions. Organic Geochemistry 27, 129-140.

Harvey, H.R., Macko, S.A., 1997b. Catalysts or contributors? Tracking bacterial mediation of early diagenesis in the marine water column. Organic Geochemistry 26, 531-544.

He, H., Rodgers, R.P., Marshall, A.G., Hsu, C.S., 2011. Algae polar lipids characterized by online liquid chromatography coupled with hybrid linear quadrupole ion trap/fourier transform ion cyclotron resonance mass spectrometry. Energy & Fuels 25, 4770-4775.

He, L., Kang, M., Zhang, D., Jia, G., 2020. Evaluation of environmental proxies based on long chain alkyl diols in the East China Sea. Organic Geochemistry 139, 103948.

Hedges, J.I., Hu, F.S., Devol, A.H., Hartnett, H.E., Tsamakis, E., Keil, R.G., 1999. Sedimentary organic matter preservation; a test for selective degradation under oxic conditions. American Journal of Science 299, 529-555.

Higgs, N., Thomson, J., Wilson, T., Croudace, I., 1994. Modification and complete removal of eastern Mediterranean sapropels by postdepositional oxidation. Geology 22, 423-426.

Hoefs, M.J.L., Versteegh, G.J.M., Rijpstra, W.I.C., de Leeuw, J.W., Sinninghe Damsté, J.S., 1998a. Postdepositional oxic degradation of alkenones: Implications for the measurement of palaeo sea surface temperatures. Paleoceanography 13, 42-49.

Hoefs, M.J.L., Sinninghe Damsté, J.S., de Lange, G.J., de Leeuw, J.W., 1998b. Changes in kerogen composition across an oxidation front in Madeira Abyssal Plain turbidites as revealed by pyrolysis GC-MS, in: Weaver, P.P.E., Schmincke, H.-U., Firth, J.V., Duffield, W. (Eds.), Proceedings of the Ocean Drilling Program, Scientific Results, 157: College Station, TX (Ocean Drilling Program), pp. 591-607.

Hoefs, M.J.L., Rijpstra, W.I.C., Sinninghe Damsté, J.S., 2002. The influence of oxic degradation on the sedimentary biomarker record I: Evidence from Madeira Abyssal Plain turbidites. Geochimica et Cosmochimica Acta 66, 2719-2735.

Holguin, F.O., Schaub, T., 2013. Characterization of microalgal lipid feedstock by direct-infusion FT-ICR mass spectrometry. Algal Research 2, 43-50.

Hopmans, E.C., Weijers, J.W., Schefuß, E., Herfort, L., Sinninghe Damsté, J.S., Schouten, S., 2004. A novel proxy for terrestrial organic matter in sediments based on branched and isoprenoid tetraether lipids. Earth Planet Sc Lett 224, 107-116.

Huguet, C., de Lange, G.J., Gustafsson, Ö., Middelburg, J.J., Sinninghe Damsté, J.S., Schouten, S., 2008. Selective preservation of soil organic matter in oxidized marine sediments (Madeira Abyssal Plain). Geochimica et Cosmochimica Acta 72, 6061-6068.

Huguet, C., Kim, J.-H., de Lange, G.J., Sinninghe Damsté, J.S., Schouten, S., 2009. Effects of long term oxic degradation on the $U^{K'}_{37}$, TEX_{86} and BIT organic proxies. Organic Geochemistry 40, 1188-1194.

Hutton, A.C., 1987. Petrographic classification of oil shales. International Journal of Coal Geology 8, 203-231.

IPCC, 2014. Climate Change 2014: Synthesis Report. Contribution of working groups I. Contribution of working groups I, II and III to the Fifth Assessment Report of the Intergovernmental Panel on Climate Change [core Writing Team, R.K. Pachauri and L.A. Meyer (eds.)]. IPCC, Geneva, Switzerland, 151 pp.

Jonas, A.-S., Schwark, L., Bauersachs, T., 2017. Late Quaternary water temperature variations of the Northwest Pacific based on the lipid paleothermometers TEX^{H}_{86}, $U^{K'}_{37}$ and LDI. Deep Sea Research Part I: Oceanographic Research Papers 125, 81-93.

Kemp, A.E., Pearce, R.B., Koizumi, I., Pike, J., Rance, S.J., 1999. The role of mat-forming diatoms in the formation of Mediterranean sapropels. Nature 398, 57.

Kim, J.-H., Huguet, C., Zonneveld, K.A., Versteegh, G.J., Roeder, W., Sinninghe Damsté, J.S., Schouten, S., 2009a. An experimental field study to test the stability of lipids used for the TEX_{86} and $U^{K'}_{37}$ palaeothermometers. Geochimica et Cosmochimica Acta 73, 2888-2898.

Kim, J.-H., Crosta, X., Michel, E., Schouten, S., Duprat, J., Sinninghe Damsté, J.S., 2009b. Impact of lateral transport on organic proxies in the Southern Ocean. Quaternary Research 71, 246-250.

Kodner, R.B., Summons, R.E., Knoll, A.H., 2009. Phylogenetic investigation of the aliphatic, non-hydrolyzable biopolymer algaenan, with a focus on green algae. Organic Geochemistry 40, 854-862.

Largeau, C., Derenne, S., Casadevall, E., Kadouri, A., Sellier, N., 1986. Pyrolysis of immature Torbanite and of the resistant biopolymer (PRB A) isolated from extant alga *Botryococcus braunii*. Mechanism of formation and structure of torbanite. Organic Geochemistry 10, 1023-1032.

Largeau, C., de Leeuw, J.W., 1995. Insoluble, nonhydrolyzable, aliphatic macromolecular constituents of microbial cell walls, in: Jones, J.G. (Ed.), Advances in Microbial Ecology, Vol 14. Springer, Boston, MA, pp. 77-117.

Lattaud, J., Dorhout, D., Schulz, H., Castañeda, I.S., Schefuß, E., Sinninghe Damsté, J.S., Schouten, S., 2017a. The C_{32} alkane-1,15-diol as a proxy of late Quaternary riverine input in coastal margins. Climate of the Past 13, 1049-1061.

Lattaud, J., Kim, J.H., De Jonge, C., Zell, C., Sinninghe Damsté, J.S., Schouten, S., 2017b. The C_{32} alkane-1,15-diol as a tracer for riverine input in coastal seas. Geochimica et Cosmochimica Acta 202, 146-158.

Lattaud, J., Kirkels, F., Peterse, F., Freymond, C.V., Eglinton, T.I., Hefter, J., Mollenhauer, G., Balzano, S., Villanueva, L., Van Der Meer, M.T., 2018. Long-chain diols in rivers: distribution and potential biological sources. Biogeosciences 15, 4147-4161.

Lattaud, J., Lo, L., Zeeden, C., Liu, Y.-J., Song, S.-R., van der Meer, M.T., Sinninghe Damsté, J.S., Schouten, S., 2019a. A multiproxy study of past environmental changes in the Sea of Okhotsk during the last 1.5 Ma. Organic Geochemistry 132, 50-61.

Lattaud, J., Erdem, Z., Weiss, G.M., Rush, D., Balzano, S., Chivall, D., van der Meer, M.T., Hopmans, E.C., Sinninghe Damsté, J.S., Schouten, S., 2019b. Hydrogen isotopic ratios of long-chain diols reflect salinity. Organic Geochemistry 137, 103904.

Lengger, S.K., Hopmans, E.C., Reichart, G.-J., Nierop, K.G., Sinninghe Damsté, J.S., Schouten, S., 2012. Intact polar and core glycerol dibiphytanyl glycerol tetraether lipids in the Arabian Sea oxygen minimum zone. Part II: Selective preservation and degradation in sediments and consequences for the TEX_{86}. Geochimica et Cosmochimica Acta 98, 244-258.

Lengger, S.K., Kraaij, M., Tjallingii, R., Baas, M., Stuut, J.-B., Hopmans, E.C., Sinninghe Damsté, J.S., Schouten, S., 2013. Differential degradation of intact polar and core glycerol dialkyl glycerol tetraether lipids upon post-depositional oxidation. Organic Geochemistry 65, 83-93.

Lengger, S.K., Hopmans, E.C., Sinninghe Damsté, J.S., Schouten, S., 2014. Impact of sedimentary degradation and deep water column production on GDGT abundance and distribution in surface sediments in the Arabian Sea: Implications for the TEX_{86} paleothermometer. Geochimica et Cosmochimica Acta 142, 386-399.

Lopes dos Santos, R.A., Spooner, M.I., Barrows, T.T., De Deckker, P., Sinninghe Damsté, J.S., Schouten, S., 2013. Comparison of organic ($U^{K'}_{37}$, TEX^{H}_{86}, LDI) and faunal proxies (foraminiferal assemblages) for reconstruction of late Quaternary sea surface temperature variability from offshore southeastern Australia. Paleoceanography 28, 377-387.

Marie, D., Partensky, F., Vaulot, D., Brussaard, C., 1999. Enumeration of phytoplankton, bacteria, and viruses in marine samples. Current protocols in cytometry, 11.11. 11-11.11. 15.

Méjanelle, L., Sanchez-Gargallo, A., Bentaleb, I., Grimalt, J.O., 2003. Long chain n-alkyl diols, hydroxy ketones and sterols in a marine eustigmatophyte, *Nannochloropsis gaditana*, and in *Brachionus plicatilis* feeding on the algae. Organic Geochemistry 34, 527-538.

Menzel, D., van Bergen, P.F., Schouten, S., Sinninghe Damsté, J.S., 2003. Reconstruction of changes in export productivity during Pliocene sapropel deposition: a biomarker approach. Palaeogeography, Palaeoclimatology, Palaeoecology 190, 273-287.

Mitra, M., Patidar, S.K., George, B., Shaha, F., Mishra, S., 2015. A euryhaline Nannochloropsis gaditana with potential for nutraceutical (EPA) and biodiesel production. Algal Res 8, 161-167.

Mollenhauer, G., Eglinton, T.I., Hopmans, E.C., Sinninghe Damsté, J.S., 2008. A radiocarbon-based assessment of the preservation characteristics of crenarchaeol and alkenones from continental margin sediments. Organic Geochemistry 39, 1039-1045.

Morris, R., Brassell, S., 1988. Long-chain alkanediols: Biological markers for cyanobacterial contributions to sediments. Lipids 23, 256-258.

Naafs, B.D.A., Hefter, J., Stein, R., 2012. Application of the long chain diol index (LDI) paleothermometer to the early Pleistocene (MIS 96). Organic Geochemistry 49, 83-85.

Nierop, K., 1998. Origin of aliphatic compounds in a forest soil. Organic Geochemistry 29, 1009-1016.

Nieto-Moreno, V., Martinez-Ruiz, F., Gallego-Torres, D., Giralt, S., Garcia-Orellana, J., Masque, P., Sinninghe Damsté, J.S., Ortega-Huertas, M., 2015. Palaeoclimate and palaeoceanographic conditions in the westernmost Mediterranean over the last millennium: an integrated organic and inorganic approach. J Geol Soc London 172, 264-271.

Nürnberg, D., Bijma, J., Hemleben, C., 1996. Assessing the reliability of magnesium in foraminiferal calcite as a proxy for water mass temperatures. Geochimica et Cosmochimica Acta 60, 803-814.

Obeid, W., Salmon, E., Hatcher, P.G., 2014. The effect of different isolation procedures on algaenan molecular structure in *Scenedesmus* green algae. Organic Geochemistry 76, 259-269.

Ohkouchi, N., Eglinton, T.I., Keigwin, L.D., Hayes, J.M., 2002. Spatial and temporal offsets between proxy records in a sediment drift. Science 298, 1224-1227.

Olofsson, M., Lamela, T., Nilsson, E., Berge, J.P., del Pino, V., Uronen, P., Legrand, C., 2012. Seasonal Variation of Lipids and Fatty Acids of the Microalgae *Nannochloropsis oculata* Grown in Outdoor Large-Scale Photobioreactors. Energies 5, 1577-1592.

Pancost, R.D., Coleman, J.M., Love, G.D., Chatzi, A., Bouloubassi, I., Snape, C.E., 2008. Kerogen-bound glycerol dialkyl tetraether lipids released by hydropyrolysis of marine sediments: A bias against incorporation of sedimentary organisms? Organic Geochemistry 39, 1359-1371.

Pancost, R.D., Boot, C.S., Aloisi, G., Maslin, M., Bickers, C., Ettwein, V., Bale, N., Handley, L., 2009. Organic geochemical changes in Pliocene sediments of ODP Site 1083 (Benguela Upwelling System). Palaeogeography, Palaeoclimatology, Palaeoecology 280, 119-131.

Pearson, A., McNichol, A.P., Benitez-Nelson, B.C., Hayes, J.M., Eglinton, T.I., 2001. Origins of lipid biomarkers in Santa Monica Basin surface sediment: a case study using compound-specific $\Delta^{14}C$ analysis. Geochimica et Cosmochimica Acta 65, 3123-3137.

Peters, K.E., Walters, C.C., Moldowan, J., 2005. The biomarker guide. Cambridge University Press.

Pitcher, A., Villanueva, L., Hopmans, E.C., Schouten, S., Sinninghe Damsté, J.S., 2011. Niche segregation of ammonia-oxidizing archaea and anammox bacteria in the Arabian Sea oxygen minimum zone. ISME Journal 5, 1896-1904.

Plancq, J., Grossi, V., Pittet, B., Huguet, C., Rosell-Mele, A., Mattioli, E., 2015. Multi-proxy constraints on sapropel formation during the late Pliocene of central Mediterranean (southwest Sicily). Earth Planet Sc Lett 420, 30-44.

Prahl, F., Cowie, G., de Lange, G., Sparrow, M., 2003. Selective organic matter preservation in "burn-down" turbidites on the Madeira Abyssal Plain. Paleoceanography 18.

Prahl, F.G., Wakeham, S.G., 1987. Calibration of unsaturation patterns in long-chain ketone compositions for palaeotemperature assessment. Nature 330, 367.

Prahl, F.G., de Lange, G.J., Scholten, S., Cowie, G.L., 1997. A case of post-depositional aerobic degradation of terrestrial organic matter in turbidite deposits from the Madeira Abyssal Plain. Organic Geochemistry 27, 141-152.

Rampen, S.W., Schouten, S., Wakeham, S.G., Sinninghe Damsté, J.S., 2007. Seasonal and spatial variation in the sources and fluxes of long chain diols and mid-chain hydroxy methyl alkanoates in the Arabian Sea. Organic Geochemistry 38, 165-179.

Rampen, S.W., Schouten, S., Koning, E., Brummer, G.J.A., Sinninghe Damsté, J.S., 2008. A 90 kyr upwelling record from the northwestern Indian Ocean using a novel long-chain diol index. Earth Planet Sc Lett 276, 207-213.

Rampen, S.W., Schouten, S., Sinninghe Damsté, J.S., 2011. Occurrence of long chain 1,14-diols in *Apedinella radians*. Organic Geochemistry 42, 572-574.

Rampen, S.W., Willmott, V., Kim, J.H., Uliana, E., Mollenhauer, G., Schefuss, E., Sinninghe Damsté, J.S., Schouten, S., 2012. Long chain 1,13-and 1,15-diols as a potential proxy for palaeotemperature reconstruction. Geochimica Et Cosmochimica Acta 84, 204-216.

Rampen, S.W., Datema, M., Rodrigo-Gámiz, M., Schouten, S., Reichart, G.J., Sinninghe Damsté, J.S., 2014a. Sources and proxy potential of long chain alkyl diols in lacustrine environments. Geochimica et Cosmochimica Acta 144, 59-71.

Rampen, S.W., Willmott, V., Kim, J.H., Rodrigo-Gámiz, M., Uliana, E., Mollenhauer, G., Schefuss, E., Sinninghe Damsté, J.S., Schouten, S., 2014b. Evaluation of long chain 1,14-alkyl diols in marine sediments as indicators for upwelling and temperature. Organic Geochemistry 76, 39-47.

Reiche, S., Rampen, S.W., Dorhout, D.J., Sinninghe Damsté, J.S., Schouten, S., 2018. The impact of oxygen exposure on long-chain alkyl diols and the long chain diol index (LDI)–a long-term incubation study. Organic Geochemistry 124, 238-246.

Robinson, N., Cranwell, P., Eglinton, G., Brassell, S., Sharp, C., Gophen, M., Pollingher, U., 1986. Lipid geochemistry of Lake Kinneret. Organic Geochemistry 10, 733-742.

Rodrigo-Gámiz, M., Martinez-Ruiz, F., Rampen, S.W., Schouten, S., Sinninghe Damsté, J.S., 2014. Sea surface temperature variations in the western Mediterranean Sea over the last 20 kyr: A dual- organic proxy ($U^{K'}_{37}$ and LDI) approach. Paleoceanography 29, 87-98.

Rodrigo-Gámiz, M., Rampen, S.W., de Haas, H., Baas, M., Schouten, S., Sinninghe Damsté, J.S., 2015. Constraints on the applicability of the organic temperature proxies $U^{K'}_{37}$, TEX_{86} and LDI in the subpolar region around Iceland. Biogeosciences 12, 6573-6590.

Rodrigo-Gámiz, M., Rampen, S.W., Schouten, S., Sinninghe Damsté, J.S., 2016. The impact of oxic degradation on long chain alkyl diol distributions in Arabian Sea surface sediments. Organic Geochemistry 100, 1-9.

Rohling, E., Hopmans, E., Sinninghe Damsté, J., 2006. Water column dynamics during the last interglacial anoxic event in the Mediterranean (sapropel S5). Paleoceanography 21.

Rohling, E., Marino, G., Grant, K., 2015. Mediterranean climate and oceanography, and the periodic development of anoxic events (sapropels). Earth-Science Reviews 143, 62-97.

Rohling, E.J., Cane, T.R., Cooke, S., Sprovieri, M., Bouloubassi, I., Emeis, K.C., Schiebel, R., Kroon, D., Jorissen, F.J., Lorre, A., Kemp, A.E.S., 2002. African monsoon variability during the previous interglacial maximum. Earth Planet Sc Lett 202, 61-75.

Romero-Viana, L., Kienel, U., Sachse, D., 2012. Lipid biomarker signatures in a hypersaline lake on Isabel Island (Eastern Pacific) as a proxy for past rainfall anomaly (1942-2006 AD). Palaeogeogr Palaeocl 350, 49-61.

Rontani, J.F., Zabeti, N., Wakeham, S.G., 2009. The fate of marine lipids: Biotic vs. abiotic degradation of particulate sterols and alkenones in the Northwestern Mediterranean Sea. Mar Chem 113, 9-18.

Rontani, J.F., Volkman, J.K., Prahl, F.G., Wakeham, S.G., 2013. Biotic and abiotic degradation of alkenones and implications for $U^{K'37}$ paleoproxy applications: A review. Organic Geochemistry 59, 95-113.

Rosenthal, Y., Boyle, E.A., Slowey, N., 1997. Temperature control on the incorporation of magnesium, strontium, fluorine, and cadmium into benthic foraminiferal shells from Little Bahama Bank: Prospects for thermocline paleoceanography. Geochimica et Cosmochimica Acta 61, 3633-3643.

Rossignol-Strick, M., Nesteroff, W., Olive, P., Vergnaud-Grazzini, C., 1982. After the deluge: Mediterranean stagnation and sapropel formation. Nature 295, 105-110.

Rossignol-Strick, M., 1983. African monsoons, an immediate climate response to orbital insolation. Nature 304, 46.

Rossignol-Strick, M., 1985. Mediterranean Quaternary sapropels, an immediate response of the African monsoon to variation of insolation. Palaeogeography, Palaeoclimatology, Palaeoecology 49, 237-263.

Sakka, A., Legendre, L., Gosselin, M., LeBlanc, B., Delesalle, B., Price, N., 1999. Nitrate, phosphate, and iron limitation of the phytoplankton assemblage in the lagoon of Takapoto Atoll (Tuamotu Archipelago, French Polynesia). Aquatic Microbial Ecology 19, 149-161.

Sangiorgi, F., Dinelli, E., Maffioli, P., Capotondi, L., Giunta, S., Morigi, C., Principato, M.S., Negri, A., Emeis, K.-C., Corselli, C., 2006. Geochemical and micropaleontological characterisation of a Mediterranean sapropel S5: a case study from core BAN89GC09 (south of Crete). Palaeogeography, Palaeoclimatology, Palaeoecology 235, 192-207.

Scholz, M.J., Weiss, T.L., Jinkerson, R.E., Jing, J., Roth, R., Goodenough, U., Posewitz, M.C., Gerken, H.G., 2014. Ultrastructure and composition of the *Nannochloropsis gaditana* cell wall. Eukaryot Cell 13, 1450-1464.

Schouten, S., Hopmans, E.C., Pancost, R.D., Sinninghe Damsté, J.S., 2000. Widespread occurrence of structurally diverse tetraether membrane lipids: evidence for the ubiquitous presence of low-temperature relatives of hyperthermophiles. Proceedings of the National Academy of Sciences 97, 14421-14426.

Schouten, S., Hopmans, E.C., Schefuß, E., Sinninghe Damste, J.S., 2002. Distributional variations in marine crenarchaeotal membrane lipids: a new tool for reconstructing ancient sea water temperatures? Earth Planet Sc Lett 204, 265-274.

Schouten, S., Hopmans, E.C., Sinninghe Damsté, J.S., 2004. The effect of maturity and depositional redox conditions on archaeal tetraether lipid palaeothermometry. Organic Geochemistry 35, 567-571.

Schouten, S., Pitcher, A., Hopmans, E.C., Villanueva, L., van Bleijswijk, J., Sinninghe Damsté, J.S., 2012. Intact polar and core glycerol dibiphytanyl glycerol tetraether lipids in the Arabian Sea oxygen minimum zone: I. Selective preservation and degradation in the water column and consequences for the TEX_{86}. Geochimica et Cosmochimica Acta 98, 228-243.

Schouten, S., Hopmans, E.C., Sinninghe Damsté, J.S., 2013. The organic geochemistry of glycerol dialkyl glycerol tetraether lipids: a review. Organic Geochemistry 54, 19-61.

Seki, O., Schmidt, D.N., Schouten, S., Hopmans, E.C., Sinninghe Damsté, J.S., Pancost, R.D., 2012. Paleoceanographic changes in the Eastern Equatorial Pacific over the last 10 Myr. Paleoceanography 27, PA3224.

Shackleton, N., 1974. Attainment of isotopic equilibrium between ocean water and the benthonic foraminifera genus *Uvigerina*: isotopic changes in the ocean during the last glacial. Les methods quantitatives d'etude des variations du climat au cours du Pleistocene, Gif-sur-Yvette, Colloque international du CNRS 219, 203-210.

Shimokawara, M., Nishimura, M., Matsuda, T., Akiyama, N., Kawai, T., 2010. Bound forms, compositional features, major sources and diagenesis of long chain, alkyl mid-chain diols in Lake Baikal sediments over the past 28,000 years. Organic Geochemistry 41, 753-766.

Sinninghe Damsté, J., Hoefs, M., de Leeuw, J., de Lange, G., 1998. Changes in kerogen composition across an oxidation front in Madeira Abyssal Plain turbidites as revealed by pyrolysis-GC-MS, Proceedings of the Ocean Drilling Program, Scientific Results, pp. 591-607.

Sinninghe Damsté, J.S., Rijpstra, W.I.C., Reichart, G.-J., 2002a. The influence of oxic degradation on the sedimentary biomarker record II. Evidence from Arabian Sea sediments. Geochimica et Cosmochimica Acta 66, 2737-2754.

Sinninghe Damsté, J.S., Schouten, S., Hopmans, E.C., van Duin, A.C., Geenevasen, J.A., 2002b. Crenarchaeol the characteristic core glycerol dibiphytanyl glycerol tetraether membrane lipid of cosmopolitan pelagic crenarchaeota. Journal of Lipid Research 43, 1641-1651.

Sinninghe Damsté, J.S., Rampen, S., Rijpstra, W.I.C., Abbas, B., Muyzer, G., Schouten, S., 2003. A diatomaceous origin for long-chain diols and mid-chain hydroxy methyl alkanoates widely occurring in Quaternary marine sediments: Indicators for high-nutrient conditions. Geochimica et Cosmochimica Acta 67, 1339-1348.

Sinninghe, D.J., Hopmans, E.C., 2008. Does fossil pigment and DNA data from Mediterranean sediments invalidate the use of green sulfur bacterial pigments and their diagenetic derivatives as proxies for the assessment of past photic zone euxinia? Environmental microbiology 10, 1392.

Smith, D.J., Eglinton, G., Morris, R.J., 1983. Occurrence of long-chain alkan-diols and alkan-15-one-1-ols in a quaternary sapropel from the Eastern Mediterranean. Lipids 18, 902-905.

Smith, M., De Deckker, P., Rogers, J., Brocks, J., Hope, J., Schmidt, S., dos Santos, R.L., Schouten, S., 2013. Comparison of $U^{K'}_{37}$, TEX^{H}_{86} and LDI temperature proxies for reconstruction of south-east Australian ocean temperatures. Organic Geochemistry 64, 94-104.

Sun, M.-Y., Wakeham, S., 1998. A study of oxic/anoxic effects on degradation of sterols at the simulated sediment–water interface of coastal sediments. Organic Geochemistry 28, 773-784.

Sun, M.Y., Wakeham, S.G., 1994. Molecular Evidence for Degradation and Preservation of Organic-Matter in the Anoxic Black-Sea Basin. Geochimica et Cosmochimica Acta 58, 3395-3406.

Sun, M.Y., Wakeham, S.G., Lee, C., 1997. Rates and mechanisms of fatty acid degradation in oxic and anoxic coastal marine sediments of Long Island Sound, New York, USA. Geochimica et Cosmochimica Acta 61, 341-355.

Teece, M., Getliff, J., Leftley, J., Parkes, R.J., Maxwell, J., 1998. Microbial degradation of the marine prymnesiophyte *Emiliania huxleyi* under oxic and anoxic conditions as a model for early diagenesis: long chain alkadienes, alkenones and alkyl alkenoates. Organic Geochemistry 29, 863-880.

Tegelaar, E.W., Deleeuw, J.W., Saizjimenez, C., 1989a. Possible Origin of Aliphatic Moieties in Humic Substances. Science of the Total Environment 81-2, 1-17.

Tegelaar, E.W., de Leeuw, J.W., Derenne, S., Largeau, C., 1989b. A Reappraisal of Kerogen Formation. Geochimica et Cosmochimica Acta 53, 3103-3106.

Ten Haven, H., Baas, M., de Leeuw, J., Schenck, P., 1987a. Late Quaternary Mediterranean sapropels, I—On the origin of organic matter in sapropel S7. Mar Geol 75, 137-156.

Ten Haven, H., Baas, M., de Leeuw, J., Schenck, P., Brinkhuis, H., 1987b. Late Quaternary Mediterranean sapropels II. Organic geochemistry and palynology of S1 sapropels and associated sediments. Chemical Geology 64, 149-167.

Ten Haven, H., Baas, M., Kroot, M., de Leeuw, J., Schenck, P., Ebbing, J., 1987c. Late Quaternary Mediterranean sapropels. III: Assessment of source of input and palaeotemperature as derived from biological markers. Geochimica et Cosmochimica Acta 51, 803-810.

Ten Haven, H., Rullkötter, J., 1991. Preliminary lipid analyses of sediments recovered during leg 117, in: Prell, W.L., Niitsuma, N., al., e. (Eds.), Proceedings of the Ocean Drilling Program, Scientific Results, 117: College Station, TX (Ocean Drilling Program), pp. 561-569.

Ten Haven, H., Eglinton, G., Farrimond, P., Kohnen, M., Poynter, J., Rullkötter, J., Welte, D., 1992. Variations in the content and composition of organic matter in sediments underlying active upwelling regimes: a study from ODP Legs 108, 112, and 117. Geological Society, London, Special Publications 64, 229-246.

Thomson, J., Higgs, N., Wilson, T., Croudace, I., de Lange, G., Van Santvoort, P., 1995. Redistribution and geochemical behaviour of redox-sensitive elements around S1, the most recent eastern Mediterranean sapropel. Geochimica et Cosmochimica Acta 59, 3487-3501.

Tissot, B., Welte, D., 1984. Petroleum formation and occurrence. Springer-Verlag, Berlin.

Urey, H.C., 1947. The thermodynamic properties of isotopic substances. Journal of the Chemical Society (Resumed), 562-581.

Valdés, F., Catalá, L., Hernández, M., García-Quesada, J., Marcilla, A., 2013. Thermogravimetry and Py–GC/MS techniques as fast qualitative methods for comparing the biochemical composition of *Nannochloropsis oculata* samples obtained under different culture conditions. Bioresource Technology 131, 86-93.

van Bergen, P.F., Blokker, P., Collinson, M.E., Sinninghe Damsté, J.S., de Leeuw, J.W., 2004. Structural biomacromolecules in plants: what can be learnt from the fossil record?, in: Hemsley, A.R., Poole, I. (Eds.), The Evolution of Plant Physiology. Elsevier, pp. 133-154.

van der Meer, M.T.J., Baas, M., Rijpstra, W.I.C., Marino, G., Rohling, E.J., Sinninghe Damsté, J.S., Schouten, S., 2007. Hydrogen isotopic compositions of long-chain alkenones record freshwater flooding of the Eastern Mediterranean at the onset of sapropel deposition. Earth Planet Sc Lett 262, 594-600.

Van Soelen, E., Lammertsma, E., Cremer, H., Donders, T.H., Sangiorgi, F., Brooks, G., Larson, R., Sinninghe Damste, J., Wagner-Cremer, F., Reichart, G.-J., 2010. Late Holocene sea-level rise in Tampa Bay: Integrated reconstruction using biomarkers, pollen, organic-walled dinoflagellate cysts, and diatoms. Estuarine, Coastal and Shelf Science 86, 216-224.

Vandenbroucke, M., Largeau, C., 2007. Kerogen origin, evolution and structure. Organic Geochemistry 38, 719-833.

Versteegh, G.J., Lipp, J., 2019. Detection of new long-chain mid-chain keto-ol isomers from marine sediments by means of HPLC APCI-MS and comparison with long-chain mid-chain diols from the same samples. Organic Geochemistry 133, 92-102.

Versteegh, G.J.M., Bosch, H.-J., de Leeuw, J.W., 1997. Potential palaeoenvironmental information of C_{24} to C_{36} mid-chain diols, keto-ols and mid-chain hydroxy fatty acids; a critical review. Organic Geochemistry 27, 1-13.

Versteegh, G.J.M., 1997. The onset of major Northern Hemisphere glaciations and their impact on dinoflagellate cysts and acritarchs from the Singa section, Calabria (southern Italy) and DSDP Holes 607/607A (North Atlantic). Marine Micropaleontology 30, 319-343.

Versteegh, G.J.M., Jansen, J.H.F., de Leeuw, J.W., Schneider, R.R., 2000. Mid-chain diols and keto-ols in SE Atlantic sediments: a new tool for tracing past sea surface water masses? Geochimica et Cosmochimica Acta 64, 1879-1892.

Versteegh, G.J.M., Zonneveld, K.A.F., de Lange, G.J., 2010. Selective aerobic and anaerobic degradation of lipids and palynomorphs in the Eastern Mediterranean since the onset of sapropel S1 deposition. Mar Geol 278, 177-192.

Villanueva, L., Besseling, M., Rodrigo-Gámiz, M., Rampen, S.W., Verschuren, D., Sinninghe Damsté, J.S., 2014. Potential biological sources of long chain alkyl diols in a lacustrine system. Organic Geochemistry 68, 27-30.

Volkman, J.K., Eglinton, G., Corner, E.D., Forsberg, T., 1980. Long-chain alkenes and alkenones in the marine coccolithophorid *Emiliania huxleyi*. Phytochemistry 19, 2619-2622.

Volkman, J.K., Barrett, S.M., Dunstan, G.A., Jeffrey, S.W., 1992. C_{30}-C_{32} alkyl diols and unsaturated alcohols in microalgae of the class Eustigmatophyceae. Organic Geochemistry 18, 131-138.

Volkman, J.K., Brown, M.R., Dunstan, G.A., Jeffrey, S.W., 1993. The Biochemical-Composition of Marine Microalgae from the Class Eustigmatophyceae. Journal of Phycology 29, 69-78.

Volkman, J.K., Barrett, S.M., Blackburn, S.I., Mansour, M.P., Sikes, E.L., Gelin, F., 1998. Microalgal biomarkers: A review of recent research developments. Organic Geochemistry 29, 1163-1179.

Volkman, J.K., Barrett, S.M., Blackburn, S.I., 1999. Eustigmatophyte microalgae are potential sources of C_{29} sterols, C_{22} - C_{28} *n*-alcohols and C_{28} - C_{32} *n*-alkyl diols in freshwater environments. Organic Geochemistry 30, 307-318.

Wakeham, S.G., Canuel, E.A., 2006. Degradation and Preservation of Organic Matter in Marine Sediments, in: Volkman, J.K. (Ed.), In: Marine Organic Matter: Biomarkers, Isotopes and DNA. Springer, Berlin, Heidelberg, pp. 295-321.

Walsh, E.M., Ingalls, A.E., Keil, R.G., 2008. Sources and transport of terrestrial organic matter in Vancouver Island fjords and the Vancouver-Washington Margin: A multiproxy approach using $d^{13}C_{org}$, lignin phenols, and the ether lipid BIT index. Limnology and Oceanography 53, 1054-1063.

Warnock, J.P., Bauersachs, T., Kotthoff, U., Brandt, H.T., Andrén, E., 2018. Holocene environmental history of the Ångermanälven Estuary, northern Baltic Sea. Boreas 47, 593-608.

Weijers, J.W., Schouten, S., Hopmans, E.C., Geenevasen, J.A., David, O.R., Coleman, J.M., Pancost, R.D., Sinninghe Damsté, J.S., 2006. Membrane lipids of mesophilic anaerobic bacteria thriving in peats have typical archaeal traits. Environmental Microbiology 8, 648-657.

Weijers, J.W., Schouten, S., Schefuß, E., Schneider, R.R., Sinninghe Damste, J.S., 2009. Disentangling marine, soil and plant organic carbon contributions to continental margin sediments: a multi-proxy approach in a 20,000 year sediment record from the Congo deep-sea fan. Geochimica et Cosmochimica Acta 73, 119-132.

Willmott, V., Rampen, S.W., Domack, E., Canals, M., Sinninghe Damsté, J.S., Schouten, S., 2010. Holocene changes in Proboscia diatom productivity in shelf waters of the north-western Antarctic Peninsula. Antarctic Science 22, 3-10.

Wörmer, L., Lipp, J.S., Schröder, J.M., Hinrichs, K.-U., 2013. Application of two new LC–ESI–MS methods for improved detection of intact polar lipids (IPLs) in environmental samples. Organic Geochemistry 59, 10-21.

Xiao, Y., Zhang, J., Cui, J., Feng, Y., Cui, Q., 2013. Metabolic profiles of Nannochloropsis oceanica IMET1 under nitrogen-deficiency stress. Bioresour Technol 130, 731-738.

Xu, Y., Simoneit, B.R.T., Jaffé, R., 2007. Occurrence of long-chain *n*-alkenols, diols, keto-ols and *sec*-alkanols in a sediment core from a hypereutrophic, freshwater lake. Organic Geochemistry 38, 870-883.

Yamamoto, M., Ficken, K., Baas, M., Bosch, H.-J., de Leeuw, J.W., 1996. Molecular palaeontology of the earliest Danian at Geulhemmerberg (The Netherlands). Geologie en Mijnbouw 75, 255-267.

Yang, Y., Ruan, X., Gao, C., Lü, X., Yang, H., Li, X., Yao, Y., Pearson, A., Xie, S., 2020. Assessing the applicability of the long-chain diol (LDI) temperature proxy in the high-temperature South China Sea. Organic Geochemistry, 104017.

Zelibor, J.L., Romankiw, L., Hatcher, P.G., Colwell, R.R., 1988. Comparitive analysis of the chemical composition of mixed and pure cultures of green algae and their decomposed residues by ^{13}C nuclear magnetic resonance spectroscopy. Applied and Environmental Microbiology 54, 1051-1060.

Zeng, Z., Liu, X.-L., Farley, K.R., Wei, J.H., Metcalf, W.W., Summons, R.E., Welander, P.V., 2019. GDGT cyclization proteins identify the dominant archaeal sources of tetraether lipids in the ocean. Proceedings of the National Academy of Sciences 116, 22505-22511.

Zhang, Z., Metzger, P., Sachs, J.P., 2011. Co-occurrence of long chain diols, keto-ols, hydroxy acids and keto acids in recent sediments of Lake El Junco, Galápagos Islands. Organic Geochemistry 42, 823-837.

Zhang, Z., Volkman, J.K., Xie, X., Snowdon, L.R., 2016. Stepwise pyrolysis of the kerogen from the Huadian oil shale, NE China: Algaenan-derived hydrocarbons and mid-chain ketones. Organic Geochemistry 91, 89-99.

Zhang, Z., Volkman, J.K., 2018. Corrigendum to “Algaenan structure in the microalga Nannochloropsis oculata characterized from stepwise pyrolysis”[Org. Geochem. 104 (2017) 1–7]. Organic Geochemistry 123, 148.

Zhang, Z.R., Volkman, J.K., 2017. Algaenan structure in the microalga *Nannochloropsis oculata* characterized from stepwise pyrolysis. Organic Geochemistry 104, 1-7.

Zhu, C., Lipp, J.S., Wormer, L., Becker, K.W., Schroder, J., Hinrichs, K.U., 2013. Comprehensive glycerol ether lipid fingerprints through a novel reversed phase liquid chromatography-mass spectrometry protocol. Organic Geochemistry 65, 53-62.

Zhu, X., Jia, G., Mao, S., Yan, W., 2018. Sediment records of long chain alkyl diols in an upwelling area of the coastal northern South China Sea. Organic Geochemistry 121, 1-9.

Zhu, X., Mao, S., Sun, Y., Jia, G., Wu, N., Yan, W., 2019. Long chain diol index (LDI) as a potential measure to estimate annual mean sea surface temperature in the northern South China Sea. Estuarine, Coastal and Shelf Science 221, 1-7.

Zhu, X., Jia, G., Mao, S., Sun, Y., Wu, N., Tian, Y., Xu, W., Yan, W., 2020. Long chain 1, 14-diols as potential indicators for upper water stratification in the open South China Sea. Ecological Indicators 110, 105900.

Acknowledgements

I arrived on Texel on a very stormy day in October 2014 and while I might have bought a better rain coat and a good pair of rubber boots within a month, I greatly enjoyed my time on the island, at the NIOZ and in the Netherlands. It hasn't always been an easy time, but I have learned a lot about science and as a person.

Stefan, thank you so much for your guidance, mentorship and especially profound patience leading me through my project, scientific crises and the world of proxies, diagenesis and green algae. The scientific journey described in this thesis was quite a bumpy ride but thanks to you, your open-door policy, discussions, problem solving and your assurance, I never earnestly thought about throwing in the towel. Jaap, thank you, for making my manuscripts much better, for asking the right questions alerting me of pitfalls and mistakes and being encouraging when needed.

I thank the reading and sitting committee for their assessment of this thesis.

This thesis would not have been possible without the MMB department and its senior scientists and technicians. Thank you especially to Denise, Jort, Caglar, Monique, Anchelique and Ellen for their support in the lab and their help working with the instruments.

Additionally, I would like to thank those that have accompanied my academic journey up to this point. Thank you to Georg Grathoff, for giving me the chance to discover mineralogy and crystallography and being a mentor and supervisor throughout my Bachelor studies. Furthermore, thank you to Daniel Conley for leading me through my Master's thesis and saying hello at the Goldschmidt conference. I also would like to thank John Volkman for in-depth, critical discussions at conferences, over email and on manuscripts.

The NIOZ, but especially the MMB department is a wonderful, international and inclusive place, that hosts a variety of people which all share a love for science. I am glad that I got to be a part of it. I thank everybody that in some way or another has contributed to this PhD and my time on Texel. I am however, especially thankful to those five, that not only possibly drank the most Gin and Tonics with me, but also humored me by going on extended coffee breaks, listening to both my problems and my rambles on new discoveries in TV, film, sailing and literature. Thank you, Laura, for being my lab mate, for listening to the good and quite possibly worst music with me, for numerous coffees and Aperol Spritz both in the Netherlands as well as in the countries we were able to discover during our conferences. Thank you to Sigrid, for being there in every situation when needed, for letting me crash in Alkmaar, for providing question marks and laughs when random gifts and chocolate appeared out of nowhere on my desk and still keep appearing in packages up to this day. Thank you, to both of you, for being my paranimfs and your support and assurance throughout the last years. Thank you to Cait, for being a nerdy pal that would sit with me for hours on end, discovering something new about anything from Harry Potter to politics to science, and who is a constant source of support on the other side of my phone. To Zeynep, for being the perfect office mate, providing me with encouragement and adventures on Texel. And last but not least, to Saara, thank you for taking the time for coffees, chats and obscure Finnish-Japanese operas and your help during these last few months of the PhD journey.

And finally, Sandra. Danke für gemeinsames jahrelanges Studieren, Exkursionen und Feldarbeit, laute Frösche auf der Moho, Sterne in der Wüste, Stromatolithen im Harz, Besuche und unzählige Skypeanrufe, die mir unheimlich viel bedeuten.

Vielen Dank insbesondere an meine ganze Familie, die mich seit jeher unterstützt und mich trotz unzähliger verpasster Familienfeiern, immer wieder mit offenen Armen empfängt, besucht, Updates und Fotos per E-Mail oder WhatsApp schickt und für mich da ist, wenn ich sie brauche. An meine Eltern, die mir immer das Gefühl gegeben habe, dass ich alles machen kann, was ich möchte und mich mit Musik, Literatur, Naturwissenschaften, „die Welt entdecken“ und mit immer neuen Entdeckungen und Obsessionen umgeben haben. Ohne euch hätte ich es nicht an diesen Punkt geschafft.

Diese Doktorarbeit ist meinen Großeltern gewidmet. Oma und Opa, vielen Dank für eure Unterstützung, ohne die ich nicht da wäre, wo ich jetzt bin. Durch unzählige Ferienaufenthalte und Urlaube, Ausflüge ins Jagdgebiet und an die Seen, sind die Abendstraße und die umliegenden Wiesen und Wälder für mich mehr eine Heimat als meine anderen Wohnorte es jemals waren. Danke, dass ihr euch immer die Zeit nehmt zuzuhören, Probleme zu besprechen und mich mit offenen Armen zu empfangen.

Und René. Ohne dich gäbe es diese Doktorarbeit nicht. Ich bin so stolz auf uns und das, was wir uns gemeinsam aufgebaut haben. Ich kann es kaum erwarten zu sehen, was die Zukunft uns bringt. If the last few years are any indication, it will be amazing.

About the author

Sophie Reiche was born on 4th March 1988 in Greifswald, Germany. She graduated from Europaschule Landesgymnasium Latina August Hermann Francke in Halle/Saale in 2007 and subsequently moved to the University of Greifswald to study Environmental Sciences. After changing her major to Geology in 2009, she graduated in 2012 with a Bachelor of Science in Geology with a specialization in Mineralogy and Quaternary Geology. Subsequently, she moved to Sweden to study at the University of Lund. She completed her Master of Science in Geology with a specialization in Quaternary Geology in September 2014 when she defended her Master thesis titled "Ascertaining the lithological boundaries of the Yoldia Sea of the Baltic Sea – a geochemical approach". Two weeks later she started her PhD position at the Royal Netherlands Institute for Sea Research on Texel, the Netherlands, under the guidance of Prof. Stefan Schouten and Prof. Jaap Sinninghe Damsté, which has led to this doctoral thesis.